



Final publishable summary report

- Publishable -

Grant Agreement number: NMP2-LA-2008-214134

Project acronym: N2P

Project title:

**FLEXIBLE PRODUCTION TECHNOLOGIES AND EQUIPMENT BASED ON
ATMOSPHERIC PRESSURE PLASMA PROCESSING
FOR 3D NANO STRUCTURED SURFACES**

Funding Scheme: Collaborative Project

Date of latest version of Annex I against which the assessment will be made: 2011-02-03

Period covered: from 01/06/2008 to 30/11/2012

Project co-ordinator: Dr. rer.nat. habil. Volkmar Hopfe, Fraunhofer IWS

E-mail: volkmar.hopfe@iws.fraunhofer.de

Project website address: www.n2p-project.eu

Index

1	Project Context and Objectives	5
1.1	Impact Areas	5
1.2	Integration	6
1.3	Consortium	7
2	Main achievements and potential impact	9
2.1	WP1/2: Plasma chemical etching for c-Si photovoltaics	9
2.1.1	Objectives	9
2.1.2	Equipment development	9
2.1.3	Process development	12
2.1.4	PV cell design – influence of surface structure	15
2.1.5	Application oriented tests	16
2.1.6	Summary of results	18
2.2	WP3/4: Structuring of TCO layers for TF-Photovoltaics	19
2.2.1	Objectives	19
2.2.2	Nano-structured TCO films	19
2.2.3	TCO surface nano-texture modification by plasma chemical post-treatment	22
2.2.4	Equipment Demonstrator for TCO deposition by AP-CVD	24
2.2.5	Evaluation of results and conclusions for exploitation	30
2.3	WP5/6: Infection control	31
2.3.1	Process and Materials studies	31
2.3.2	Application demonstrator for infection control	34
2.3.3	Road mapping exercise	39
2.3.4	Evaluation of results and conclusions for exploitation	39
2.4	WP7/8 Energy storage	41
2.4.1	Process and materials R&D	41
2.4.2	Application demonstrator for energy storage	45
2.4.3	Evaluation of results and conclusions for exploitation	49
2.5	WP9/10: Interface Technologies for Durable Adhesion	51
2.5.1	Process and materials development	51
2.5.2	Application Demonstrator for Interface Technologies	58
2.6	WP11: Cross-cutting equipment development	65
2.6.1	Objectives	65
2.6.2	Plasma sources	65
2.6.3	Power supplies	67
2.6.4	Process monitoring and control	70
2.7	Dissemination activities and exploitation of results	72

GLOSSARY

AFM	Atomic Force Microscopy
AP	Atmospheric Pressure
AP-PCE	Atmospheric Pressure Plasma Chemical Etching
AP-PECVD	Atmospheric Pressure Plasma Enhanced CVD
AP-CVD	Atmospheric Pressure Chemical Vapor Deposition
APP	Atmospheric Pressure Plasma
AZO	Aluminium doped Zinc Oxide (ZnO:Al)
BSF	Back Surface Field
CAD	Computer Aided Design
CdTe	Cadmium Telluride
CFD	Computational Fluid Dynamics
CIGS	Copper Indium Gallium di Selenide
CNT	Carbon Nano-Tube
CoO	Cost of Ownership
CFRP	Carbon Fibre Reinforced Polymers
c-Si PV	Crystalline Silicon Photovoltaic
CVD	Chemical Vapor Deposition
DBD	Dielectric Barrier Discharge
DC	Direct Current
DLC	Double-Layer Capacitor
DEM	Demonstration activities
DoW	Description of Work (= project workplan, contractual)
ESBL	Extended Spectrum Beta-lactamase
FA-CVD	Flame-Assisted CVD
FTIR	Fourier Transformed Infrared Spectroscopy
FCA	Free carrier absorption
FTO	Fluorine doped Tin Oxide (SnO ₂ :F)
GA	Grand Assembly
GD	Glow Discharge
GDBD	Glow (discharge) Dielectric Barrier Discharge
GDOES	Glow Discharge Optical Emission Spectroscopy
GOX	Glucose Oxidase
GRE	Glycopeptide Resistant Enterococci
GWP	Global Warming Potential
HAI	Hospital Acquired Infection
HCAI	Health Care Associated Infections
HEV	Hybrid Electric Vehicle
HF	Hydrofluoric acid
HV	High Voltage
IP	Impact Area
MBTC	Monobutyl Tin Trichloride
MIR	Mid Infrared
MRSA	Methicillin Resistant Staphylococcus aureus

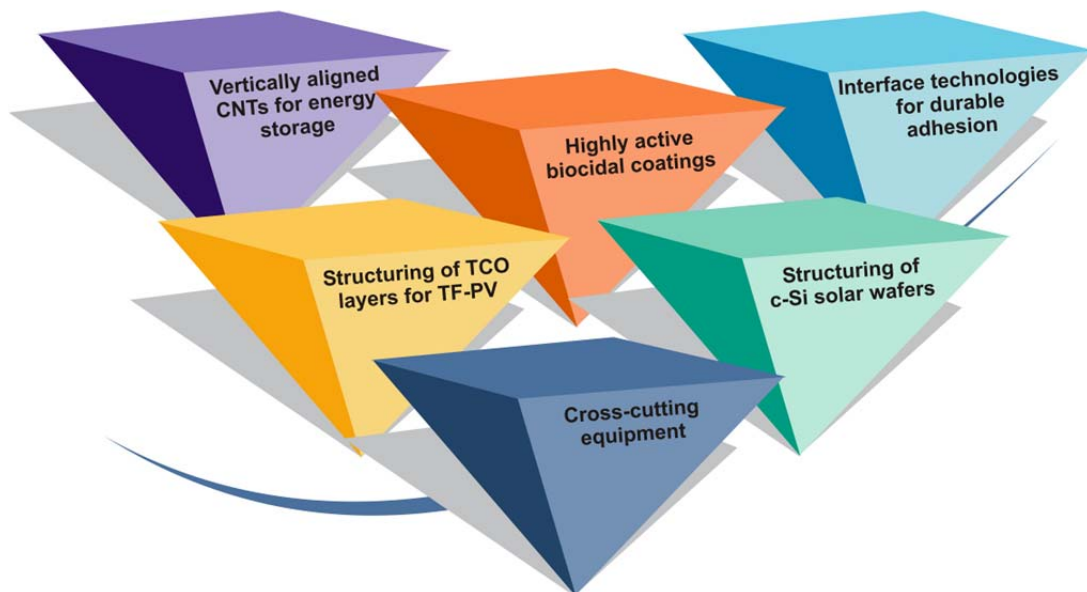
MW	Microwave
NIR	Near Infrared
PANI	Polyaniline
PPy	Polypyrrole
PCA	Principal Component Analysis
PCE	Plasma Chemical Etching
PCC	Project Coordination Committee
PLS	Partial Least Squares
PSG	Phosphorous Silicate Glass
PV	Photovoltaic
QAC	Quaternary Ammonium Compounds
QCL	Quantum Cascade Laser
R2R	Roll-to-Roll
RT	Room Temperature
RTD	Research and Technology Development incl. Coordination
SAL	Sterility Assurance Level
SEM	Scanning Electron Microscopy
Si	Silicon
SoA	State of the Art
SW-CNT	Single-Walled Carbon Nano-Tubes
TCO	Transparent Conductive Oxide
TFA	Trifluoroacetic Acid
TF-PV	Thin Film Photovoltaics
TD	Diffuse Transmittance
TT	Total Transmittance
TTC	Tin Tetrachloride
UV	Ultra violet light
VIS	Wave length region of the visible light
VRE	Vancomycin Resistant Enterococci
WPC	Work Package Committee
XPS	X-ray Photoelectron Spectroscopy
XRD	X-ray Diffraction

1 Project Context and Objectives

Outstanding progress has been made in recent years in developing novel structures and applications for direct fabrication of 3D nano-surfaces. However, exploitation is limited by lack of suitable manufacturing technologies. In this project we develop innovative in-line high throughput technologies based on atmospheric pressure surface and plasma technologies. The two identified approaches to direct 3D nano-structuring are etching for manufacturing of nano-structures tailored for specific applications and coating.

The overall project aims are:

- bridge the gap between advanced R&D results in nano-technology and industrial production
- demonstrate introduction of nano-technology into high impact application areas
- establish a sustainable network of leading European players, comprising
 - Industrial oriented R&D supplier
 - Equipment supplier
 - End-user industries



1.1 Impact Areas

The targeted applications are grouped in two main areas with wide interest both commercial and societal:

- Energy
 - Energy production, e.g. solar energy
 - Energy storage, e.g. for e-car
 - Energy savings; e.g. lightweight vehicles
- Health
 - Medicine, e.g. biocidal walls for hospitals

- Hygiene, e.g. in high visitor traffic areas

Four major impact areas were selected, demonstrating different application fields:

Impact Area 1 - Photovoltaics is aimed on efficient power production based on solar cells, one of the major and fastest growing renewable energies. The overall efficiency of such devices is significantly affected by an optimised “light management” to improve the energy harvesting properties of the solar cell.

We are aiming for two areas with high commercial impact: (1a) Crystalline Silicon Solar Cells currently comprising a major market share for power production and (1b) Thin Film Silicon Solar Cells having high potential for market growth.

Impact Area 2 – Infection control is aimed on biocidal surface structures where there is clear potential for 3D nano-structures and need for new manufacturing approaches. Increasing concern about infections is leading to the conclusion, that only multi-action approaches for the control of infection transfer can be effective. We combine such surfaces with 3D nano-structures, which will both immobilise and deactivate pathogenic organisms on surfaces. Widespread application in areas such as medical related (hospital environments), hygiene in areas with high visitor traffic, and food handling are represented within the consortium. Potential commercial and societal benefits are wide and significant.

Impact Area 3 – Energy storage is directed at direct growth of aligned carbon nano-tubes (CNT) on electrode surfaces. The targeted 3D nano-structures with very high aspect ratios offer a unique combination of properties, e.g. combining high specific conductivity with high ion mobility making them candidate material for use in, e.g. super-capacitors with high power density. The components envisage a strongly expanding market potential, e.g. as energy storage systems for electric cars, if they can offer unique performance and can be manufactured cost efficiently.

Impact Area 4 – Interface technologies for durable adhesion is focussed on three major high volume market segments:

Aeronautics: Next generation of lightweight airliners needing durable bonding of carbon fibre reinforced polymers with lightweight metals, and

Automotive: Durable high-tech organic coating systems for lightweight (polymer) vehicle parts. Target is to reduce energy consumption by introducing lightweight materials.

Steel: Lightweight construction panels with high stiffness manufactured from steel strips and embossed steel sheets. Target is to reduce materials consumption and manufacturing of high add-on value parts for clients.

Common for these three sub-areas is that interface control by 3D nano-structuring is crucial for achieving maximum shear strength (cohesive break) and extended life time i.e. stabilization of the interface between substrates and “coating” (paint/adhesive). Target is to substitute manufacturing technologies with higher cost and environmental impact by economic atmospheric pressure plasma technology for plasma-chemical surface modification and coating on 3D shaped immobile parts for aircraft and automotive as well as, for continuous coating on panels for steel industry.

1.2 Integration

A key aspect of this “Integrating Project” is the potential benefit from cooperation cross-over boundaries of traditional areas. Whilst we have focused the R&D activities along the four “Impact Areas” being selected, we have established strong horizontal “cross-cutting” technology links based on the underpinning technologies for high throughput manufacturing.

Horizontal technology platforms to support “cross fertilisation” have been established in:

- Atmospheric pressure CVD technologies,
- Atmospheric pressure plasmas,
- Surface treatment / etching and nucleation strategies for 3D nano-structuring,

- Surface 3D nano-structure and thin film analysis, and
- Process monitoring & control, quality assessment.

1.3 Consortium

The N2P consortium comprises 21 partners from 8 countries, having a complimentary knowledge, and covering the complete R&D chain

- 5 Universities
- 4 (industrial) Research Institutes
- 1 Public Body
- 6 SMEs
- 5 Industry (large)





2 Main achievements and potential impact

2.1 WP1/2: Plasma chemical etching for c-Si photovoltaics

2.1.1 Objectives

Development of Atmospheric Pressure Plasma Chemical Etching (AP-PCE) processes for application in silicon solar wafer processing was main objective. The method has potential for performance enhancement of PV cells by introducing tailored micro- and nano-structures on both front and rear surface. Main target for getting higher performance is to increase the light trapping effect for solar radiation in the near infrared region (NIR). The AP-PCE technology can be used within the c-Si solar cell production to replace some standard wet chemical etching steps, e.g.:

- Front surface texturing (to reduce the total optical reflectance)
- Removal of phosphorus glass together with “dead” layer” (highly phosphorus doped sub-surface layer) after P diffusion (before the anti-reflective ARC coating) to increase the blue response and also V_{oc} of solar cells
- Edge isolation (removal of shunts between the front and rear sides) by etching the n^+ layer from the rear side
- Modification of the rear side surface morphology to maximize the light trapping within the cell structure

All these technological approaches were studied and tested with a range of supporting tools for PV wafer diagnostics, optical characterisation, and modelling.

2.1.2 Equipment development

Two types of atmospheric pressure plasma sources are implemented into the prototype equipment for continuous processing of wafers:

- An linearly extended DC arc plasma source with 250 mm working width; the source has been quite positively assessed for high rate rear-side wafer etching but suffers from homogeneity being not sufficient for front-side etching
- Microwave plasma source with 250 mm working width was successfully evaluated for all processes being critical with respect to surface homogeneity, e.g. dead layer removal and front surface texturing

The etching gases (alternatively NF_3 , SF_6 , HCl or COF_2) are introduced into the afterglow plasma region of the reactor.

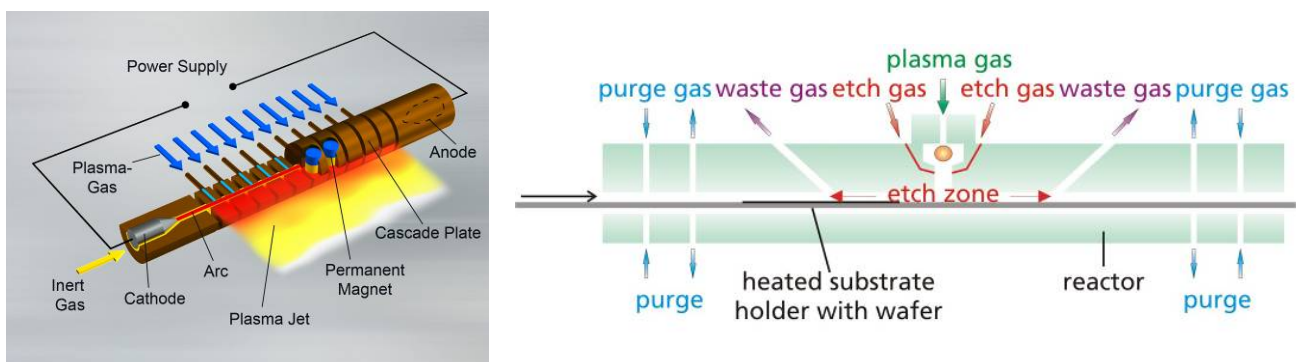


Figure 1: Principle of the linearly extended DC arc plasma source (left) and the plasma-chemical etching reactor for atmospheric pressure operation (right)

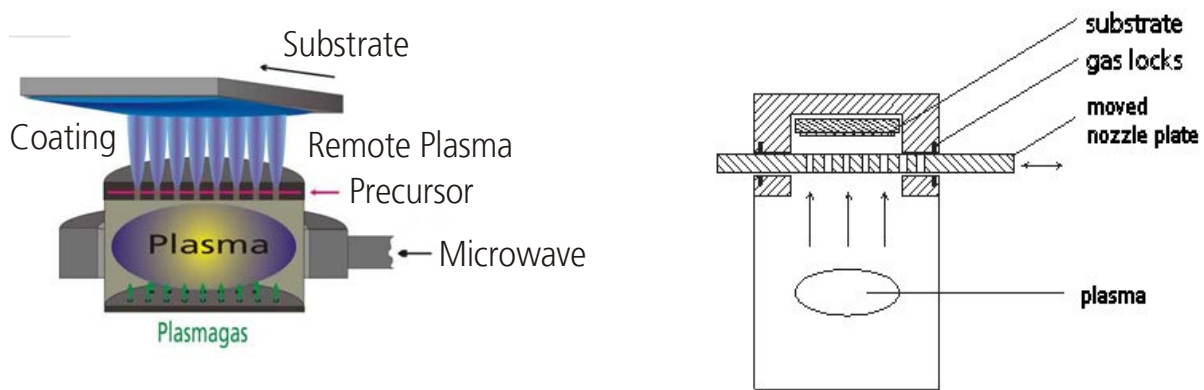


Figure 2: Schema of the microwave AP-PCE equipment (left) and working head with movable extraction nozzles (right)

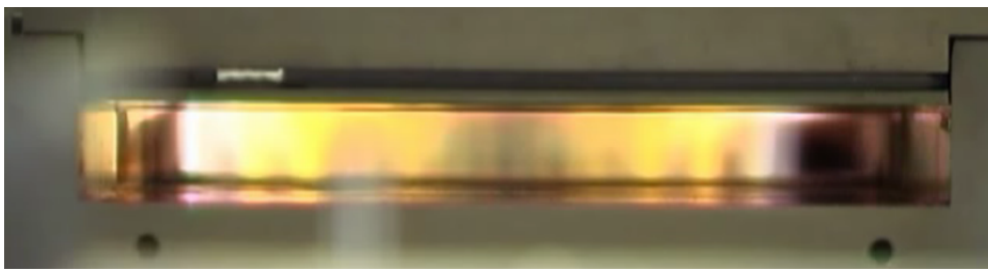


Figure 3: View into the microwave reactor under running conditions with remote plasma operation

The microwave plasma reactor has been successfully used for all etching tests during the last project period. Enhanced etching homogeneity allowed industrial tests for both rear side wafer processing and front side “dead layer” removal. Examples of the sheet resistance maps after application of the front side 3D nano-etching are shown below. Homogeneity of the sheet resistance values is within 10% tolerance being sufficient.

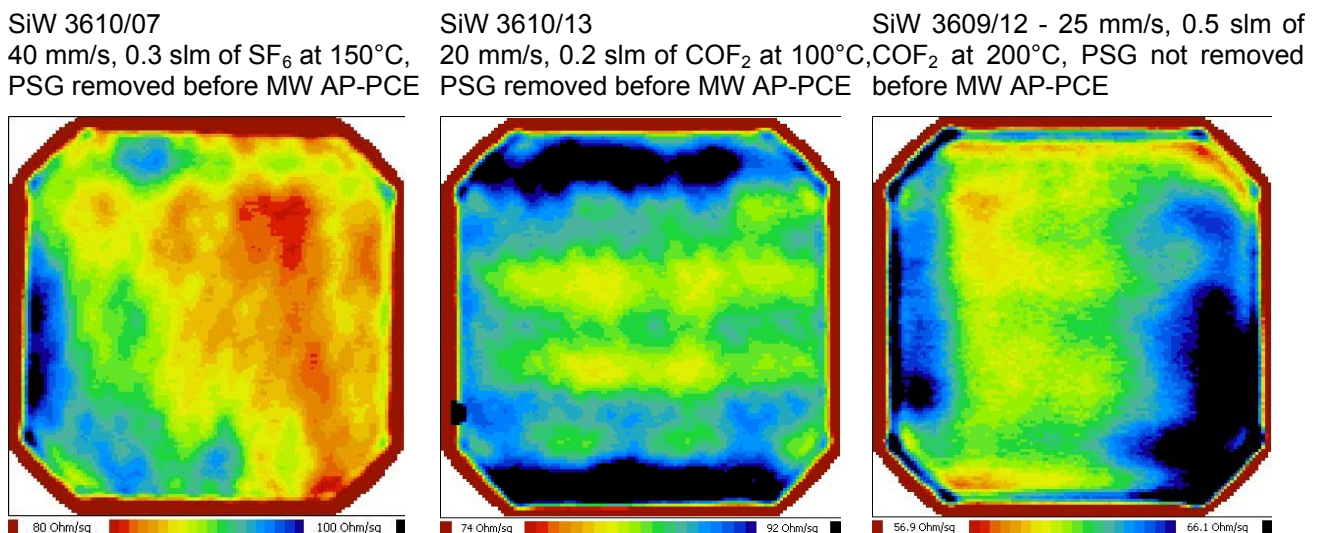


Figure 4: Sheet resistance maps after various “dead layer removal” experiments done in microwave AP-PCE apparatus at different temperatures, wafer displacement velocities and in different etching gases (SF_6 or COF_2)

Prototype AP-PCE Reactor

Aim was the development of an equipment demonstrator for continuous processing of solar wafers by AP-PCE to explore industrial feasibility of the technologies being developed within N2P. Target parameters were:

- Atmospheric pressure plasma sources (DC arc and microwave), working width > 156 mm
- Heat able substrate stage for (single) wafer processing; continues/controllable displacement with velocities up to 50 m/min
- Wafer throughput of up to 1000/h (nominal), depending on etching task



Figure 5: Prototype AP PCE equipment including exhausted reactor cabinet, linear substrate displacement system and gas delivery system –right; AP PCE reactor with DC plasma source –left ©Fraunhofer IWS

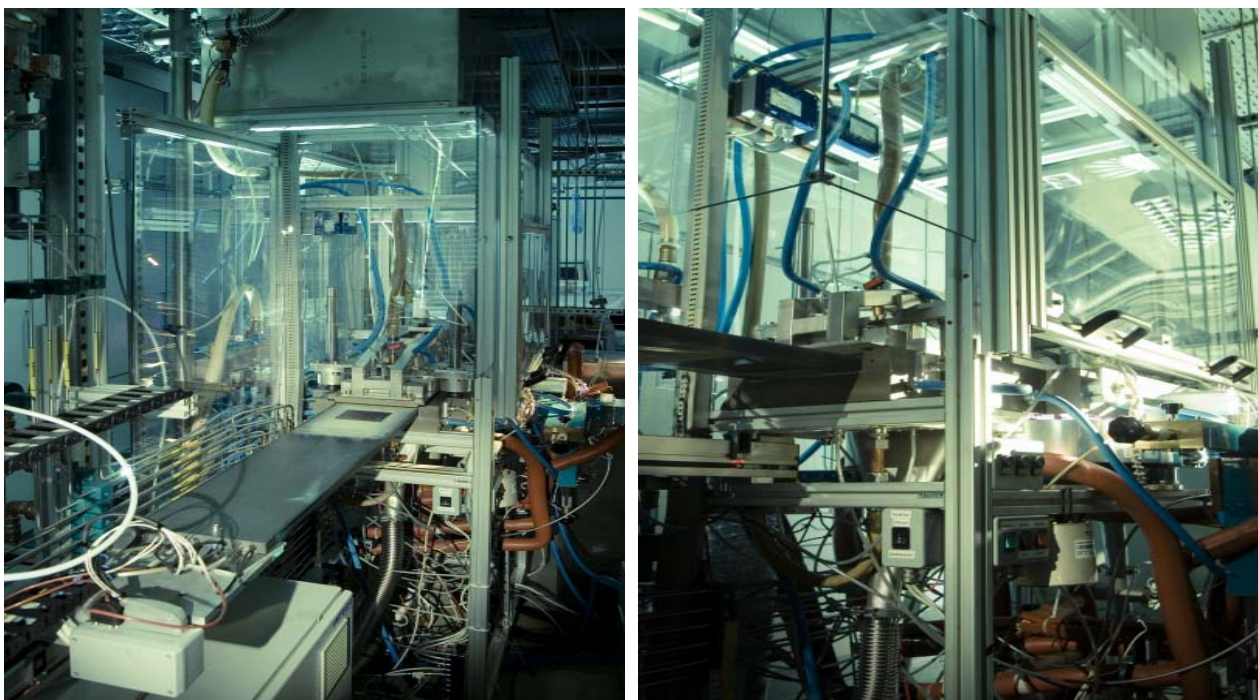


Figure 6: Microwave AP PCE prototype equipment (established outside N2P). Picture of the whole plasma equipment including reactor cabinet, linear substrate displacement system and gas delivery system -left; AP PCE reactor with microwave plasma source-right ©Fraunhofer IWS

Higher etching uniformity and increased process purity in MW APPCE reactor determines the higher exploitation potential for this apparatus. Moreover lower energy consumption for the plasma generation (10 kW of microwave power compared to 35 kW from DC arc) results in a lower thermal budget being absorbed locally within the Si wafer and thus reduces risk for any stress induced materials degradation.

2.1.3 Process development

The AP-PCE technology was applied for c-Si solar cell technology as an alternative process of some standard wet chemical etching steps, namely:

- Front surface texturing; to reduce the total optical reflectance
- Modification of the rear side surface morphology; to maximize the light trapping within the cell structure (mainly for cells with dielectric rear side passivation)
- Edge isolation: removal of shunts between the front and rear sides by etching the n+ layer from the rear side
- Dead layer removal: removal of „phosphorus glass“ (mixture of SiO_2 and P_2O_5) and „dead layer“ (highly phosphorus doped surface layer) after P diffusion to increase the blue response and V_{oc} of solar cells

2.1.3.1 Etching precursors

Four different etching gasses have been tested which were selected as preferred options for c-Si wafer treatment: NF_3 , SF_6 , COF_2 and HCl (alternatively in mixture with O_2 or H_2O). The first two gases are widely used in plasma silicon etching (at reduced pressure), and result in surface structures being distinctly different: etching with SF_6 leads to a smoothening effect where NF_3 creates surface with high aspect 3D surface structure and sometimes inverted pyramids at the Si $\langle 100 \rangle$ surface.

It has been demonstrated that the initially low degree of conversion of SF_6 into the active etching species can be enhanced (from about 15% to more than 80%) by oxygen addition. Furthermore beneficial is that the etching rate of silicon can be increased by a factor of about 4.

Decomposition of both NF_3 and SF_6 in the AP plasma is very high, approaching nearly 100% (for NF_3). This result is beneficial both for economic and environmental reasons: Cost is decreased because of high usage of the (expensive) etching precursors and furthermore reduction of expensive waste gas treatment.

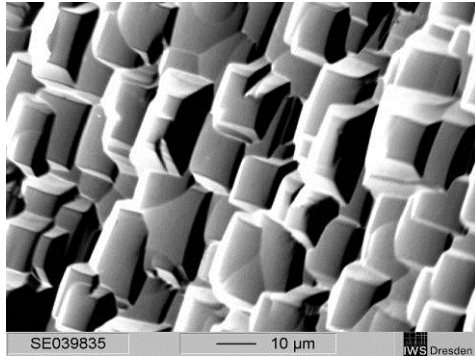
A generic disadvantage for both SF_6 and NF_3 is their “global warming potential” (GWP) which is high. This can be contra-productive for application in PV industry. Therefore the development work was widened out to test a new etching candidate gas – COF_2 , implying a low GWP, equal to CO_2 . Although the resulting surface morphology is different from SF_6 etching the subsequent application oriented tests (rear side etching for “edge isolation”) demonstrate a quite high cell performance when using COF_2 .

A further generic aim of the etching process is to remove metallic contaminations from the surface to increase carrier lifetime. However, this seems not to be possible with pure fluorine based chemistry. Therefore the AP-PCE investigations have been widened out into a combined fluorine-chlorine based chemistry; by introducing HCl and HCl/SF_6 gas compositions. This fluorine-chlorine based etching should lead to higher etching process purity mainly with respect to reducing level of metallic contamination. Furthermore beneficial is, that this etching gas mixture results in formation of surface roughness with a rms value in the order of tens nanometers. As a consequence optical reflection in the visible region decreases, being beneficial for energy harvesting.

2.1.3.2 Front surface texturing

Plasma etching in NF_3 gas results in surface roughening (nano-texturing) of the initial micro-structure. The process is well controllable without any side-reactions.

Wafer 1530, Reference, 45° view, not etched, 1000x



Wafer 1530, position 2 after etching, 45° view, 1000x

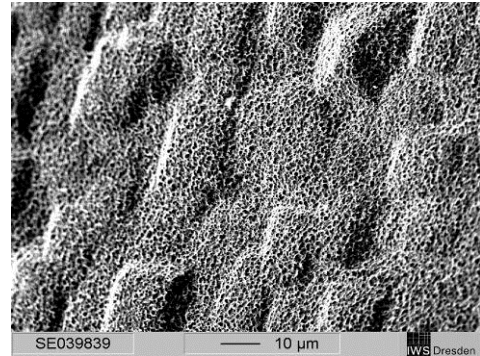


Figure 7: SEM images of wafer 1530 after saw damaged etching in KOH (left) and after plasma-chemical etching in NF_3 (right)

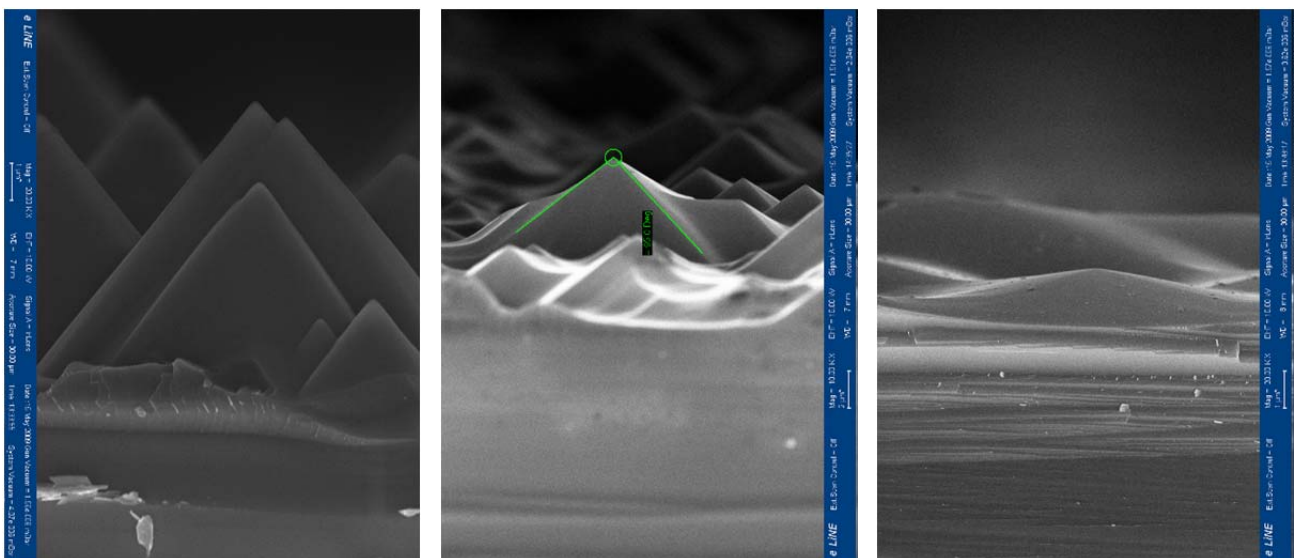


Figure 8: Increase of internal reflectivity of cell structure from 65-70% for standard screen-printed Al to > 90% by adjusting of top pyramid angle of c-Si by variation of gas composition: no etching (left), etching in SF_6 - O_2 mixture (middle) and etching in pure SF_6 (right) © Academy of Sciences of the Czech Republic, Institute of Physics (ASCR)

2.1.3.3 Modification of the rear side surface morphology / edge isolation

Rear side surface modification was realised (in combination with edge isolation) with both plasma generation systems and quite similar results concerning the surface morphology were observed.

We focused our attention mainly to the surface morphology modification by the gas mixture of SF_6 and O_2 which (applied to the Si surface with random pyramids) and NF_3 leads to a pyramid angle modification. For a cell structure with dielectric rear side passivation an optimal back Si morphology can be achieved. Figure 9 shows results of the surface morphology after AP-PCE treatment when pure SF_6 and 1:1 mixture of SF_6 and O_2 was applied. In both cases average silicon removal by etching was about 5 μm; therefore, as an additional benefit, it might be sufficient also for the “edge isolation” (removal of phosphorus doped layer from the rear side). Pre-requisite would be a good homogeneity over the whole wafer area.

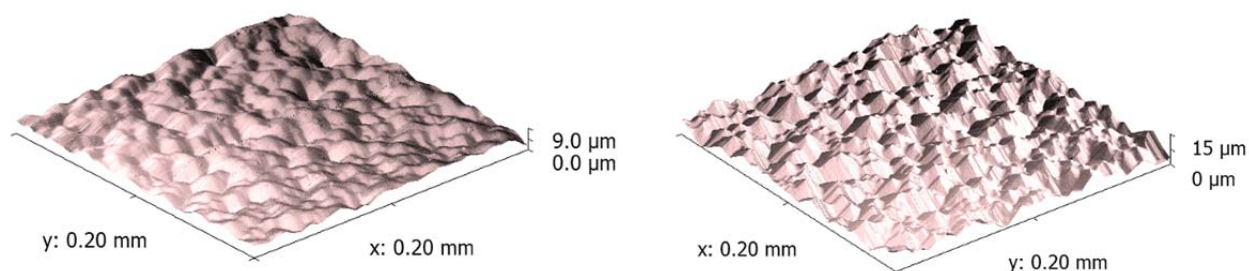


Figure 9: AFM scans of modified rear surface morphology using APPCE method. left - higher smoothing when etching is carried out in pure SF₆, resulting average top pyramid angle is 145°; right - etching result when mixture of SF₆ and O₂ was used, resulting average top pyramid angle is 106°

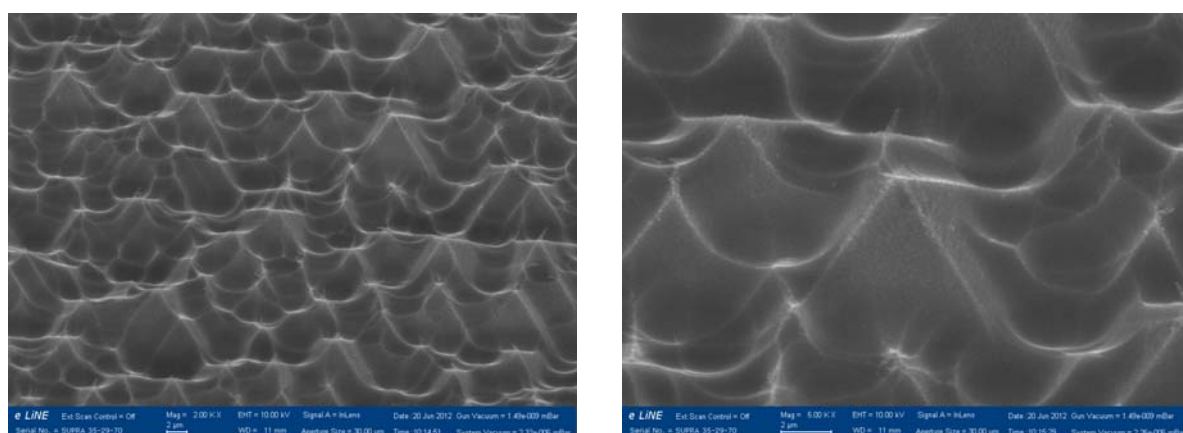


Figure 10: SEM results (2 various scales) of the front surface morphology of Si wafers after MW AP-PCE in COF₂ resulting in “sharpening” of the original pyramidal surface with “flat” valleys between pyramids.

2.1.3.4 Dead layer removal

Removal of “dead” layer is probably the most critical process because requirements for homogeneity of the etching process are high to avoid “over-etch”. Best results were achieved with MW APPCE apparatus and COF₂ as an etching gas.

Etching process is thermally activated: when the substrate temperature is increased from 100 to 200°C, etching rate increases of about 60%, while for a temperature enhancement from 200 to 300°C etching rate increases of about 30%. These values are valid for relatively low flow rates of etching gas (0.2 - 0.3 slm) thus this “saturation” effect can be attributed to the nearly complete gas utilization.

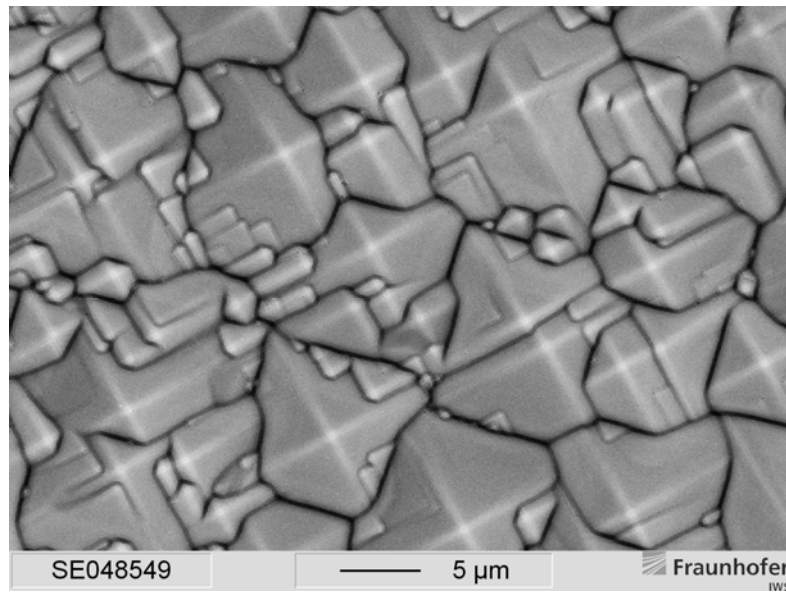


Figure 11: APPCE in COF_2 removes the PSG homogeneously, thus APPCE dead layer removal is possible without necessity to etch the PSG by wet chemistry

2.1.4 PV cell design – influence of surface structure

Key factor towards future high efficiency PV cells is seen in optimizing the light capturing properties. Most of all a well-tuned internal reflection schema should substantially increase light trapping in the near infrared. From physical point of view the topic is quite complex therefore we started at first with optical modelling and subsequently we tried to verify the modelling results by targeted etching experiments. Aiming to derive design rules for optimal optical cell concepts the c-Si solar cell structures were modelled by combined coherent optics and a Monte-Carlo approach. The first modelling results for simple c-Si structures with various surface morphologies (but without any other layer or coating) were verified by T/R spectroscopy, where particular Si surface morphologies after AP-PCE treatment were evaluated by AFM, SEM and by measurement of the angular distribution of scattered light.

After model verification the optical behaviour of more complicated cell structures was calculated. The results show high potential for light trapping enhancement of c-Si structures with modified rear side morphology and dielectric rear side passivation. Moreover, a relative wide acceptable range of pyramid angles on the rear side ($110\text{--}150^\circ$) for good light capture of encapsulated cell structures was identified as crucial for the yield of solar cell production. Higher thickness of the dielectric layer on the rear side leads to a better light trapping effect due to elimination of parasitic absorption of the evanescent wave at the Si-SiO₂ interface. Figure 12 summarizes the optical modelling results of this structure where pyramid angle and thickness of the rear SiO₂ are the key parameters (note, that in this case SiO₂ optical data were used but maybe from electronic point of view Al₂O₃ could even be more beneficial).

- Modelling parameters:
- Angle of incidence Θ with respect to the normal incidence (0, 15, 30, 45 and 60°)
 - Angle of incidence Φ with respect to the pyramid base orientation (0, 15, 30 and 45°)

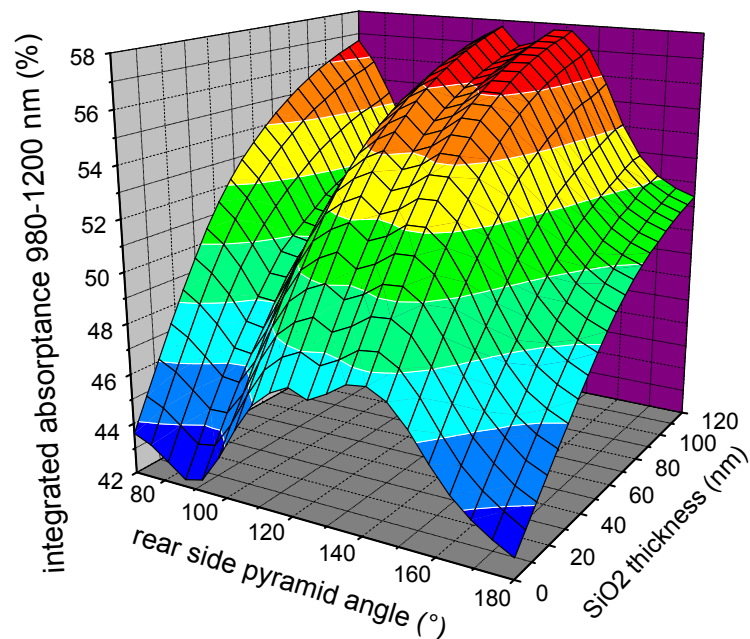


Figure 12: Dependence of the integrated absorbance for all modelled angles of incidence Λ (spectral range 980 – 1200 nm) on the rear side pyramid angle and thickness of SiO₂ layer on the rear side (beneath the Al contact).

Comparison of the modelled results for solar cell structures with dielectric passivation and results of commercial PC1D modelling confirmed the abilities to achieve values of internal reflectivity well above 90% (internal reflectivity of standard screen-printed Al contact is 65-70%). Keeping also the high electronic quality of the solar cell structure into account, e.g. high bulk minority carrier lifetime and low rear surface recombination velocity, we see high potential for an efficiency increase.

Additional economic potential for the researched AP-PCE technologies is seen for the future generation of very thin Si wafers which substantially reduce materials consumption and cost.

Further cell efficiency improvements can be realized by surface structures with selective or shallow emitters. These structures should not only increase the generated current density (known as “blue response”) but also the voltage parameters due to lower front surface recombination velocity. Even higher performance potential has the structure where a shallow emitter is realized from standard or deep emitter by the etch-back process. In this case we need to remove highly doped subsurface silicon layer with a thickness of 15 to 30 nm with the highest concentration of gettered impurities such as iron. These “dead layer removed” structures were realized both by MW AP-PCE, and wet chemistry for reference.

2.1.5 Application oriented tests

Standard product of Solartec (PV end-user) is mat blue c-Si solar cells having conversion efficiency at time of N2P project launch of about 15.0%. As a result of thorough process optimisation as well as with significant contribution of R&D work within the N2P project, conversion efficiency of standard solar cells with screen-printed Al back contact (standard CZ grown silicon) was increased to 18.0 - 18.5% (Spring 2012).

The first application oriented test results with the AP-PCE rear side morphology modification/edge isolation were encouraging. Partial smoothing of the rear side led to a better Al BSF formation and slightly higher internal reflectivity of IR radiation. Best results (from the DC Arc AP-PCE) were achieved when etching was provided by COF₂; leading to efficiency enhancement up to 2 rel.%.

Further experiments were carried out in the MW AP-PCE apparatus to compare the rear side treatment with SF₆ and COF₂. The following table summarizes the achieved results.

group	value of	Isc (A)	Voc (V)	Impp (A)	Vmpp (V)	Pmpp (W)	FF (%)	Eff (%)	Rso (Ohm)	Rsh (Ohm)
standard process	best cell	5.780	0.630	5.570	0.517	2.878	79.0	18.41	0.008	20.7
	average	5.780	0.630	5.532	0.515	2.850	78.2	18.23	0.008	14.3
SF ₆	best cell	5.780	0.631	5.557	0.520	2.887	79.2	18.47	0.008	10.6
	average	5.776	0.630	5.517	0.518	2.859	78.6	18.29	0.008	7.0
COF ₂	best cell	5.709	0.623	5.480	0.513	2.810	79.0	17.98	0.008	8.4
	average	5.681	0.620	5.423	0.509	2.759	78.4	17.65	0.008	6.9

Higher cell performance compared to the reference process was achieved for wafers etched with SF₆ while COF₂ treatment (contrary to the previous similar study realized in DC arc AP-PCE) leads mainly to cell voltage degradation.

A further set of industrial trials was targeting at dead layer removal. Best results were obtained by COF₂ nano-etching being suitable for both PSG removal and dead layer removal. When SF₆ is used as an etching gas then PSG has to be removed before dead layer removal; otherwise a porous structure is formed onto the silicon surface with deeper holes at the places of pyramid edges and valleys between pyramids.

Removal of less than 15 nm of highly phosphorus doped silicon in COF₂ leading to a sheet resistance of 55 to 60 Ohm/sq. (from original 50 Ohm/sq.) results in slight I_{sc} enhancement (+0.4%). When a higher etching temperature is used (200°C instead of 100°C) corresponding to a removed thickness of about 25 nm the increase in I_{sc} is even higher, close to 0.7%.

A further set of industrial trials was focused on advanced PV cell structures with dielectric rear side passivation. More than 3000 wafers in total passed the tests where cell performance was assessed by referencing advanced AP-PCE procedures against standard Solartec's processing. Some AP-PCE treatments are beneficial for the final cell performance but other leads to cell parameter degradation. Here the purity and self-cleaning ability of the etching process plays a dominant role. There is room for further process improvement.

2.1.6 Summary of results

- Feasibility of atmospheric pressure plasma chemical etching was confirmed for all process steps under consideration: front surface structuring, rear surface morphology modification (in combination with edge isolation) and, dead layer removal.
- Combined nano-micro structure substantially increases light harvesting in the near infrared region: efficiencies up to 17.8 % achieved for PV cell structures with conventional Al back surface field (BSF).
- High potential for efficiency improvement (up to 0.8 abs.%) was found for cell structures with dielectric passivation of the rear side after AP-PCE morphology modification; the combined nano-micro structure substantially increase light harvesting properties of the cells (by tuning pyramid angles).
- Throughput target of about 1000 wafers/h have been confirmed for dead layer removal (for one plasma source)
- R&D activities within the N2P project significantly contributed to the standard solar cell performance improvement at Solartec: from 14.5 - 16.0% (at project launch) to the current efficiencies of 18.0 – 18.8%

2.2 WP3/4: Structuring of TCO layers for TF-Photovoltaics

2.2.1 Objectives

The main objective of WP3 is to increase the efficiency of thin film solar cells by introducing tailored 3D nano-structured layers with high light trapping performance, suitable for the next generation of solar cell technology. The aim is to achieve this by deposition of nano-structured TCO films, in a stable reproducible process, and by development of a plasma post treatment process for TCO surface nano-texture modification. The objective is to improve the efficiency of thin film photovoltaics by between 10% and 25% (relative, compared to the use of standard TCO), enabling routes to thin-film PV cells with lower €/Wp manufacturing costs.

2.2.2 Nano-structured TCO films

Transparent Conductive Oxides (TCO) are used for silicon high efficient thin film PV cells, e.g. tandem cells. The coatings have been deposited by Atmospheric Pressure Chemical Vapour Deposition (AP-CVD) from a range of different precursors and co-reactants.

Two materials are investigated: fluorine-doped tin oxide (FTO) and zinc oxide. The former is mainly focused on the effects of the AP-CVD parameters on the fabricated solar cells, while the latter concentrates on the challenges involved producing films of zinc oxide at AP-CVD.

In order to maximize the photo-generated current and cell efficiency in thin film photovoltaic devices, a TCO preferably should have the following properties:

- high diffuse transmittance (TD), i.e. high haze, light scattering
- low free carrier absorption (FCA), i.e. high total transmittance (TT)

In general, an increased diffuse transmittance is obtained by increasing film thickness and roughness. A low FCA is achieved by reduced doping levels. Both properties are controlled by the TCO growth process and need to be carefully counter-balanced to achieve high performing TCO layers.

2.2.2.1 AP-CVD deposition of fluorine-doped tin oxide (FTO)

As part of the activities within this Work Package, fluorine-doped tin oxide ($\text{SnO}_2\text{:F}$) nano-structured TCO films (FTO) have been deposited by AP-CVD from a range of different precursors and co-reactants. These films have been characterized with respect to their optical properties (light scattering, transmission, and absorption) and electrical properties (resistance, carrier concentration, mobility). In turn, the characterisation results from the TCO films were correlated with the results from the fabricated solar cells.

A wide range of parameter variations were provided as follows:

- Variation of deposition temperature for MBTC/TFA derived films
- Variation of growth rate for MBTC/TFA derived films
- Effects of annealing on AP-CVD TCOs.
- Effect of doping level on optical properties

The overall results are summarized as follows:

- Increased deposition temperatures gave lower FCA, improved mobility, slightly higher surface roughness, but higher sheet resistance
- Reduced doping level result in decrease of FCA.
- Growth rate changes caused little difference to the surface roughness, although the morphology became more irregular and variable in feature size as the growth rate increased. Electrical measurements showed, for an increase in growth rate, a decrease in resistivity, along with an increase in carrier concentration and a small decrease in mobility.

- The use of different CVD precursors shows a strong influence on TCO properties. Two precursors were investigated: TTC and MBTC. Opposing trends were shown for resistivity and similar trends with surface roughness. Also, use of MBTC showed trends with carrier concentration, while TTC showed little change. However, although use of TTC still gave higher optical haze the FCA were too high. Due to this it was decided to concentrate on the MBTC derived films as these had the lower FCA which was considered the most important factor for efficiency improvements in PV cell performance.
- Annealing in air established the very high thermal stability of AP-CVD deposited $\text{SnO}_2\text{:F}$, with little to no change in electrical, optical and morphological properties.

TCO-FTO performance assessment by PV cell testing

Solar cells have been produced using these TCOs, and their performance in terms of photo-generated current and efficiency has been compared to commercially available standard TCOs.

The main result from these investigations is that thin film amorphous silicon solar cells with the best TCO, developed by the online AP-CVD process, show an efficiency of 17.5% higher than cells on industrially available online TCO (9.4% cell efficiency for typical project related N2P-TCO compared to 8% efficiency for cells on industrial TCO TEC-8). Furthermore, they are comparable to the efficiency of cells deposited on AGC U-type, a widely used off-line TCO. This is an outstanding result as these off-line products are more expensive and of better quality than their online counterparts. Within this project there is a clear outlook on further improvement of properties towards higher efficiencies.

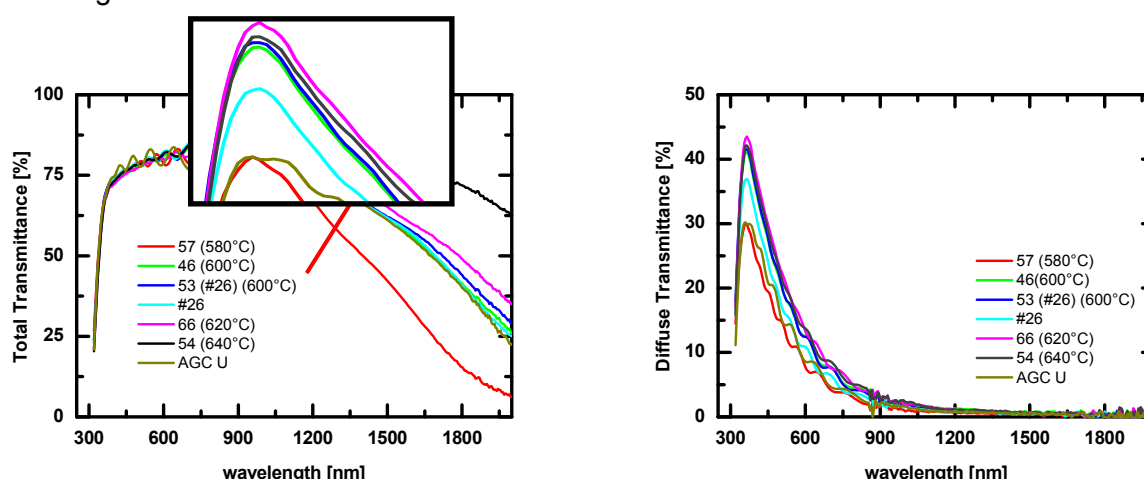


Figure 13: Optical performance of N2P- TCO samples compared to reference industrial TCO. ©USAL, EPFL

AP-CVD deposition of ZnO

ZnO is widely used in TF-PV industry because of excellent electrical and optical properties; e.g. low FCA. In comparison to FTO the drawbacks for ZnO are both high cost (deposited mainly by vacuum methods) and low durability (thermal, chemical, tendency for cracks).

The N2P work is aiming to deposit ZnO by low cost high throughput AP-CVD. A further aim is to control surface structure towards high performing TCO properties.

Growth and Control of Surface Texturing

During project period a number of breakthroughs have been made in regards to zinc oxide growth. Current work is focused onto producing fluorine doped films with high surface roughness. Outlined below is the sequential ordering of developments and the rationale behind the approach:

An initial problem with the zinc oxide growth was the surface topology of the films which routinely produced smooth films with very low roughness values ($\text{rms} = 12 \text{ nm}$). Substrate temperature was shown to contribute a significant amount to the surface texture of deposited films. Process optimisation lead to highly textured growth at 440°C

The next stage was to optimise the doping levels, surface texture and the growth conditions for scaled up operation for deposition onto larger substrate surfaces using one of the newly designed dual flow AP-CVD heads.

The initial work has produced un-doped coatings with high uniformity, while good conductivity could be achieved with doped films. However, the films were unevenly doped, suggesting either uneven distribution of the dopant or fast reaction at the point of precursor entry. Further research and spatial in-situ monitoring of the chemistry round the coating head is required to elucidate these results and hence improvements in deposition conditions.

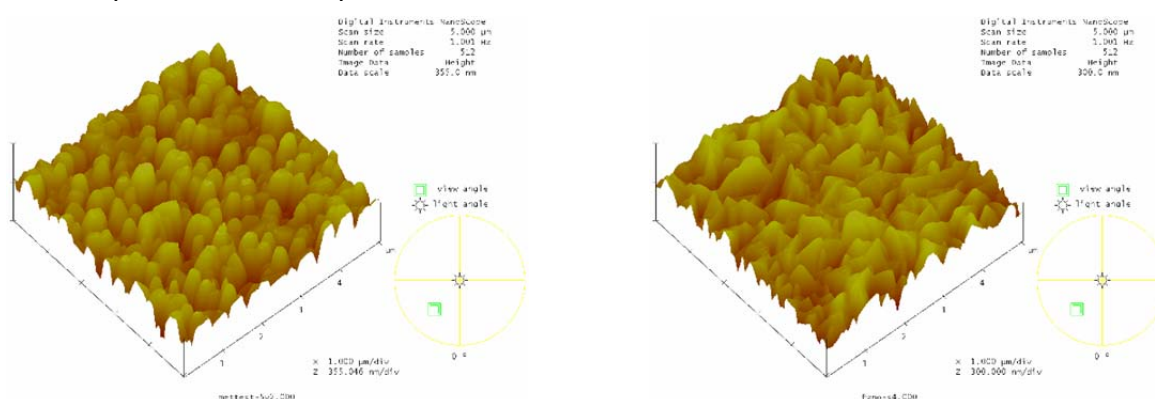


Figure 14: AFM of high temperature AP-CVD deposited zinc oxide; undoped (left); F-doped (right) ©USAL, CTEC

Roll-to-Roll TCO-FTO deposition, characterization, and solar cell deposition

In the existing pilot line for AP-CVD deposition of $\text{SnO}_2:\text{F}$ by roll-to-roll (R2R) at Helianthos, a single injector is used for supply of reactive gases to the aluminium foil substrate. In order to enhance the capabilities of this process and to increase the throughput a second injector and gas supply system have been built and integrated into the existing system. Deposition trial runs with 2 injectors have been performed on the 350 mm wide foil (Figure 15).

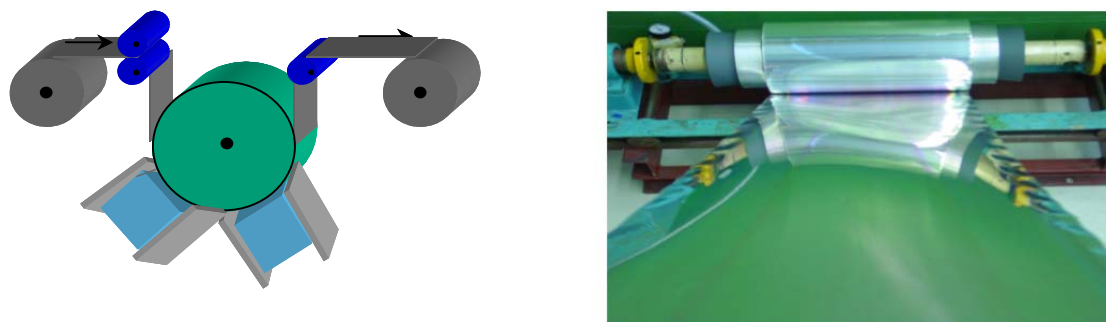


Figure 15: R2R deposition of $\text{SnO}_2:\text{F}$ on 350 mm wide aluminium foil, from two AP-CVD injectors ©Helianthos

Growth from two injectors at increased web speed, gives comparable values for the sheet resistance (R_{sq}), while integrated current (J_{int}) values are lower for the two-injector TCO layers. The surface morphology of the TCO layers has been studied by SEM. All layers exhibit typical surface textures with pyramid-shaped grains shown in Figure 16.

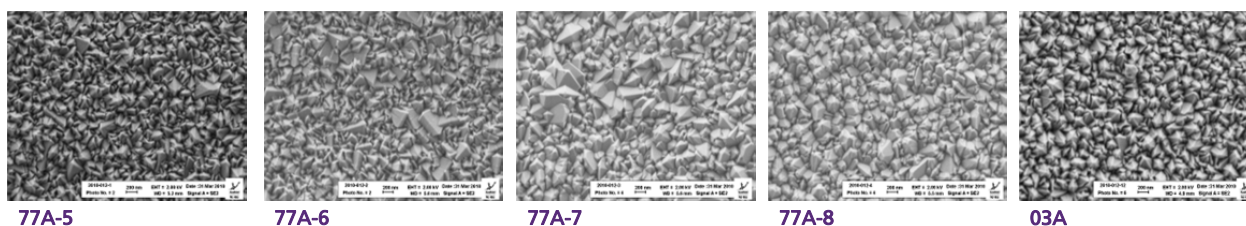


Figure 16: Surface of TCO layers from single injector and 2-injector growth (Type 2 foil, 03A is Type 1 foil) ©Helianthos

From the above results it has been concluded that Al foil substrate roughness has a strong influence on light scattering properties of the TCO, contributing largely to high haze values. Scattering is enhanced by TCO having a pyramid texture. 2-Injector growth appears to produce smoother TCO than single injector. Results of solar cell production have been highly encouraging.

2.2.3 TCO surface nano-texture modification by plasma chemical post-treatment

One approach to deliver tailored 3D nano-structuring of TCOs is plasma chemical etching. This treatment is seen as an optional route (in addition to growth control) toward getting optimised light management properties of TCOs.

The concept is to replace traditional wet chemical or low pressure plasma systems with a low cost, easily integrated and scale-able system capable of continuous inline processing at line speeds compatible with the AP-CVD growth. The etch treatment must provide modification in the <100 nm range, with the objective of retaining or enhancing optical performance whilst minimising the risk of structural defects in the completed cell.

With respect to the development of a plasma post treatment, experimental set-ups for two different atmospheric plasma techniques have been built:

- linear DC arc plasma (FhG-IWS)
- DBD remote plasma (USAL)

The plasma sources have been tested for their ability to modify TCO surfaces. Surface nano-texture modification was successfully demonstrated, as indicated by changes in surface morphology and conductivity measurements.

DC arc plasma etching

Asahi U type $\text{SnO}_2\text{:F}$ samples and also ZnO:Al (AZO) samples have been treated successfully with HCl plasma at atmospheric pressure. Promising results have been obtained at both types of TCO layers with respect to increase in the total transmission and haze. In contrast to the FTO layers, AZO layers were etched at relatively mild conditions. The surface wrinkling measured by AFM (R_a) was app. 20% for $\text{SnO}_2\text{:F}$ and up to 700% for ZnO.

In the case of FTO etching it was found that an increase of HCl flow and plasma energy result in an increased roughness and haze, but also in decreased total transmission and increased sheet resistance. With parameter optimisation it was possible to adjust the etching conditions that haze was improved by 20% whereas the sheet resistance was increased by not more than 7%.

Plasma etching of ZnO:Al is much faster than etching of $\text{SnO}_2\text{:F}$. Already with moderate plasma parameters and with relative low HCl flows a strong etching occur which result in a drastically change of surface structure. With careful parameter optimisation the haze could be enhanced by 52% with only a marginal increase of sheet resistance.

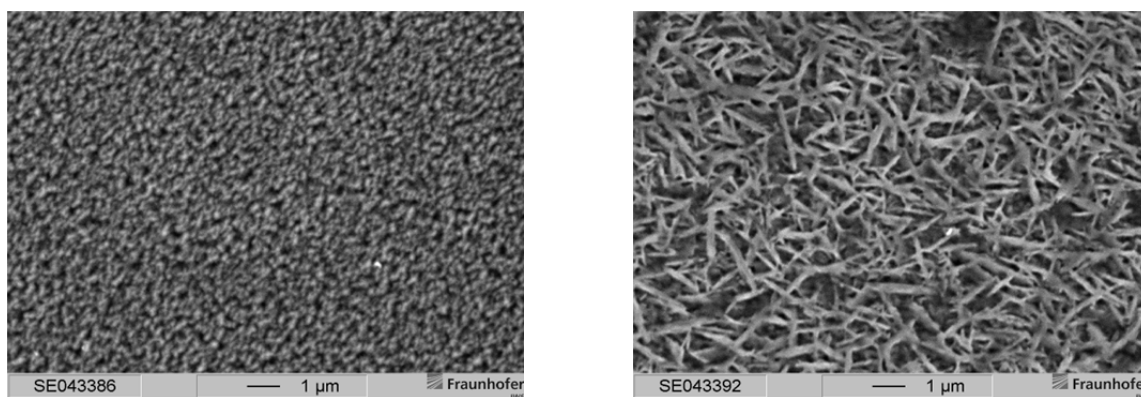


Figure 17: Surface morphology of a ZnO:Al sample (SEM), left: reference, right: after HCl plasma treatment
©Fraunhofer IWS

DBD based plasma etching

The etch system is based on remote DBD atmospheric plasma; both the plasma source and the dedicated ultra-short pulse power supply is described in WP11.

The remote AP plasma etch system proved effective in providing a controllable modification of both F:SnO₂ and ZnO films via adjustment of process parameters, with significant potential to contribute to cell performance. For example, Figure 18 below shows a F:SnO₂ film which was modified using an activated N₂ and HCl gas mixture to selectively expose the larger surface features. It can be seen that the optimised etch process changes the size and distribution of the surface features, apparently preferentially removing the smaller peaks. This results in larger surface structures which may be expected to increase light scattering, with the possibility of reducing interface related defects in the subsequently deposited µc-Si:H.

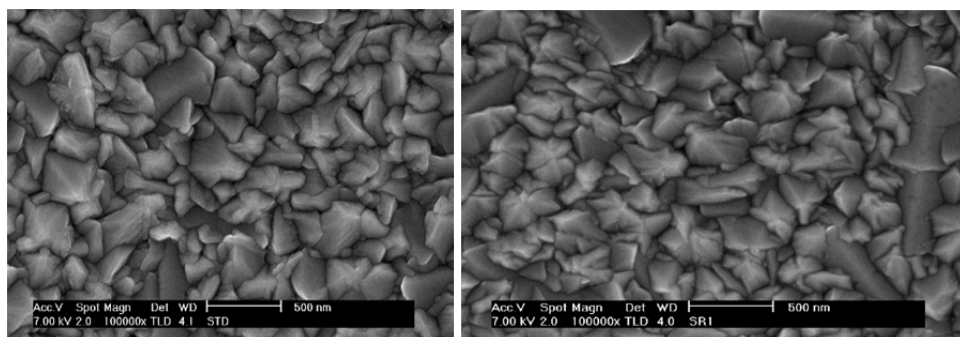


Figure 18: SEM images showing the as-deposited FTO surface (left) and the etched surface (right) ©CTEC, USAL

The ability to selectively remove small sharp features was also observed for the modification ZnO, achieved using only nitrogen, oxygen and water vapour in the process gas mixture.

Optical characterisation exhibits that the changing topography has a drastic influence on the forward light scattering, with clear advantage for photovoltaic performance.

2.2.4 Equipment Demonstrator for TCO deposition by AP-CVD

2.2.4.1 Objectives

Objective for is to increase the efficiency of thin film solar cells by introducing tailored 3D nano-structured layers with high light trapping performance, suitable for the next generation of solar cell technology. The aim is to achieve this by deposition of nano-structured TCO films, in a stable reproducible process.

- Equipment demonstrator for on-line TCO layers on glass
- simulate production scale for both in-line operation and multi-coaterhead approach
- working width for continuous operation will be 100 mm;
- Multi-layer demonstration capability: barrier layer, TCO-multilayer
- Approaches for 3D nano-structuring of TCO layers will be both growth control and plasma chemical etching (feasibility study)
- Deliver samples for PV cell demonstrator: FTO, ZnO
- Application demonstrator for advanced silicon based thin film PV cells on glass
- Size of PV cell demonstrator on glass: 100x100 mm²; size of test cells 40x40 mm²
- PV cell demonstrator for: Amorphous silicon; Tandem cells

A further aim is to establish advanced process monitoring concepts to demonstrate increased process stability and PV cell performance. Two approaches will be established:

- Gas phase monitoring for control of critical reactor parameters
- In-line surface monitoring of TCO layer properties being critical for cell performance (incl. monitoring on heated substrates)

2.2.4.2 Equipment Design and Engineering of the Inline Coater (ILC) Demonstrator System

The main part of the activities has been the design and construction of the Equipment Demonstrator for deposition of fluorine-doped tin oxide (SnO₂:F) nano-structured TCO films by Atmospheric Pressure Chemical Vapour Deposition (AP-CVD). The Equipment Demonstrator had to simulate production scale for both inline and multi-head approaches across a 100 mm sample width.

Novel design head concept was developed which achieved significantly faster growth rates. The uniformity for a 10x10 cm² was best uniformity to date (i.e. +/-5% @ 650 nm film thickness) – highlighting the improvements in cross-ribbon distribution uniformity.



Figure 19: Photograph of the AP-CVD in-line equipment demonstrator system © CTEC

3D nanostructure multi-layer concept TCO-FTO

Building on the progress made in WP3 further work was conducted to develop the TCO properties to optimise for the demonstrator samples.

These samples have been characterised for their optical and electrical properties. These samples were then turned into PV cells.

A range of CVD parameters were investigated with the specific objective of improving PV cell performance:

- Water to tin ratio
- Titanium dioxide interface/index grading layer
- Reduced (further) FCA

The overall results are summarised below:

Water to tin: Carrier concentration decreased with increasing water content. RMS roughness decreased with increasing roughness. The transparency increased with increasing water to tin ratio. Haze also increased with increasing water to tin ratio.

The titanium dioxide layers were thin <100 nm, so showed little effect on the electronic properties. Titanium dioxide on the surface resulted in a 'graded' index design.

2.2.4.3 TCO-FTO Performance Assessment by PV cell testing (mini-modules on 10x10 cm² cell)

Based on the results achieved it was decided to use 10x10 cm² TCO films deposited with two pre-optimised water:Sn ratio and to compare to the industrial online product TEC (AFG) TCO and industrial high end offline standard AGC-U TCO. In order to test the homogeneity of the TCO surface, two approaches were used:

- The 10x10 cm² cell deposition was laser scribed in 20 smaller 1x1 cm² independent cells.
- A full interconnected mini-module was achieved in which each 1x8 cm² segment is connected in series

Sample 271 provided the best efficiency (mean on 20 cells) of 10.75%, with a low result spreads indicating the good homogeneity of the substrate surface. The industrial online standard (to which the TCO is compared for) shows efficiency close to 9.5%.

This corresponded to a relative gain of 13% compared to the industry standard, well above what was expected at the beginning of the project. As a bonus, comparison of the cell data for the sample TCO to the high-end offline industrial sample AGC-U, which is the current state-of-the-art for SnO₂:F (which had a mean efficiency around 10.2%) shows a gain of 5%.

The optical properties of the TCOs are compared to the industrial standards, both online and offline. Figure 24 shows the progress that has been made in exceeding current online and offline SnO₂:F benchmark products. It also demonstrates the significant progress has been made in understanding and controlling the effect of the AP-CVD process parameters on the TCO and subsequent PV cell performance that has been achieved within this project.

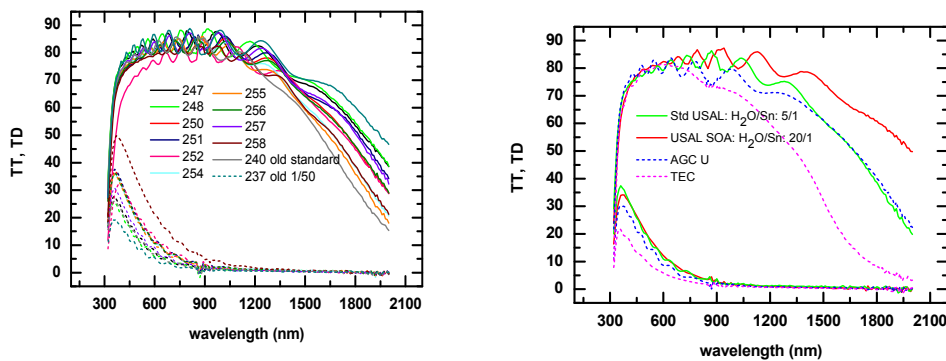


Figure 20: Optical properties of industrial standards and sample TCO films

ZnO Application Demonstrator

Fluorine doped zinc oxide deposition was transferred to a 'dual flow' coater for large area sample preparation. Dimethylzinc, triethylamine, trifluoroethanol and ethanol were used as precursors.

Properties of ZnO:F Films

Un-doped zinc oxide had a preferred orientation of (002), leading to a plate-like structure on the surface. ZnO:F films had a mixture of (200) and (101) phases, Thick ZnO:F films had a single (101) peak, giving a needle-like surface morphology.

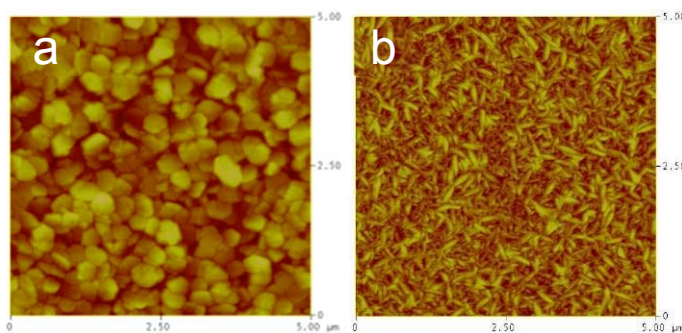


Figure 21: ZnO:F surface morphology for un-doped ZnO (left) and F doped ZnO (right) ©USAL, CTEC

1000 nm films have a sheet resistance of 10 Ω /sq.

FTO / ZnO:F PV testing

The first test samples had a maximum efficiency of 8.9%. Free carrier absorption in the near infrared was too high. For the second sample set, the amount of fluorine dopant was reduced to reduce free carrier absorption. The efficiencies were all over 8%. The reduced efficiency was compared to the first sample set was due to an increase in surface roughness. This reduced the fill factor of the cells. The best cell had a 700/300 nm FTO to ZnO:F structure with an efficiency of 8.7%.

2.2.4.4 Demonstration of Process Monitoring

In order to develop a stable, reproducible process, in-situ spectroscopic monitoring techniques have been developed for integration into the equipment demonstrator. Process monitoring and simulation have been applied successfully to improve the overall efficiency of the AP-CVD process.

Figure 22 shows an overview of the applied techniques. The process monitoring instruments developed during WP11 were used for measurements at the new CTEC demonstrator to monitor

gas phase absorber concentrations. The in-line precursor (MBTC monobutyl tin trichloride) concentration was analyzed with the IR grating absorption spectrometer (IR-GAS) directly after the bubbler and hydrogen chloride (HCl) was measured at two positions in the reaction zone with the NIR laser absorption system (NIR-LAS) simultaneously. The measurements showed the capability of both instruments to detect minor variations of process parameters which have an influence on the process efficiency.

CFD (fluid dynamics) simulation was used to evaluate and improve the coater head design. Based on these results, a contribution from the spectroscopic process monitoring of the gas phase to the improvement of efficiency was evaluated with 5.2 % for an industrial process line.

The optical surface monitoring equipment was installed on the CTEC demonstrator to monitor surface properties. The following part describes how spectroscopic measurements (IR-GAS and NIR-LAS) and optical surface monitoring (Reflection, haze measurements) contribute to an overall simulated process efficiency improvement of 15 % (Deliverable defined as 10%).

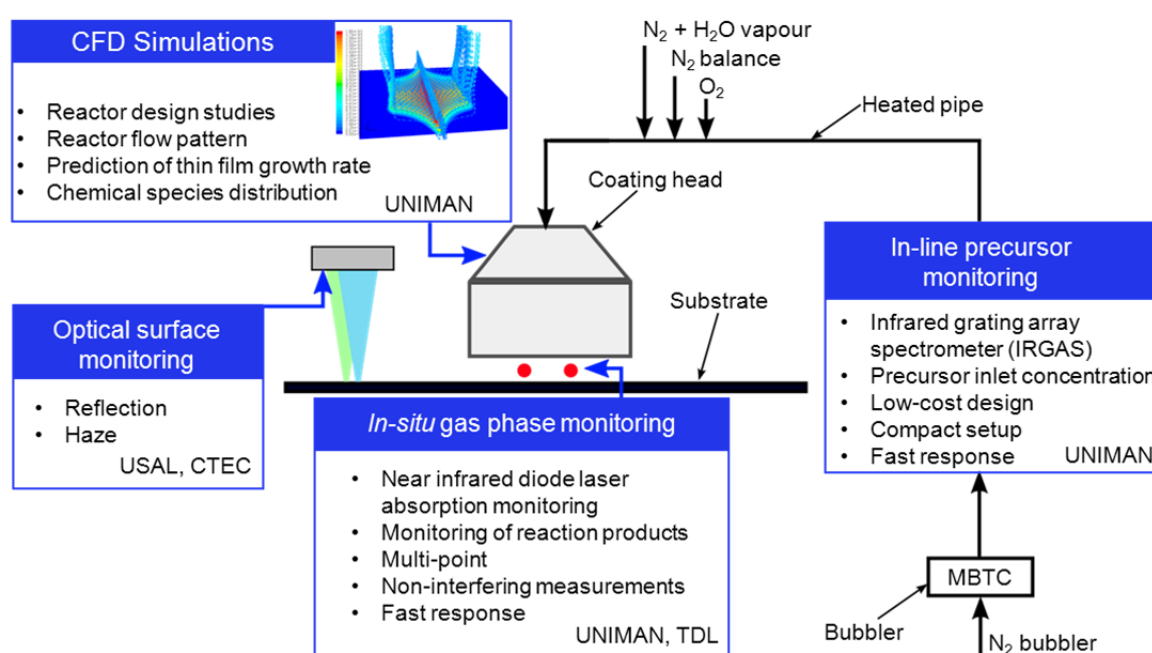


Figure 22 Integrated monitoring concept for improvements to process efficiency ©UNIMAN, CTEC

Combined Online Optics Head for Surface Monitoring

A bench top reflection spectrometer was constructed based on a proven Ocean Optics unit. The system is a 'one side' design, making it compatible with online applications. The system is capable of measuring colour, thickness and refractive index (when combined with CTEC proprietary models/software); for more details refer to WP11/Process monitoring.

Online TCO Monitoring: Software and Modelling

This method for the determination of film thickness and refractive index of thin films on glass substrates requires the measurement of the position and intensity of the first maximum reflection peak. Therefore having taken the sample measurements, it becomes necessary to model these results to determine film properties such as refractive index and thickness. Proprietary modelling software has been developed at CTEC to allow accurate and rapid processing of reflection spectra results. An example of the determination of film properties – based on actual measurements – is shown in Figure 23.

In summary, the processes developed within the model are:

1. Substrate modelled, including n, k & d, and accounts for back reflection – critical for film modelling
2. Calculated models and measured R T values have shown that reliable n d values can be obtained using only reflection data for consistent film/substrate combinations
3. Further development and use of constants related to material properties allows index and thickness values to be obtained for two thin films on a known substrate
4. Model extended to allow characterisation of a three layer system and predict the influence of layer thickness on color

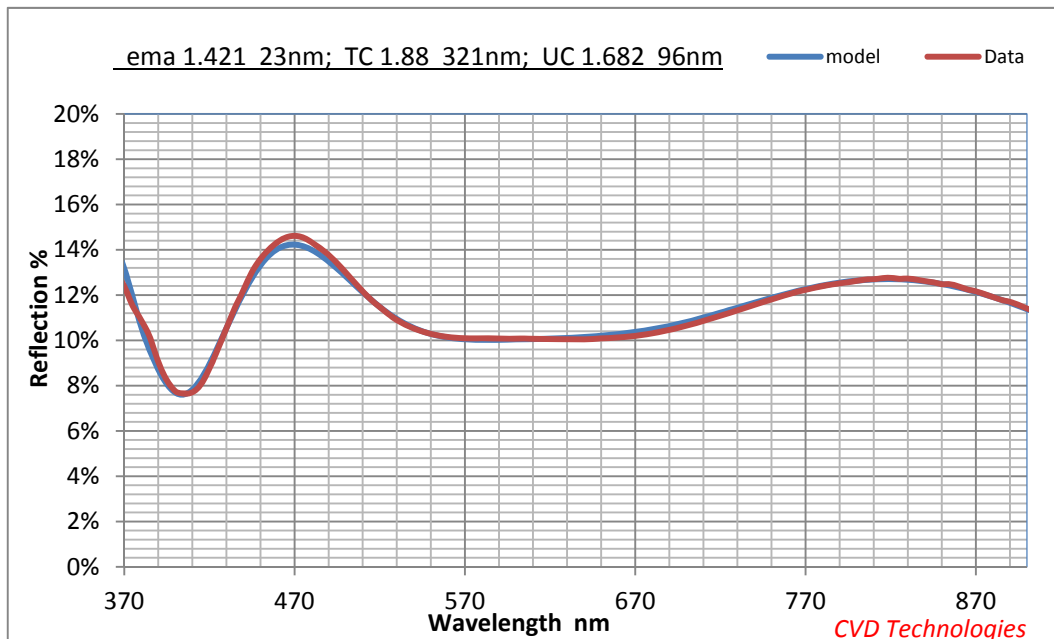


Figure 23: Example of measurements taken using the optical monitoring system to analyse a 3 layer stack © CTEC

Computational fluid dynamic reactor simulation

A 3D model with the dimensions of the lab-scale CVD reactor at CTEC/USAL was built for simulation with ANSYS FLUENT. The model predicts film growth rates and spatial chemical species concentrations.

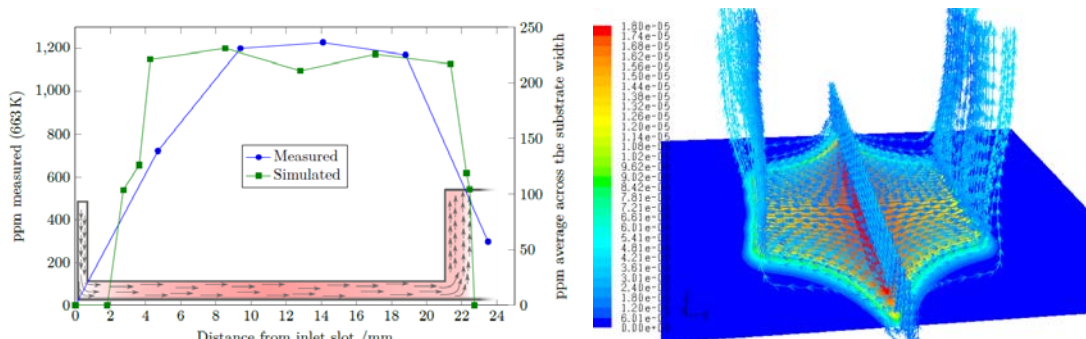


Figure 24: Correlation of simulation and actual measurements (left) and visualization of model (right) © UNIMAN

Computational fluid dynamic simulations have used to characterize a CVD process. It is shown that CFD simulations correctly predict

- Film growth rates (quantitatively)
- Chemical species distribution (qualitatively)
- Reactor flow patterns (uniformity of gas injection and distribution)

Shortcomings in the reactor design have been identified by tracing particle pathlines in the fluid domain of the model. Further, the predicted distribution of HCl in the reactor gas phase was used to identify fixed monitoring points for the NIR-LAS instrument on the CTEC prototype reactor.

2.2.4.5 Process monitoring by FTIR and NIR-DLS

A novel IR-GAS process spectrometer has been developed and the spectral range for its operation has been identified with in-situ FTIR measurements. In-situ measurements were made in the reaction zone of the CVD reactor (stationary coating) with varying process parameters like gas temperatures, addition of water, flow rates and substrate temperatures. Concepts for qualitative measurements with the IR-GAS and NIR-DLS instrument have been established

Optimal sensor positions for the NIR-DLS instrument have been determined. HCl was monitored at 11 equidistant points across the width of a lab-scale reactor coating head. Small amounts of HCl are found under the inlet slot where unreacted precursor gas mix impinges on the substrate surface. After increasing close to the inlet slot, the concentration of HCl reaches a more constant level throughout the reaction zone as the reaction on the substrate progresses. It was found that monitoring near the ends of the reaction zone yields the most reliable measurements of HCl concentration as fluctuations are small compared to monitoring near the inlet. Only small traces of HCl are found at points centrally in the exhaust zone.

Several measurements showed that both measurement instruments can be used complementary to achieve best process control performance. The measurements at the new demonstrator proved the applicability of the developed measurement systems under realistic CVD process conditions.

Simulated improvement in overall process efficiency

Process monitoring and simulation can be used to increase the efficiency of industrial CVD processes. Various measurements at the AP-CVD equipment demonstrator showed the potential of optical process analysis. A transfer of these new process control opportunities to an industrial glass production line allows an estimation of the possibilities in process efficiency improvement.

Two approaches have been reported – gas phase monitoring and optical surface monitoring. The equipment developed has the potential to realized real gains in a float line operating situation. In order to simulate this, the effect of optical surface monitoring on the start-up phase of a coating campaign, and the effect of the gas phase monitoring on the established process operation are simulated.

- A float glass production line with a line speed of 500 m/hour and a width of 3.4 m produces about 13600 m² of glass in an 8 hour shift.
- During the start-up phase the optical surface monitoring has the capacity to save 40 minutes waiting for analysis. Transferring these 40 minutes into production time equates to an increase in 8.3% uptime.
- Once the process is established and running the gas phase monitoring has the capability to increase an average production run by at least 30 minutes. This equates to an increase in uptime of 6.3%.

So overall simulated improvements in process efficiency equate to 14.6%.

2.2.5 Evaluation of results and conclusions for exploitation

The equipment demonstrator has produced sample TCOs upon which mini-modules has been deposited. The stability and homogeneity of the TCO has been demonstrated, with the performance exceeding current state-of-the-art reference TCO. Concept demonstrator samples of ZnO TCO have also been deposited, delivered and had cells made upon the TCO with encouraging performance.

A range of TCOs have been developed, analysed and turned into solar cells during the project. Significant knowledge has been gained in understanding the interplay between the TCO properties and the resulting cell performances. The requirements of the deliverable have been met (and exceeded). Relative increases in haze (greater than 50%) and decreases in absorption (greater than 25%) have been demonstrated. The end result was a cell produced on the project TCO showing a 13% improvement over the commercially available AFG TCO.

Based upon the achievements outlined within the results of WP4 a number of exploitation opportunities have been identified.

1. Manufacturing process for advanced TCO-FTO for integration into floatline applications

AP-CVD deposition and plasma etching treatment processes for production of nano-textured TCO-FTO for photovoltaics, would offer higher efficiency thin film PV modules from enhanced light trapping by nano-textured TCO.

2. Manufacturing process for advanced TCO-FTO for in-line coating of glass panels –

Offering ability to optimise and tune TCO-FTO to best customise and match to individual TF-PV needs via multilayer capability including undercoat + FTO. Option for combination of AP-CVD with plasma etching for production of nanotextured TCO-FTO for photovoltaics.

3. On-line surface monitoring tools (equipment, including software)

Robust process integrate-able fibre spectrometer based system. Designed to be compatible with noisy/dusty/vibration/heat of float glass lines. Customised software developed for application needs.

2.3 WP5/6: Infection control

2.3.1 Process and Materials studies

2.3.1.1 Objectives

Objectives for WP5 on infection control are to develop a highly active biocidal coating and cleaning protocols to allow a minimum 5 year activity in application environment, and a targeted viability count of 5 log reduction in 4 hours in laboratory testing and 3 log reduction in the field. These coatings will exhibit a multi-functionality well beyond current state of the art, i.e. use multiple biocidal actions to act against a wide range of organisms incl. bacteria, viruses, fungi, and bacteriophage that are important in human and animal health and food microbiology.

The influence of nano-structuring on viability will be explored, the developed technology in a real application area such as hospitals, food services and public sanitary areas demonstrated, and research will be linked into studies on hospital infection monitoring.

2.3.1.2 Coating technology for biocidal surfaces

Three processes having been defined which achieve the target activity:

- DBD plasma process (aerosol assisted AP-PECVD)
- Combined hybrid DBD and FA-CVD process
- FA-CVD process

Processes that meet target activity have been defined depending on substrate: FA CVD on ceramic and glass, DBD plasma on steel and plastic surfaces. For the first time biocidal coatings have been produced which combine both high biocidal activity and mechanical durability. The coating technology being applied is inherently scalable.

Low temperature DBD plasma was used for deposition of biocidal coatings. While coatings with intrinsic antibacterial properties could be obtained, bacterial kill rate was not within project targets. Therefore, combinations with antibacterial agents that can leach out of the coating were necessary. Two different approaches were studied:

- Plasma deposition of antibacterial salts dissolved in a monomer
- Plasma deposition of antibacterial nano particles dispersed in a monomer

Best results were obtained by coating silver nitrate solutions in APEO on coated steel. Transparent, homogeneous coatings were deposited that exceeded the project application targets. Combination of flame CVD and plasma DBD coatings show even better results.

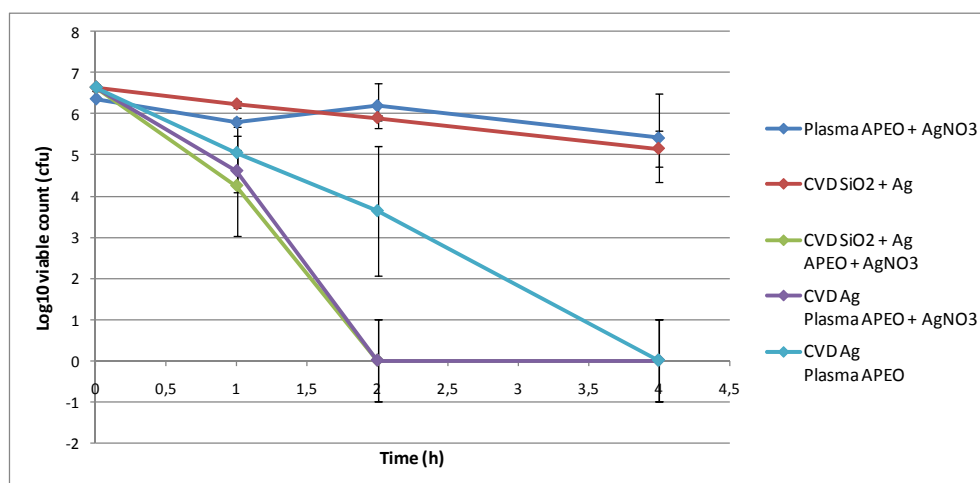


Figure 25: Bacterial reduction of plasma DBD coating, flame CVD coating and combinations © Vito, CTEC

Also deposition of biocidal plasma coatings on structured surfaces was studied. While this did not result in improved performance up to now, different results are expected in real environments, which is still to be tested.

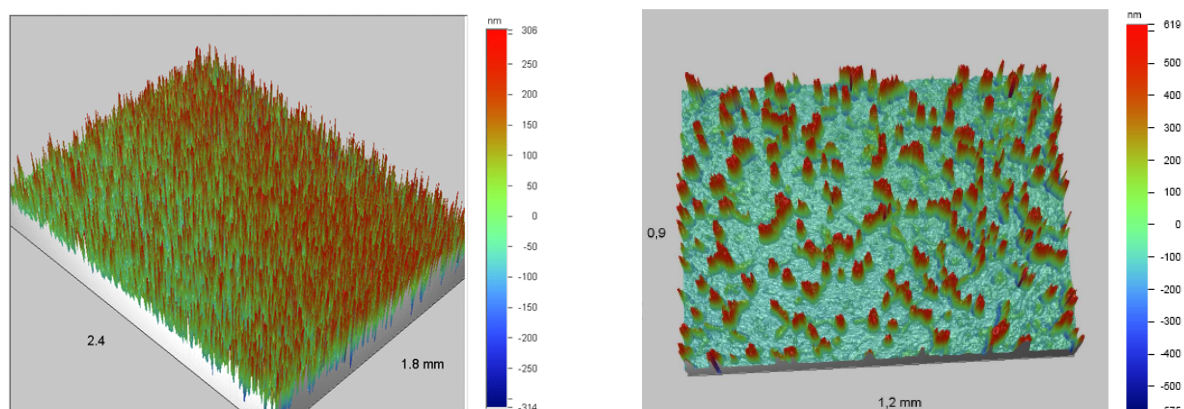


Figure 26: Surface roughness of plasma deposited ODAMO coatings at low (left) and high (right) plasma power.
© Vito

In conclusion the plasma DBD deposition process and the hybrid DBD and FA-CVD combined process have successfully deposited films that exceed the target activity and thus the original objective of the deliverable has been met.

FA-CVD is a cheap and easily engineered chemical process. The heat for activation is provided by the flame and unheated substrates can be used. The films have shown they have efficacy in laboratory tests against all common strains of bacteria. Ag/SiO₂ and Cu/SiO₂ have exceeded the 5 log 4 hour reduction target. The films can coat all metallic and ceramic/glass substrates. Once efficacy is proven in real environment situations the process and chemistry has the potential to be exploited and used in commercial processes.

Highly active anti-bacterial surfaces with nano-meter coatings can be produced by means of FA-CVD. In particular, layered “sandwich” coatings are very active in lab testing. The coating has a very good optical aspect and do not change the appearance of the substrate.

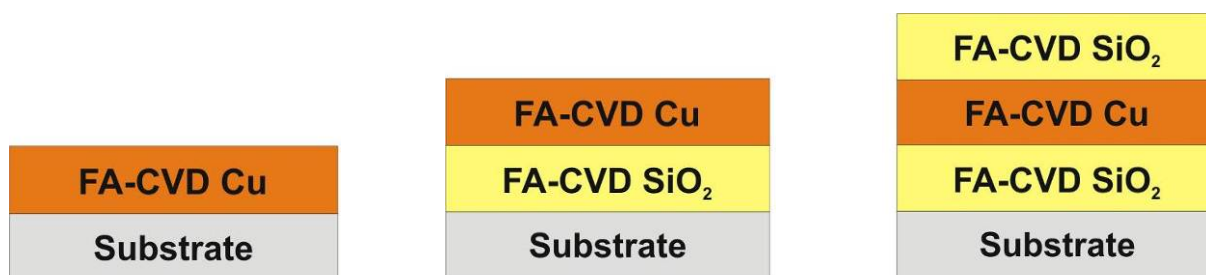


Figure 27: Layer systems that were deposited on top of the substrates © CTEC, OCAS

A start was made to explore the durability of such coating systems. Wash ability testing has been undertaken using a standard cleaning agent used on hard surfaces in hospitals. Durability of the standard film has been assessed. A quality control technique for FA-CVD films has been established to ensure product standardization.

The link between “real application” performance and lab test results are however, not clear. The difficulty lies mainly in the “standardising” of cleaning operations and its influence on bacterial growth. Potential customers/applications generally demand proven anti-bacterial effects, but fail to describe the circumstances under which the anti-bacterial effects should be met.

Screening tests for biocidal activity

The biocidal activity of the coatings was screened against a range of pathogens. This section describes the results of testing for antibacterial activity of coatings against the major objective of a 5 log reduction in viability of standard laboratory test organisms within 4 h. This entailed the adaption of standard test methods for antimicrobial plastics as there are no standard tests for glass coatings.

Photocatalytic films comprising Ag and CuO overlaid with TiO₂ were also tested and showed promising activity. The coatings were sufficiently active to proceed to testing under environmental conditions.

The results show that coatings of SiO₂ with both Ag and CuO had excellent antibacterial activity. The interference with activity caused by the presence of protein was not unexpected as both Ag⁺ and Cu²⁺ will bind to protein. However the presence of protein can be expected in the healthcare environment. For example serum contains approximately 8% protein. However it was possible to overcome this inhibition by increasing the amount of use of higher starting concentrations of Ag and Cu when preparing the films.

The results for the TiO₂ coatings showed that the films had high activity. Although the times for a >5log kill were longer than we have reported previously this is probably due to the lower light levels used for irradiation (10% of previously used levels) and competition for photocatalysis by the organic matter present when the recently introduced BS method for determining photocatalytic antibacterial activity was used. The availability of Ag may also have been reduced by binding to components of the low levels of nutrient broth used for re-suspension. However the results show that the films were still capable of giving a high killing activity within a short time even at the reduced light levels in the test method used. The results from these tests have been published.

Application oriented tests of biocidal activity

Substantial resources were invested into evaluation of biocidal surfaces against pathogens in “real use” situations. The results show that, although the coatings were active against hospital pathogens these were, as expected, in some cases more resistant than standard laboratory strains. One objective was to achieve a 3 log reduction within 4 h. This was met for some but not all pathogens.

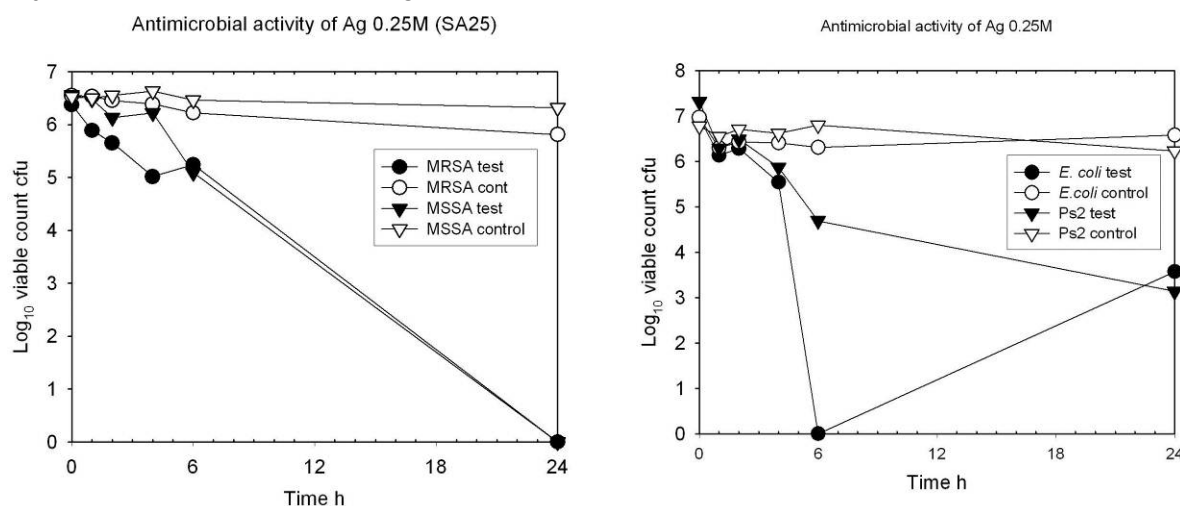


Figure 28: Activity of 0.25M Ag-SiO₂ films against hospital pathogens MRSA and MSSA (left) and Pseudomonas strain 2 (right) © USAL-bio

In situ exposure of coated samples showed further reduction in rate of killing. The reasons for this are not clear but may relate to the type of organisms (e.g. present as resistant endospores rather than vegetative cells) and availability of antimicrobial agents at the surfaces.

There is a need to develop test methods that more closely reflect the *in situ* activity. There was reduced activity which was to be expected as the antimicrobial activity of the films depends on diffusion of the antimicrobial (Ag^+ or Cu^{2+}) from the surface and into the bacteria. This may be expected to be reduced when in the natural environment e.g. of a hospital where the surfaces will be dry. It should be pointed out that the surfaces here were not cleaned in any way. Washing the surfaces, as would happen *in situ*, will remove many of the microorganisms on the surface and may allow further diffusion of ions onto the surface.

The activity of the photocatalytic surfaces against pathogens at the lower light levels used is more relevant to potential real life situations. The hospital related pathogens were more resistant than the standard disinfectant testing strains but were still reduced by 95-99.9% on the surfaces. The Ag-TiO₂ films gave a higher activity in the dark but the Cu(O)-TiO₂ films were more active when illuminated with UVA despite a much reduced photocatalytic activity. It will be interesting to determine the activity of the latter films against hospital pathogens and preliminary results showing visible light activity need to be investigated further.

In conclusion the results show that the antimicrobial activity in situ is reduced compared to laboratory tests. The reasons for this are not fully understood. Furthermore there are no standard tests for antimicrobial activity that replicate in situ use. However the activity is sufficient to warrant further long term testing in hospital and other environments and further development of test methods is required.

The difference in activity of biocidal films in laboratory and real environments has not been truly investigated by any parties and as such the results will be state-of-the-art and of great significance to a wider audience.

2.3.2 Application demonstrator for infection control

2.3.2.1 Objectives

Aim is to develop demonstrators to confirm activity of coatings in real life application areas and develop appropriate test methods for application areas:

1. Equipment demonstrator: Development of an equipment demonstrator for coating of test panels of (minimum) size 200 mm x 300mm to show the capability for future scale up potential.
2. Application demonstrator: Development of materials demonstrators to confirm activity of coatings in real life application areas and development of appropriate test methods for these areas. The methodology will involve small scale sample exposure to multiple environments, sanitary, hospital, food, complemented by a larger scale exposure in a field environment such as a sanitary facility and a showcase application in a purpose built house environment.
3. Road mapping exercise: Preparation of a literature review and reporting to inform wider scientific and industrial communities with respect to the application potential of biocidal coatings in real life environments. Identification of knowledge gaps and barriers to exploitation (e.g. ethical approval), set-up decision trees, conclusions and recommendations for way forward for exploitation

2.3.2.2 Equipment demonstrator

A DBD plasma equipment demonstrator for deposition of nano coatings with antibacterial properties was established at VITO. The equipment was originally planned to be able to treat samples up to 200 mm wide and about 300 mm long (A4 size). The final DBD plasma demonstrator system is able to treat samples of 300 mm with up to lengths of 1.2 m.

The system has a fixed plasma reactor and a moving substrate holder which are positioned in a ventilated hood with electromagnetic shielding to ensure safe operations. (Figure 29) The substrate holder is able to move at speeds from 1 m/min up to 50 m/min and the number of treatment passes can be freely selected.

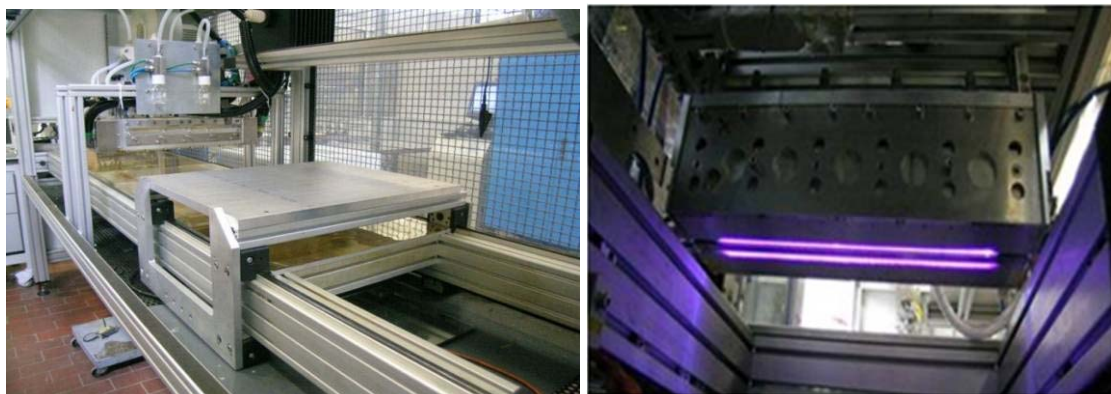


Figure 29: Hybride DBD (aerosol assisted) plasma equipment demonstrator system ©VITO

The DBD plasma demonstrator system is able to use a wide variety of gas mixtures and allows the injection of liquid or dispersed chemistries in the form of nano-sized aerosols by means of pressure atomization. Uniform coating deposition has been demonstrated as well as continuous stable operation over more than 24 h.

The demonstrator system has been used for the production of antibacterial coated A4-sized pre-painted steel panels for application demonstration in medical environments in WP6 and for interface adhesion improvement of lacquered steel based composite panels in WP10.

2.3.2.3 Application demonstrator

Application demonstrators have been constructed to confirm activity of films in real life application areas. Lacquered steel test samples of 0.2 m by 0.3 m have been coated on the DBD plasma demonstrator system for application trials.

Three such demonstrators have been constructed and FA-CVD or DBD plasma test panels introduced. The areas being two environments in a hospital, a female toilet facility and a bathroom in a purpose built house for material development analysis. Humidity in the bathroom can be changed allowing performance in different environments to be assessed. Test methodologies have been developed to allow in-situ testing in application areas



Figure 30: Field test in application areas: Gastrointestinal Surgical Ward 37 (Sluce Room)/Site 2 –left; Renal Ward 12 (Sluce Room)/Site 1 –right © HPA, USAL-bio

Results on Durability / Adhesion / 'Washability' testing

In parallel to the field tests and in-use activity tests in toilet and hospital environments, a preliminary washability test protocol was developed in order to assess the durability and washing resistance of antibacterial coatings. A practical usage of anti-bacterial coatings requires them to be active during soiling and/or to be able to withstand cleaning cycles. In real life, guidance on cleaning procedures and specifications (type of sponges, cleaning agents, cleaning frequency) for coated parts and sheets is often missing and, consequently, wash ability test results can be hardly compared.

A test methodology was set up for washability tests on ceramic tiles. By using abrasive sponges, it was possible to remove the SiO_x/Cu layer in a controlled way. This type of sponge (with and without additional weight) was selected to remove various amounts of Cu from a set of tiles (LOW, MEDIUM, HIGH). After the washing tests, these samples were sent for bacterial testing.

Washing will result in coating removal and/or leaching of the bioactive compounds. By means of a washability tester, the amount of bioactive compounds, e.g. CuO in SiO_2 layer, was reduced in a controlled way by rubbing with an abrasive sponge wetted by 5% Mr.Proper cleaner. Afterwards, the biocidal behavior of the washed samples was evaluated for the reduced amounts of Cu. An abrasive sponge was selected to accelerate the washing process.

In real life, the use of abrasive sponges is not encouraged as the silica based bioactive coatings are easily removed by the hard abrasives on the surface of the sponges. Cleaning of bioactive coatings by means of soft sponges fits better. Although high washing resistance was shown for silica based films when rubbed with soft sponges (up to 20 000 rubs), the Cu compounds were slowly leached out the silica matrix.

The following washing conditions were selected:

- **LOW** Cu removal (test 1): 100 rubbing cycles with abrasive sponge without additional load (Cu removal between 24 and 46 %)
- **MEDIUM** Cu removal (test 2): same as test 1 + 500 additional rubbing cycles with abrasive sponge and additional load of 335 g (Cu removal between 56 and 68%).
- **HIGH** Cu removal (test 3): same as test 2 + 400 additional rubbing cycles with abrasive sponge and additional load of 335 g (Cu removal between 65 and 100%, quite high deviation in XRF quantification due to low Cu signal).

Although activity was greatly reduced for the highest intensity washing there was still residual antimicrobial activity giving a 2 log₁₀ reduction (99%) after 24 h (Figure 31). Lower intensity washing cycles did not reduce the activity as much and a >5log₁₀ kill was achieved after 24 h.

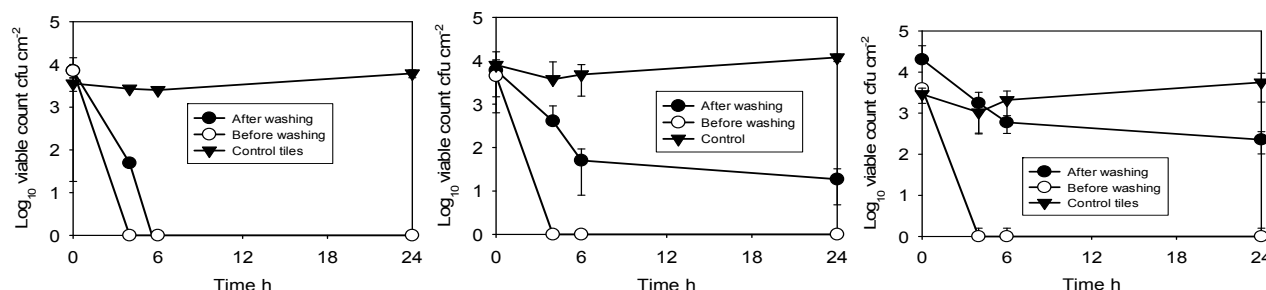


Figure 31: Effects of washing on antimicrobial activity of coated tiles - Low wash (left), medium wash (middle), long wash (right) © OCAS, USAL-bio, CTEC

Activity against hospital pathogens

Significant progress has been made towards the evaluation of the activity of the coatings against pathogenic bacteria of current importance in hospitals and in evaluating novel test methods. We

have tested the activity of three types of coating, CuO-TiO₂, CuO-SiO₂ and Ag-SiO₂ against a range of pathogens.

Although coatings with CuO-TiO₂ showed promising activity against pathogens and some evidence for visible light induced photocatalytic disinfection activity there were problems with durability of the coatings which requires further fundamental studies in the CVD parameters to optimise the coatings. The work so far has been published¹.

Activity of the Ag-SiO₂ coatings was also promising but the activity was greatly inactivated by the presence of protein and although the inhibition could be overcome by increasing the amount of Ag in the film this had an adverse effect on durability.

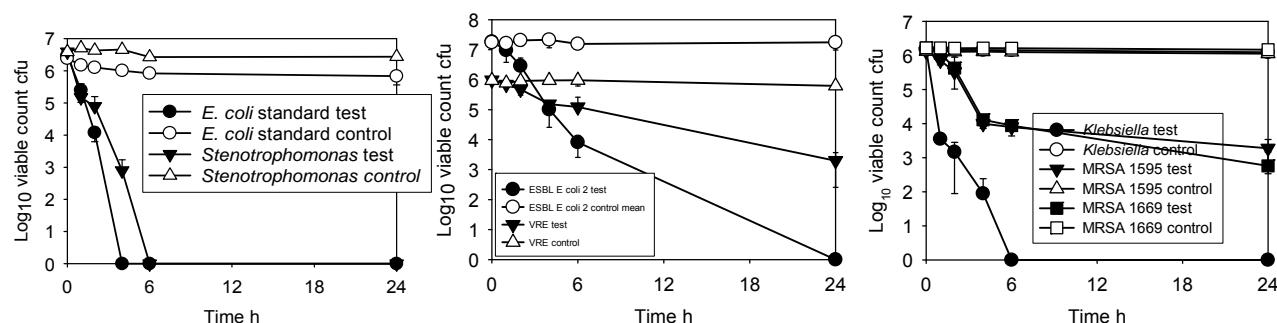


Figure 32: Activity of Cu-SiO₂ coatings against hospital pathogens

The CuO-SiO₂ coatings had promising antimicrobial activity giving a 5 log₁₀ reduction in standard test organisms and at least a 2 log₁₀ reduction in even the antibiotic resistant pathogens such as MRSA, VRE and ESBL-producing Gram-negative bacteria within 24 h (Figure 32). Because of the good antimicrobial activity and their reduced cost compared to Ag-based coatings Cu-SiO₂ coatings were used in tests of in use performance.

There are no standard tests to determine *in situ* activity of antimicrobial coatings. We have investigated a number of methods for determining this performance. Firstly coated tiles were placed in the sluice rooms of two hospital wards at St Mary's Hospital, Manchester, UK. Secondly, test samples of coated glass, ceramic tiles and steel were placed in a toilet facility at the University of Salford.

DBD plasma coated samples were evaluated together with CVD coated samples in a field application tests. The results show consistent reduction in contamination for the first 4 months on the coated tiles and glass. After 6 months the tiles were cleaned with soap and water. This left residual contamination and a high level of contamination which slowly reduced over the next two months.

The tiles were then thoroughly cleaned which reduced the overall contamination and the test tiles once again reduced the contamination compared to the controls. These results show that activity can be maintained although the activity may be inhibited by soiling.

Thirdly, samples were contaminated with hand prints to determine the potential for suppression of transfer of infections by hands. In these cases the coated surfaces together with uncoated controls were contaminated by naturally occurring microorganisms as were samples using a swabbing protocol. Finally samples were contaminated with test cultures under conditions of controlled temperature and humidity in a showcase test facility at The University of Salford.

The results confirmed that the antimicrobial activity seen in laboratory tests was maintained with significant reduction of levels of microbial contamination for all tests.

The results show consistent reduction in contamination for the first 4 months on the coated tiles and glass. After 6 months the tiles were cleaned with soap and water with the intention of removing the

¹ Foster *et al.*, 2012 Antimicrobial activity against hospital-related pathogens of dual layer CuO/TiO₂ coatings prepared by CVD, Chem. Vap. Deposition 2012, 18, 140–146

high levels of contamination in order to determine whether the tiles were still giving antimicrobial activity. However this left some residual contamination which had spread from the control to the test tiles. Although this slowly reduced over the next two months it was decided that a thorough clean was necessary. The tiles were then cleaned and rinsed with sterile water which reduced the overall contamination back to starting levels and all the test tiles once again reduced the contamination compared to the controls over the next three months with the exception of the VITO APEO+CuSO₄ samples (Figure 33). These results show that activity can be maintained although the activity may be inhibited by soiling

VITO APEO coating

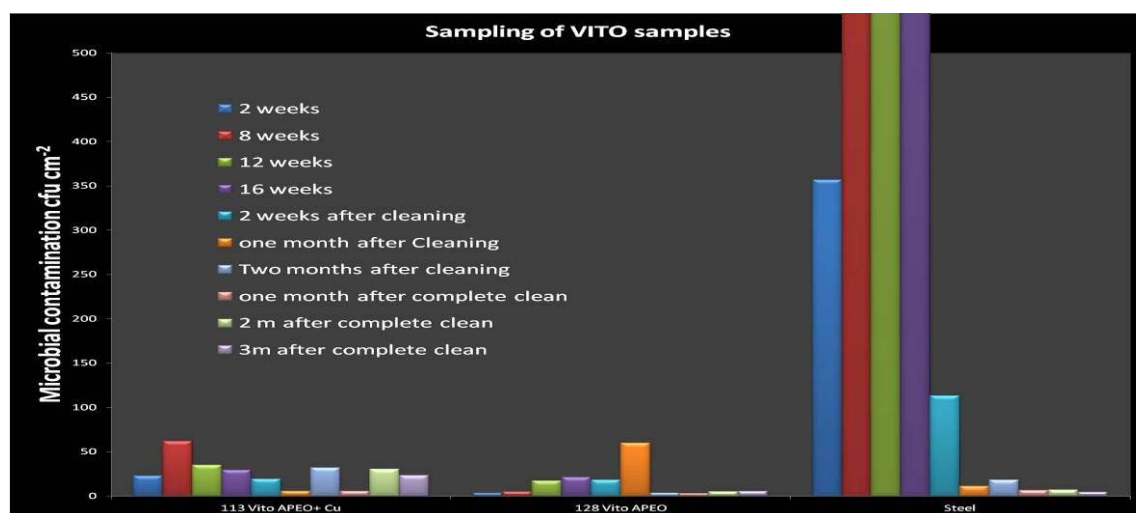


Figure 33: In use testing of coated tiles and steel in toilet facility © USAL-bio, Vito

The test tiles in the hospital continue to perform well. Overall levels of contamination were lower than on previous occasions in Ward-37 after 8 months (Figure 34). Both test tiles had lower total contamination levels than the control tiles. The test tile next to the bench had more staphs than the control tile but the staphs on the tile next to the sink were undetectable whereas they were present on the control tile. Contamination will be a random event and this type of result is not unexpected. No enterococci were detected on this occasion. The results suggest a larger scale trial would be worthwhile.

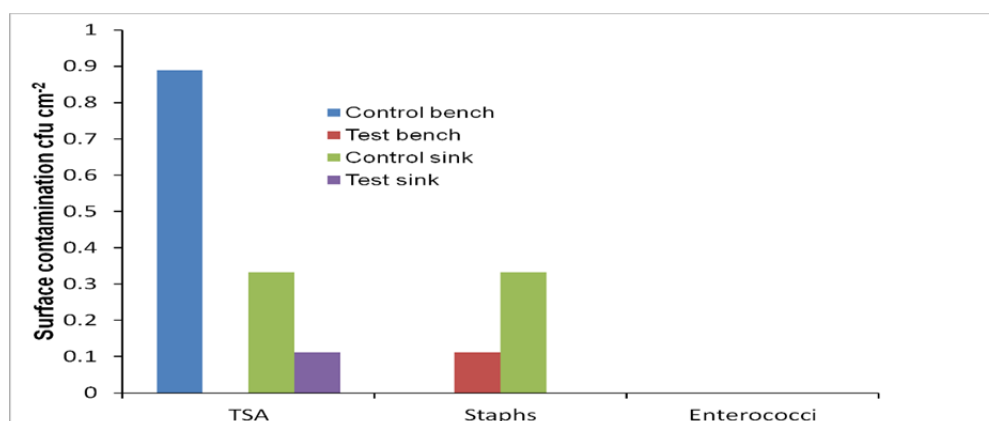


Figure 34: Performance of tiles in the sluice room of Ward 37 at St Mary's Hospital, Manchester UK after 8 months

The effectiveness of the antibacterial coating was evaluated by following up the colony forming units per square cm over time. The results show a very good performance, even upon cleaning. Evaluation of DBD plasma coated samples in application tests in real life environments (sanitary facility) show a strong (3 log) reduction in colony forming units which clearly demonstrates effective biocidal properties.

2.3.3 Road mapping exercise

The purpose of the road mapping exercise is to inform wider community and fill knowledge gaps and to conclude and make recommendations to the way forward through to exploitation. Exploitation is dependent on a number of factors which are beyond the control of the project such as ethical approval for health care application and affect of coatings on infection control not just bacterial load reduction.

- ⇒ Roadmapping is going to be prepared as a separate document which can be downloaded from N2P webpage

2.3.4 Evaluation of results and conclusions for exploitation

From evaluation of the state-of-the art for “Infection Control” and re-assessing exploitation potential we have gained the following conclusions:

- The main advantage of CVD deposited anti-bacterial coatings is that they are more easily cleanable than traditional anti-bacterial coatings employed in industry and hence should be more active in “real life” situations. Also, the nm-scale coatings are optically less noticeable than current anti-bacterial solutions. Currently employed anti-bacterial coatings are mainly based on anti-bacterial agents being dispersed in organic or silicone polymers of the coating have a thickness in the μm -range.
- The hydrophilicity of the FA-CVD coating makes the removal of e.g. sunflower oil with “wet” cleaning easier compared to polymer based surfaces, such as polyethylenoxide, polyethyleneimine and polypropylene.
- It has become increasingly clear that biocidal property alone needs to be supported by end-user focused benefits e.g. reduction in infection transfer. One example referring to our original key application area “Infection Reduction in Hospitals” may demonstrate the underlying changes in expert’s thinking: these are the “Design bugs out” and Healthcare Associated Infections Technology Innovation programmes of the UK Department of Health. There is a clear potential for our coatings to be incorporated into both of these initiatives but the true potential for suppression of infections will need to be clearly demonstrated as well as potential cost benefits. Significant further work is needed (and is indeed underway externally) to explore this and we anticipate multiple reports being available during the next 1 to 3 years.
- The relevance of the testing protocols used is unclear. We sense a clear need for developing certified testing procedures being application specific. A real demonstration of beneficial effects of antimicrobial surfaces in reduction of infection rates in a hospital environment would be a very resource intense task which clearly goes beyond N2P.
- Exploitation potential is compromised and slowed down by lack of this (and other) information. Whilst there are potential niche applications in shorter term, the large area / large volume market exploitation will require more substantive evidence of efficacy and at least a supported testing protocol which gives confidence.

Risk factors which may influence exploitation

- One major obstacle for widespread adoption in the Healthcare sector is that, because of the cost of installation, it will be necessary to demonstrate not only a reduction in levels of environmental contamination by pathogenic organisms but also to demonstrate that this leads to a reduction in infections. This will require extensive further studies (see roadmap).
- The publications that show reduction of levels of microbial contamination by use of copper and copper alloys on frequently touched surfaces (e.g. tap handles, door handles, door push plates, bedside locker drawer handles) in hospital wards demonstrate that there is a role for antimicrobial surfaces in reducing environmental contamination. Copper and copper alloys are already well established for this and it will be difficult to compete with

this. However, we envisage that the coatings developed in the project will be complementary to these rather than direct competitive products especially as they provide alternative materials to copper and copper alloys namely coated glass, ceramic tiles and steel. A combination of these products should further reduce levels of environmental contamination by microorganisms and have a positive contribution to reduction of transmission of infections

- The main concern of potential customers with respect to the proposed anti-bacterial coatings are the durability of the latter, since they are of nm-scale. The total amount of bactericidal agent present in the coating is limited in comparison to polymer-based systems.

Exploitation of results is seen in different directions:

- Exploitation via mass produced parts from steel with improved performance/functionality
The steel industry considers the following applications for biocidal coatings:
 - application in heating, ventilation and air-conditioning (HVAC)
 - application in the area of pre-painted steel. For the high end market white goods (e.g. fridges), there is interest if the coatings are optically transparent.
 - for stainless steel, biocidal coatings can be marketed in the field of food applications; in parts that are currently cleaned by antiseptic solutions.
- Equipment (+process) for in-line coating of biocidal surfaces (Vito, CTEC)
- A major route for exploitation is envisaged through use in the Healthcare sector (see roadmap)
- Exploitation for reduction of infection in other areas e.g. both public bathroom and toilet facilities.

2.4 WP7/8 Energy storage

Double layer capacitors (DLCs) are seen as key components for energy storage systems, e.g. for economic hybrid electric vehicles. Due to their high power density and outstanding cycle stability, as compared to batteries, DLCs are advantageous in applications like energy recuperation from braking. However, comparatively low energy density and high costs limit their application and performance improvement is required. Within various possible electrode materials, vertically aligned carbon nano-tubes are expected to provide many advantageous properties towards next generation DLCs due to their unique structure and their electrical properties. However, production cost and unsuitable substrates are currently seen as barriers for supercap applications. The DLC components envisage a high market potential and high societal benefit, if they can be manufactured in a cost-efficient mass production.

2.4.1 Process and materials R&D

2.4.1.1 Objectives

Main objective is the development of economic growth processes for aligned carbon nano-tubes on metal electrode surfaces. This comprises the development of dedicated catalyst seed layers with controlled 3D nano-structure to stimulate growth of high aspect conducting CNT materials. To achieve the economic targets high throughput processing by continuous atmospheric pressure CVD for CNT growth and in-line dip-coating for catalyst layers are envisaged. The transferability of the coating process to cost efficient lightweight electrodes, as aluminium foil, is a further economic goal.

Further objectives are the development of electrochemical cell configurations with high dual layer capacity, and power density. Non-aqueous (organic) electrolytes are targeted to achieve high cell voltage and energy density. Application oriented tests will be performed to demonstrate the improved charging efficiency, long-term stability and useful lifetime of the optimized devices.

2.4.1.2 General synthesis method

Fast and scalable deposition processes for catalytic thin films and for the growth of carbon nanotube (CNT) films were established based on wet-chemical dip-coating and chemical vapour deposition at atmospheric pressure.

An innovative route for the catalyst deposition has been developed to replace the mostly used vacuum based sputter deposition. Solution based precursors were applied for deposition of thin alumina layers and subsequently the actual catalyst thin films. The method allows for homogeneous mixing of metal precursors and therefore for alloying various metals into a nanostructured film by dip-coating and post treatment. Fe-based catalysts have been identified as most promising, while doping with Co or Mo lead to enhanced growth rates and different CNT film structures.

The precursor solutions offer very good wet-ability even on metallic surfaces allowing for a precise control of nano-sized catalyst coatings. For the dip-coating process withdrawing speed and precursor concentration were the main parameters to adjust the film thickness of the layers. Precursor films were transformed into metal oxide layers through oxidizing thermal treatment.

The reducing atmosphere during the AP-CVD growth step caused reduction of the transition metal thin film and yielded the desired nano-particulate catalyst.

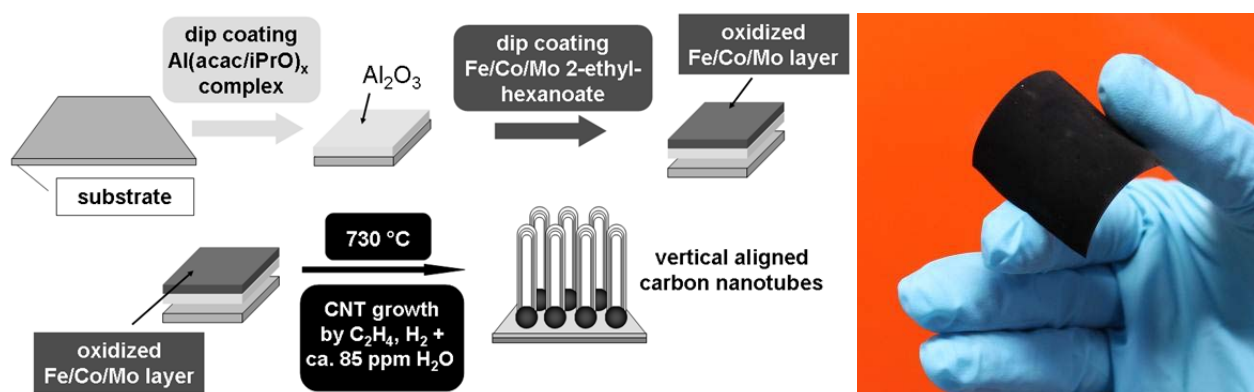


Figure 35: Process scheme for CNT synthesis (left), photograph of CNT-coated metal foil (right) © Fraunhofer IWS, TUD

Dense, homogeneous carbon nanotube films with a strong vertical alignment and a height up to $200\ \mu\text{m}$ were synthesised via thermal AP-CVD at 730°C on nickel substrates. In the first 20 min the growth rate ranges between 7.0 and $8.5\ \mu\text{m}/\text{min}$ for an optimized 2:3 (Fe:Co) system. After 30 min growth time the rate decreases significantly due to catalyst inactivation, diffusion limitation and CNT decomposition.

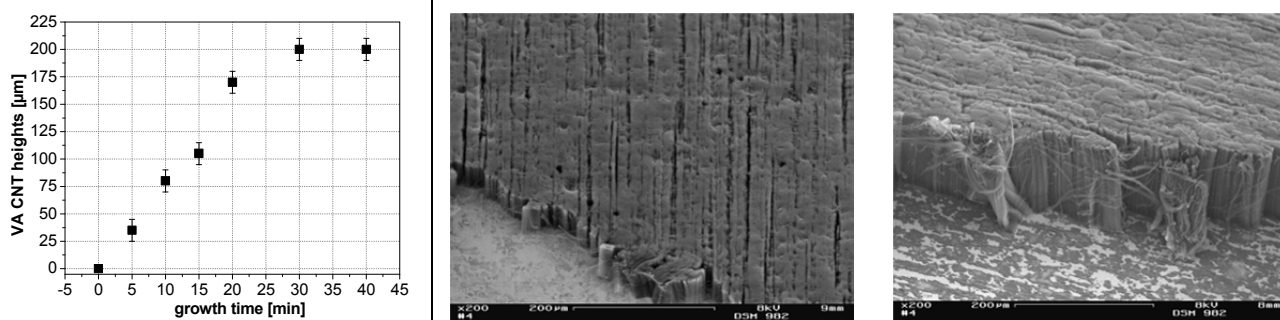


Figure 36: growth kinetics (l.); SEM images of samples after 5 (m.), 20 (r.) minutes growth time © Fraunhofer IWS, TUD

By adjustment of the process the deposition temperature was lowered down to 645°C and direct vertical aligned CNT growth on aluminium foil was observed via AP-CVD for the first time. The transferability to aluminium substrates and the scalability of the processes open up the feasibility of the CNT-based electrode approach. This Al-electrode approach is seen as a leap forward towards cost saving cell concepts. Al based electrodes are furthermore imperative for any mobile application of supercap components.

In addition the wet-chemical catalyst deposition allows for the coating on 3-dimensional substrates, such as foams or fibre mats through infiltration. Efficient 3-dimensional CNT growth on various carbon fibre materials has been demonstrated, opening further opportunities for application. Carbon fibres not only could further reduce the substrate weight, but can also significantly enhance the long time stability of the electrodes, because metal corrosion is one of the degradation mechanisms in supercapacitors.

2.4.1.3 3D nanostructures

Catalyst composition and film thickness were found to strongly influence resulting CNT film properties. Doping the Fe-catalyst with Co lead to enhanced growth rates, while with Mo addition small particle sizes could be stabilized and thus denser CNT films and lower CNT diameters could be achieved. By decreasing the thickness of the Fe/Mo catalyst films the average CNT diameter could be adjusted in the range of $4\text{--}22\ \text{nm}$. The existence of single walled nanotubes was evidenced for low catalyst film thicknesses by both Raman spectroscopy and TEM. Decreasing the thickness of the Fe/Co catalyst films on the other hand lead to inhomogeneous, very inefficient CNT growth. It

was found that for the Fe/Co system particles are not stabilized and tend to agglomerate forming larger particles. Stabilization of small catalyst particles as achieved by Mo doping was found to be crucial for 3D-nanostructure control.

The direct influence and control of the CNT nanostructure, even for the growth on technical rough metal foil substrates, is an outstanding result and a crucial step towards enhanced CNT-based supercapacitor electrodes.

The direct influence of catalyst film thickness on CNT diameter was found for the high temperature process on nickel as well as for the reduced temperature process on aluminium substrates. As expected, specific surface area of CNT material was enlarged significantly with decreasing diameter and was 265 m²/g for 20 nm thick CNTs and 506 m²/g for 4 nm thick CNTs according to BET adsorption measurements.

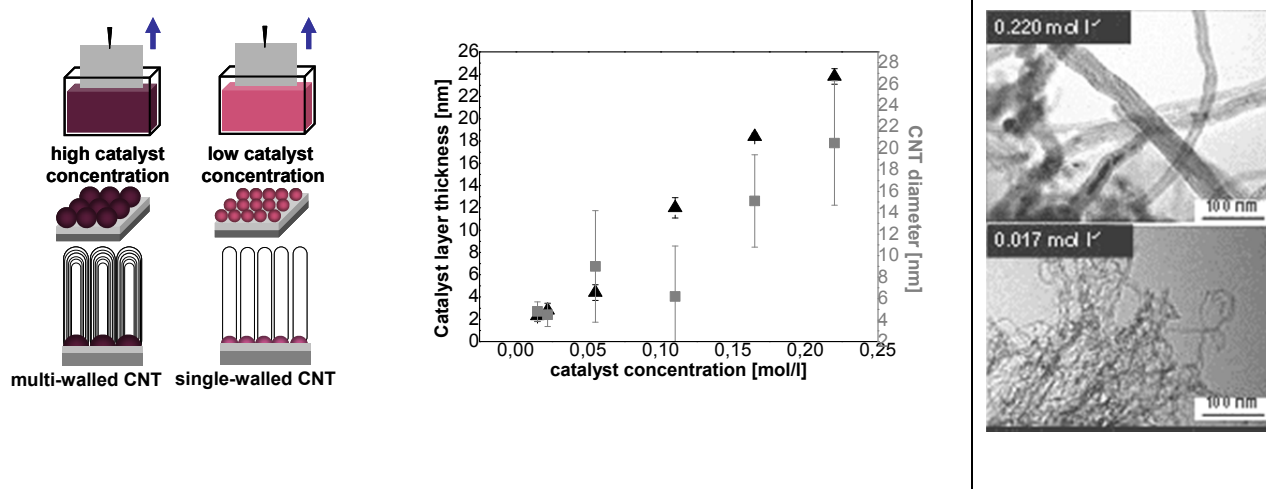


Figure 37: scheme for adjusting CNT diameter through catalyst concentration (l.); dependence of catalyst film thickness and CNT diameter from catalyst concentration in the precursor solution (m.); TEM micrographs for two selected samples © Fraunhofer IWS, TUD

2.4.1.4 Electrochemical testing

The CNT electrodes were tested and evaluated in a symmetric electrochemical test cell set-up with various electrolytes. TEABF₄/acetonitrile which is the standard electrolyte in commercial DLC cells was found to be suitable for CNT based supercaps as well. Additionally ionic liquids were tested as candidate electrolyte materials offering an enhanced voltage range.

For characterization of supercapacitor performance, the following investigations were done on the samples:

- Impedance spectroscopy at different bias potentials, in order to characterize the voltage dependence of capacitance
- Cyclic voltammetry with 10, 20 and 50 mV/s sweep rate between the voltage range from -2 V to 2 V.
- Galvanostatic charge-discharge cycles:
 - with different current densities in order to calculate the Ragone plot and determine the power density and energy density
 - long-term stability test up to 2000 or 10000 cycles with 1 A/g current density
- Preliminary self-discharge tests; because the fast self-discharging process is a critical problem of supercapacitors in general.

Electrochemical testing revealed the huge potential of the CNT-films for energy storage applications. Specific capacities strongly depend on the specific surface area of the electrode material and thus are directly influenced by the CNT diameter. For samples with the lowest CNT diameter capacities of up to 60 F/g were obtained.

A symmetrical, quite regular box-like shape of CV was detected by cyclic voltammetry on aligned CNT electrode, with small potential dependence, similarly to the reference active carbon material. The voltammetry characteristics prove a good charge propagation of both materials. CV curves show the capacitance difference between the two electrodes, similarly to the ac impedance results. The capacitance for CNT is lower than for active carbon. The main reason for this is the lower BET surface area. On the other hand, the ohmic drop of CNT/Ni electrode (initial slope of CV at -2 V on forward and at 2 V on reverse sweep direction) is magnitudes lower than that of the reference electrode, indicating the lower R_{esr} . No current peaks related to accompanying electrochemical reactions are visible on the curves, indicating a good operating performance, and suggesting a long-term cycling stability.

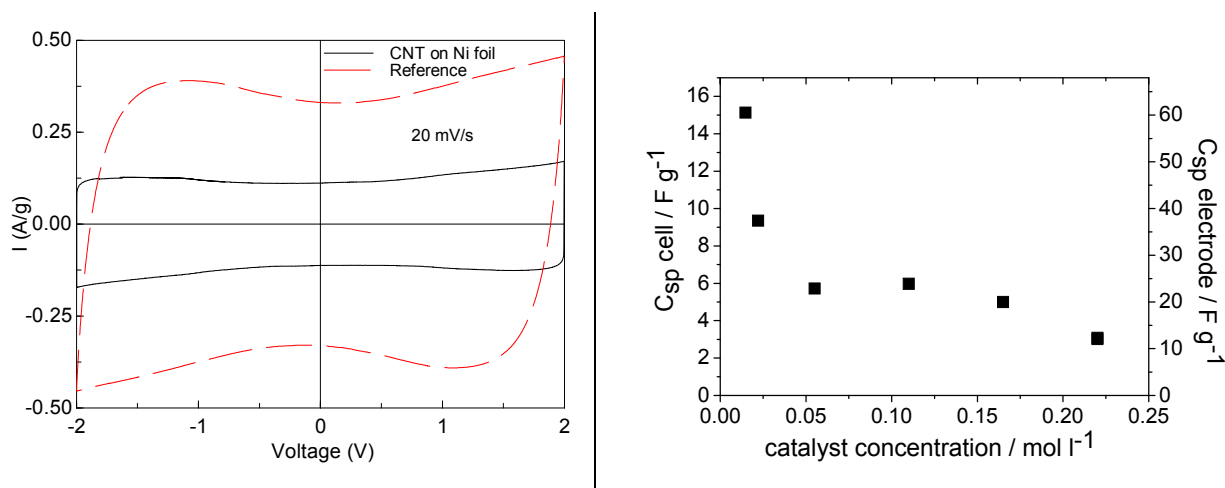


Figure 38: Corrected cyclic voltammetry curves of CNT/Ni and porous carbon/Al reference, measured at 20 mV/s sweep rate in TEABF₄/acetonitrile electrolyte; dependence of catalyst concentration (CNT diameter) on specific capacity © RCNS, Fraunhofer IWS

Very low series resistance was measured indicating the excellent contacting of the aligned CNT forest to the metallic electrode and fast ion diffusion kinetics within the high aspect ratio 3D structured CNT films. This is confirmed by impedance data revealing a low decrease of capacitance with increasing frequency.

This frequency dependence and the overall low resistance of CNT electrodes can clearly be attributed to their unique structural properties. While in active carbon based electrodes particle-particle resistance and complex micropore geometry add to limited charge and electrolyte ion transport, CNT electrodes profit from their completely different architecture:

- every single CNT is in direct contact to the current collector
- electronic resistance along the CNT is very low
- surface area is completely accessible
- intertube channels (pores) are larger than 10 nm and are directed towards the other electrode thereby leading to a very fast ionic transport.

These properties make the CNT based supercaps superior in areas where high power density, high frequencies or high pulse currents are essential.

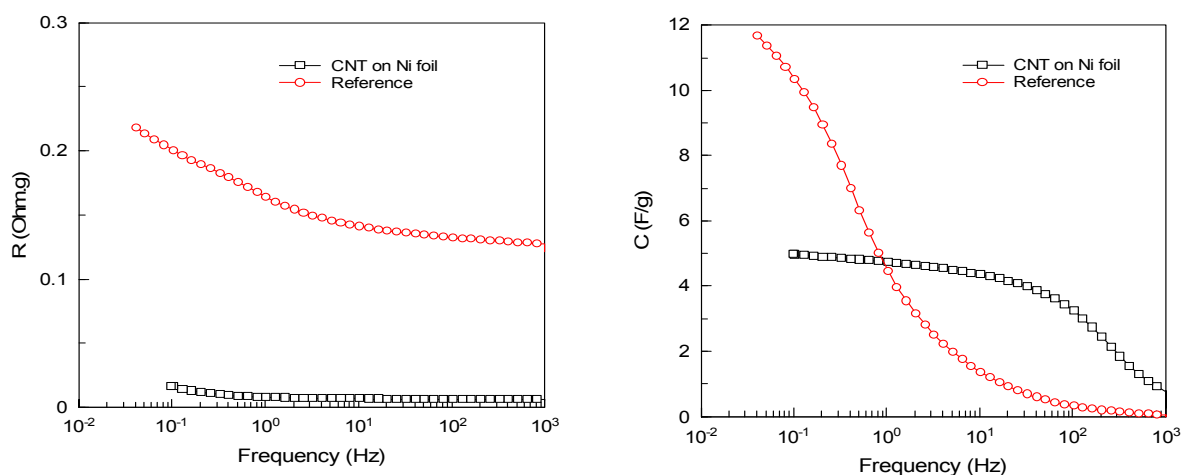


Figure 39: Series resistance of CNT/Ni in comparison to porous carbon/Al as commercial reference cell (left) and frequency dependence of specific capacitance in TEABF₄/acetonitrile as electrolyte (right) © RCNS, Fraunhofer IWS

Furthermore long-term tests with up to 1.000.000 charge-discharge cycles demonstrate excellent stability of the CNT test cells. In contrast to commercial active carbon based electrodes no degradation in terms of increase in series resistance or decrease in capacitance was observed in these long term experiments revealing another advantage of the CNT electrodes.

This difference can be attributed to the perfect 3D surface structure of the CNTs when compared to activated carbon. Low amount of functional groups limit side reactions and thereby degradation during cycling.

Summary: Fast and scalable CNT synthesis methods were established. The 3D nanostructure of the CNT electrodes was optimized towards enhanced performance in the DLC application and finally the superior properties of CNT-based electrodes over existing technologies were demonstrated through electrochemical testing. At high charging rates and in high-power applications CNT-electrodes are clearly superior against existing supercapacitor technologies.

2.4.2 Application demonstrator for energy storage

2.4.2.1 Objectives

Target is to demonstrate scalability of the CNT based electrode approach to industrial level. Based on the results being achieved in the R&D phase the process recipe will be transferred into higher scale (bench type) equipment demonstrator targeting to demonstrate feasibility of a continuous production route for CNT-based electrodes.

A further aim is to demonstrate performance increase of CNT based supercap against SoA commercial solutions. For the final phase it is planned to provide CNT based electrodes for manufacturing industrial size supercap cells. The components will be assembled and evaluated by an external supercap producer; outside N2P.

2.4.2.2 Equipment demonstrator

As a first step toward high-throughput manufacturing of CNT based electrodes a reactor was build-up to demonstrate quasi-continuous AP-CVD processing. A quartz chamber with 70 mm width is placed in a rectangular 3-zone furnace. Homogeneous coatings on samples with a dimension of 140 x 400 mm² were obtained through substrate folding. The thermal AP-CVD process is very stable and was found to be very reproducible.



Figure 40: Photograph of the reactor for a quasi-continuous growth of aligned CNT by AP-CVD (l.); Photograph of electrode with format of 140 x 400 mm² © Fraunhofer IWS

2.4.2.3 Application demonstrator – coin cell

For evaluation of the electrode performance a coin cell fabrication tool was installed. The cell is constructed from one pair of stainless steel cell cases with PP sealing O-ring, stainless steel spring and spacers. Electrodes are examined as two-electrode system with sandwich type arrangements.



Figure 41: Coin cell design and electrode © Fraunhofer IWS

Coin cells enable extended performance tests, including determining energy and power density, internal resistance and cycle stability. A wide range of samples with different 3D nanostructure and various substrate types have been studied and compared to commercial active carbon based electrodes.

Estimation of energy density and power density

The energy density and power density is estimated with the following optimised results obtained for aligned carbon nanotube layers on nickel substrate:

- Voltage window in acetonitrile solution: 2 V
- Separator: Ethyl-cellulose 25 µm thick
- R_{esr} for 2 * 1 cm² electrode pairs: 0.7 Ω
- $C_{\text{dl,sp}}$ for 1 g active layer of CNT in two-electrode cell: 10 F/g (highest achieved)
- $C_{\text{dl,sp}}$ for single electrode: 40 F/g (equivalent to three-electrode system)
- Thickness of the Ni substrate: 10 µm
- $\rho_{\text{Ni}} = 8.912 \text{ g/cm}^3$
- $\rho_{\text{electrolyte}} = 0.9 \text{ g/cm}^3$

Table 1: Specific capacitance, specific resistance, energy density and power density calculated to active mass, mass of electrode, and mass of supercapacitor cells

	$R_{esr,sp}$ mΩ.g	$C_{dl,sp}$ F/g	$C_{dl,sp}^*$ F/g <small>single electrode</small>	E_{sp} Wh/kg	P_{sp} kW/kg
active layer	0.7	10	40	5.5	1400
electrode (substrate + active layer)	7	1		0.55	142
total EC cell (substrate, active layer, electrolyte, separator)	8.75	0.8		0.44	115

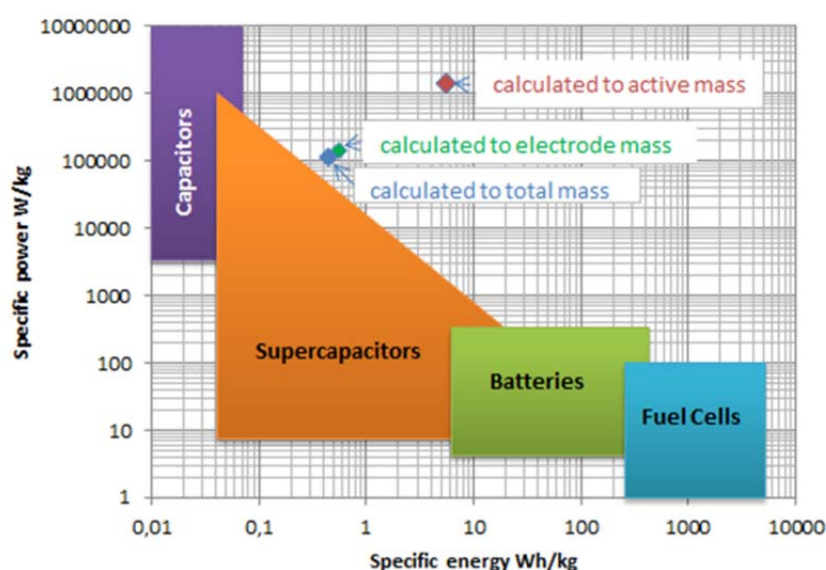


Figure 42: CNT on Ni electrode performance in the ragone plot © Fraunhofer IWS, RCNS

Two components were not taken into account for the calculations: the resistance of current collectors, and the mass of the supercapacitor cell container. The contribution of these two factors to both power density and energy density being related to total mass depend on the size of the final product.

The usual resistance of the metallic parts of supercapacitor cells is ~10 mΩ. The contribution of this resistance is increasing with size of CNT supercap.

In conclusion, the very high power density of CNT supercapacitor test cell is by far exceeding the DoW target criteria (>50 kW/kg for electrode material). The very low serial resistance is due to the fast ion-transport in the aligned intertube channels, and the high electric conductivity of the CNTs. Furthermore, when replacing the nickel substrate by aluminium, three times larger energy- and power density on electrode and cell level can be achieved.

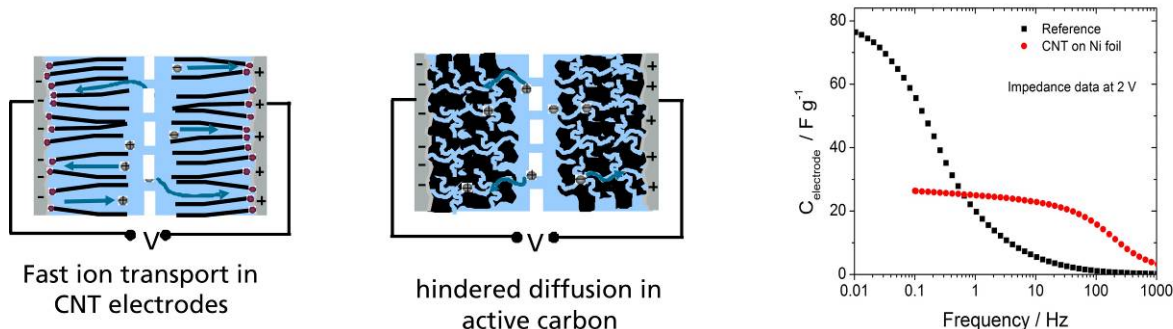


Figure 43: Scheme of ion transport for CNT based electrodes (left) in comparison to conventional active carbon based electrodes (mid); frequency dependence of specific capacitance in TEABF₄/acetonitrile as electrolyte of CNT/Ni electrodes in comparison to porous carbon/Al as commercial reference cell (right) © Fraunhofer IWS, RCNS

Aluminum current collectors

Electrochemical measurements prove the successful transfer of CVD process from Ni to Al substrate. The specific capacitance of VA-CNT/Al electrodes varied between 25.6 – 61.2 F g^{-1} depending on the catalyst complex mixture composition and concentration. The electrodes have a very small value of effective serial resistance at 0.42 – 0.15 $\text{m}\Omega \text{ g}$ indicating a potential candidate as electrode material in high power supercapacitor application. Excellent cycle stability of supercapacitors has been demonstrated up to 300,000 cycles.

The energy and power density were estimated taking into account the cells' components including the mass of CNT, mass of 50 μm thick aluminum substrate, the mass of separator and electrolyte, but excluding the cell house.

The power density of the here described VA-CNT/Al EDLCs are approximately 80 kW kg^{-1} , and practically independent on the density of CNT layer. This is 1-2 magnitudes higher than the typical power density of supercapacitors made from activated carbon (AC) (0.5 – 10 kW kg^{-1}). This is due to the very low internal resistance of CNT EDLC owing to the fast ion-transfer process in the inter-tube channels of aligned CNT layers, high electronic conductivity of the CNTs, and direct binder-free contact between CNT layer and aluminum substrate. On the other hand, the energy density varies between 0.1 – 0.15 Wh kg^{-1} depending on the density of the CNT layer. This is a magnitude lower than the energy density which can be reached with AC electrodes 1 – 10 Wh kg^{-1} . The major reason of the lower energy density is the loose packing of tubes in the active layer resulting low density 0.15 – 0.4 mg cm^{-2} , in contrary to the AC based electrodes having a typical active mass loading around 10 mg cm^{-2} .

Our electrochemical results indicate the advantage of VA-CNT/Al supercapacitors in applications that require high power density or high frequency.

Carbon fibre current collectors

As mentioned before, CNT directly grown on carbon fibre materials could be another option for light weight electrodes with a very high CNT mass load.

Measurements have been performed and a energy density of 0.8 Wh/kg on electrode level was calculated. Power density was as high as 4 kW/kg .

Outstanding results have been obtained in terms of cycle stability. While reference electrodes reveal a decrease in capacitance and increase in series resistance over the first 50.000 cycles. The values for CNT@carbon fibre electrodes were stable over 1.000.000 cycles.

This result can be attributed to the more stable and defect-free surface of CNTs as compared to active carbon, but also the metal-free electrode approach helps to avoid corrosion and other degradation effects related to the metal / carbon interface.

2.4.2.4 Application demonstrator – prismatic cell

A prismatic DLC cell was manufactured by an associated industrial partner applying CNT coated aluminium foil electrodes. The coated area was 35 x 35 mm² for each electrode and 4 single electrodes were assembled to a 3-cell system. The cell was filled with TEABF₄/acetonitrile electrolyte and tested by industrially established standards.

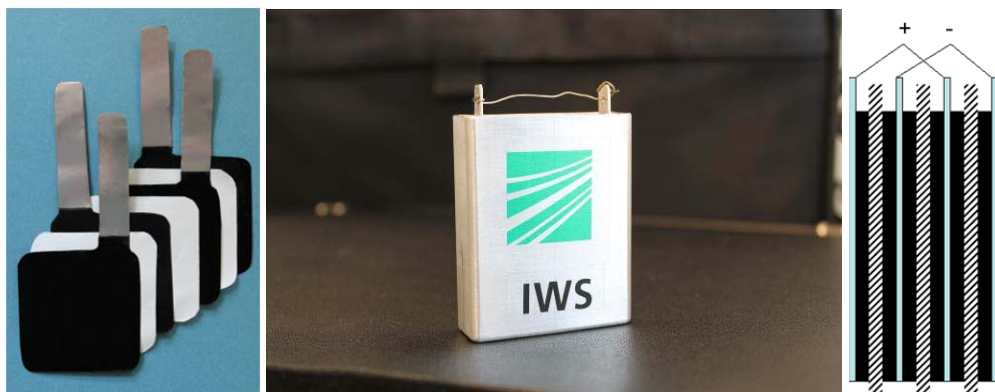


Figure 44: stack assembly of CNT coated aluminum foil electrodes (l.) ; industrially manufactured prismatic cell (m.); scheme of the 3-cell assembly (r) © Fraunhofer IWS

As a result a very low series resistance of 7 mΩ when compared to reference electrodes (37 mΩ) was determined confirming the lab scale results on coin cells.

Extrapolating these results to a larger cell would result in a lowered capacitance of 3,4 F and a substantially decreased series resistance of 0,2 mΩ for the CNT electrodes as compared to 250 F and 10 mΩ for the reference cell.

According to the assessment from the cell manufacturer the outstanding performance in the high frequency range can not be matched by other supercapacitor type, opening new possible applications.

It should be mentioned, that the CNT coated aluminium foil was optimized towards low resistance and is only one possible design for a CNT based supercapacitor. As already demonstrated, properties of the CNT-electrodes can be varied over a broad range by the 3D nanostructure of the CNT and by applying different substrates.

2.4.3 Evaluation of results and conclusions for exploitation

Results of this Workpackage reveal new approaches for the production of CNT-based electrodes. Synthesis on low cost / low weight substrates has been demonstrated as well as the scalability of the atmospheric pressure processes for growth of 3D nanostructures.

Based on these results an industrial CNT-electrode production can be envisaged, being competitive when compared to slurry based state-of-the-art production technologies. The next steps would be the transfer of process steps to roll-to-roll equipment and to increase the coating width.

In terms of performance significant differences were observed for the CNT-electrodes when compared to active carbon reference electrodes. While capacitance and thus energy density was lower for all CNT samples, clear advantages and superior performance has been demonstrated for

their high current properties. Significantly lower series resistance, enlarged frequency range and higher power density were found to result from the unique material architecture of vertical aligned CNT films.

CNT-based supercapacitor cells are a new class of energy storage devices closing the gap between state-of-the-art supercapacitors and electrolytic capacitors. While maximum energy densities are required for energy storage devices for HEV and EV, enhanced cycle stability, frequency range and power density are more important to consumer electronic applications. Here a significant market potential for CNT-based supercapacitors can be envisaged.

2.5 WP9/10: Interface Technologies for Durable Adhesion

2.5.1 Process and materials development

2.5.1.1 Objectives

Main objectives are the development of interface technologies to improve bond strength of adhesively bonded or painted components in the aerospace, automotive, and steel industry. The applications are focused on three high volume market segments:

- Next generation of very large airliners ("black aircraft") which need durable bonding of carbon fibre reinforced polymers with lightweight metals; target is to reduce fuel consumption,
- Durable organic coating systems for lightweight (polymer) vehicle parts, and for
- Lightweight construction panels with high stiffness, e.g. for facades; target is to provide high add-on value parts for clients with reduced materials consumption and increased durability.

Main aim for aeronautic industry is to increase bond strength of adhesively bonded parts of both titanium and carbon fibre reinforced plastic substrates with respect to long term stability of adhesion.

Focus of automotive industry is to reduce failure rate of painted thermoplastic surfaces (polypropylene PP) and the improvement of paint adhesion to cost efficient lower grade thermoplastic materials.

Focus of steel industry is to increase bond strength and durability of stainless steel and organic pre-painted galvanised steel for construction panels (sandwich panels with high specific stiffness) being manufactured from steel strips and embossed steel sheets.

Common ground for all these application areas is that high throughput surface processing technologies are envisaged. A range of atmospheric pressure plasma and flame coating methods were assessed concerning their potential for scale-up to industrial stage.

A further main aim is the development and evaluation of test methods to assess the quality of innovative plasma-chemical surface modification with respect to adhesion strength achieved.

Application oriented test methods need to be developed for the correlation of process data vs. product performance

2.5.1.2 Equipment demonstrator for treatment of 3D shaped parts

The technology head based on a DC-Arc plasma source with 150 mm working width (extendable to 300 mm) was mounted in a test bench and the substrate was moved in front of the fixed plasma source. The tech bench is equipped with a linear substrate movement system, capable of speed up to 50 m/min. To simulate treatment of 3D shaped parts the working distance between plasma source and substrate is adjustable in a wide range. All variants of chemical surface functionalizations and coatings on flat and shaped parts can be provided with this type of equipment.

To achieve both high working distance and high process speed a high activity of the remote plasma is necessary. Based on extensive fluid dynamic modelling the design and construction of a new remote gas feeding system with hole type nozzles for increasing gas velocity was finalised. With this upgrade a substantial higher tolerance for the distance between plasma head and substrate has been achieved. This is imperative for treatment on 3D shaped components.

The up-graded technology head was also equipped with a newly designed gas feeding system for CVD precursors. Due to the high gas speed and substantially increased activity of the remote plasma high deposition rates of up to 300 nm*m/ min have been achieved. This setup was used for providing coatings for both aeronautics and steel applications.

The developed “technology head” was furthermore assessed with respect to implementation into a robot which is relevant for applications in automotive (high speed treatment) and aeronautics (moderate speed treatment). Based on a re-design and the use of lightweight-components a substantial weight reduction was demonstrated being pre-requisite for any high speed treatment. Feasibility of the generic approach was confirmed but the robot based application require substantial more development work to meet requirements (being out of scope for N2P).



Figure 45: Lab-scale test bench coater for flat and (slightly) 3D shaped components in operation, plasma source is an extended DC-Arc with 150 mm working width (left), stainless steel substrate after high rate deposition of SiO_x based coatings, with rates of about 300 nm*m/min (right) © Fraunhofer IWS, FGW

2.5.1.3 Equipment demonstrator for treatment of painted metals

A DBD plasma equipment demonstrator for surface treatment and 3D nano-structuring of flat (or embossed) steel materials was established at VITO. The equipment was originally planned to be able to treat samples up to 200 mm wide and about 300 mm long (A4 size).

Due to the exploitation potential of this approach, being high, it was decided to further scale-up the equipment demonstrator (beyond DoW specification). The final DBD plasma demonstrator system is now able to treat samples of 300 mm width up to a length of 1,2 m. The system has a fixed plasma reactor and a moving substrate holder both positioned in a ventilated hood with electromagnetic shielding to ensure safe operations.



Figure 46: Aerosol assisted DBD plasma equipment demonstrator system ©VITO, AFS.

The DBD plasma demonstrator system is able to use a wide variety of gas mixtures and allows the injection of liquid or dispersed chemistries in the form of nano-sized aerosols by means of pressure atomization. Uniform coating deposition has been demonstrated as well as continuous stable

operation over more than 24 h. A software program has been developed to monitor and log all process parameters.

The demonstrator system at VITO is used for application demonstrator developments in which the interface adhesion of lacquered steel based composite panels is studied. The same demonstrator system is also used in WP6 to produce samples for antibacterial surfaces for medical environments.

Dynamic deposition rates of aminopropyl triethoxysilane (APEO) deposited with the VITO PlasmaLine system are 5 to 10 nm³/m/min and mainly depends on the gas flow in the plasma reactor. The increase of the gas velocity towards the substrate surface results in a higher deposition efficiency, see Figure 47.

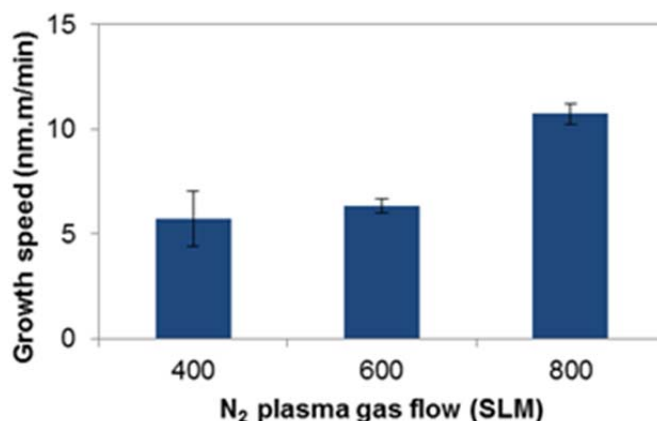


Figure 47: Dynamic deposition rate of APEO as precursor in dependence of gas flow ©VITO

2.5.1.4 Process development and testing

From previous process evaluation results it became obvious that increased adhesion on the targeted polymer / composite/ metal surfaces can be achieved by combining three effects:

- 3D nano structuring; partially in combination of controlled nano/micro-structuring,
- Chemical surface functionalisation, and
- Applying functional coatings as thin interface layer

Target materials being selected for the different application areas were:

- For aeronautics: two substrates (CFRP and light weight metal, pref. Ti)
- For automotive: two substrates (thermoplastic materials)
- For steel industry: two substrates (stainless steel flat/embossed and, pre-painted galvanised steel)

Plasma treatment of titanium based alloys for aeronautic application

As a result of extensive screening experiments best results were achieved with SiO_x coatings from HMDSO and TEOS precursors. Application related testing by means of wedge tests exhibit better long-term adhesion properties than the industrial reference process Turco 5578.

Durability against ageing is crucial for aeronautics applications. For differentiation of ageing behaviour the wedge test has to be used. For this test ageing up to 1500 h was performed. Benchmarking process is alkaline anodisation, NaTeSi, with nearly no loss of adhesion by ageing.

For atmospheric pressure plasma treated samples the results after ageing of samples showed, that plasma cleaning without chemistry involved has no positive effect on the long term stability of

adhesively bonded Ti. In contradiction to that SiO_x layers demonstrated a significant improvement of adhesion stability; crack propagation is in between the results for NaTeSi and Turco 5578 treatment.

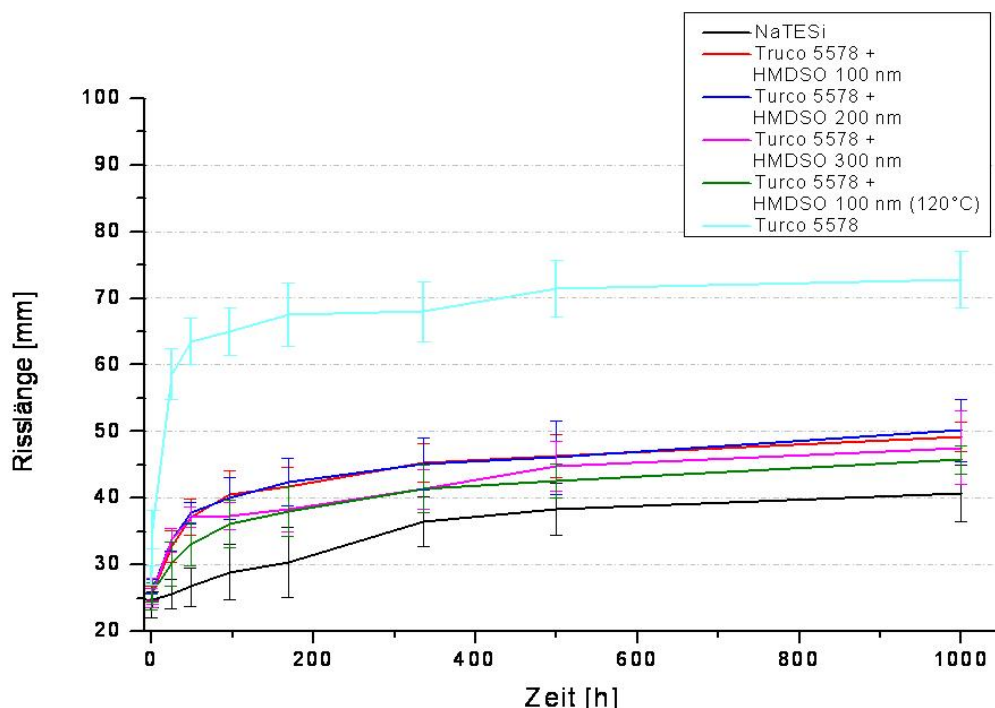


Figure 48: Crack growth for monitoring long term stability of Ti bondings – thickness variation of interface layer © EADS

Plasma treatment of CFRP for aeronautic application

Successful exploratory tests were done for elimination of residues of peel ply which is used to remove CFRP components from the mould. All plasma activations lead to a modification of the contact angle, CO_2 containing plasma results in lower water contact angle than O_2 containing plasmas. Pull-off tests showed sufficient adhesion with selected plasma parameters taking into account the results from polypropylene substrate treatment.

For a detailed insight in the behaviour of the interface of bonded CFRP specimen application specific G_{Ic} tests are necessary. Cleaning and activation of CFRP result in bonded specimen that fails in the substrate and not in the bonding interface.

Plasma activation of PP for automotive application

With the up-graded DC Arc- plasma source in combination with the new substrate movement system the industrial target parameters (50 m/min line speed and substrate distance 7 cm) for PP substrates could be tested for the first time.

Surface analytics confirmed that atmospheric plasma treatment results in nano-structured, chemically modified surfaces. The plasma treatment roughens the surface uniformly. Despite of the fact that surface characterisation results and adhesion testing show no straightforward correlation from current database it can be deduced that best adhesion correlates with medium surface energy, medium roughness and medium amount of C=O groups being detected in IR-ATR spectra.

Test series showed that the adhesion of the primer was sufficient at parameters of 50 m/min and substrate distance < 4 cm or 20 m/min and 7 cm. This parameter set does not meet specification for treatment of (strongly) shaped parts in automotive, e.g. painting of EMPP bumpers. The reason is supposed to be the decreasing activity of the remote plasma with increasing substrate distance.

Because the plasma activation is working in principle, the lacquering of sillboards was identified as potential application for further investigations. Sillboards are less shaped parts therefore smaller treatment distances did not fall into account in comparison to the originally selected bumpers having a 3D-geometry. With the plasma processing on 4 cm treatment distance and a treatment speed of 50 m/min also good adhesion results were achieved in the scratch test. This result is notable because different polypropylene compounds (different contents of inorganic filler, e.g.) are used for this applications.

Plasma treatment of stainless steel and pre-painted galvanised steel, for steel applications

Targeting to adhesion control for manufacturing of lightweight panels for construction, three coating technologies were investigated:

- Coater head equipment based on extended DC Arc plasma source for coating on stainless steel; both flat and embossed substrates (at IWS)
- Aerosol assisted DBD plasma for treatment and coating on pre-painted galvanized steel (at VITO)
- Flame assisted CVD (at OCAS)

Best results for stainless steel were achieved with DC arc plasma by applying a SiO_2 layer with controlled thickness in combination with plasma post-treatment. This treatment procedure results in complete cohesive failure of the glue, meaning that upper limit of joint strength have been achieved; no further improvement would be possible with this glue type. The durability of the joints was drastically improved compared to untreated stainless steel.

The DC arc plasma technology from Fraunhofer-IWS has been up-graded to be used for high-throughput coating having the potential to meet economic goals. Preliminary tests showed that the technology can be used for flat steel sheets as well as for embossed panels.

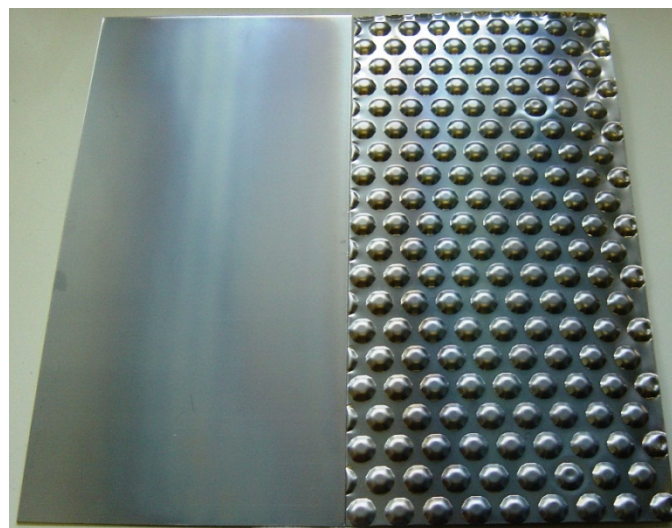


Figure 49: Deposition of SiO_xC_y layer on embossed steel plate by extended DC-Arc plasma technology; sample size: 10 cm x 30 cm © Fraunhofer IWS

The flame assisted CVD from partner OCAS (1-step deposition process without post-treatment) resulted in coatings on stainless steel being comparable with DC arc but less performing than the DC arc post treated plasma coatings in application testing. The joint strength was relatively high but it was lower than for the depositions made with the 2-step AP plasma coating process at IWS. The durability of the flame assisted CVD layers was also improved compared to untreated stainless steel.

For pre-painted steel both DC-Arc plasma and flame assisted CVD technology were not applicable probably because the heat load is too high. Degradation of the polymer surface resulted consistently in lower adhesion strengths than the untreated samples. Therefore an alternative approach was

researched based on the aerosol assisted DBD plasma technology from partner VITO which can be applied at low temperatures. Samples were treated using various gas mixtures and precursors. Evaluation was done by means of lap shear tests, after joining two painted panels by thermoplastic polyethylene (PE)-based and polyethylene/polypropylene (PE/PP) 2-layer films which are industrially used for sandwich panel manufacturing.

Surface characterization

A wide range of state-of-the-art surface analytics was applied to investigate the surface structure after plasma treatment. Motivation for these extensive investigations was to identify correlations between surface structure and application oriented properties targeting to derive rules for a science based platform for process development. Nevertheless that this aim only partly could be achieved (which is understandable in the light of complexity of the area) some substantial progress was made.

For Titanium, a correlation between surface micro/nano-roughness could be identified. As a consequence a pre-treatment of Titanium for high performing adhesive bonding should result in a nanostructured surface topography as shown in the picture below. To study this interface behaviour more in detail an investigation of the substrate after the ageing process was started. As a result a correlation between the micro/nano-structure of the surface and the long term stability of adhesive bonds was noticed. The smoother the surface of the treated substrate is the lower the long term stability will be.

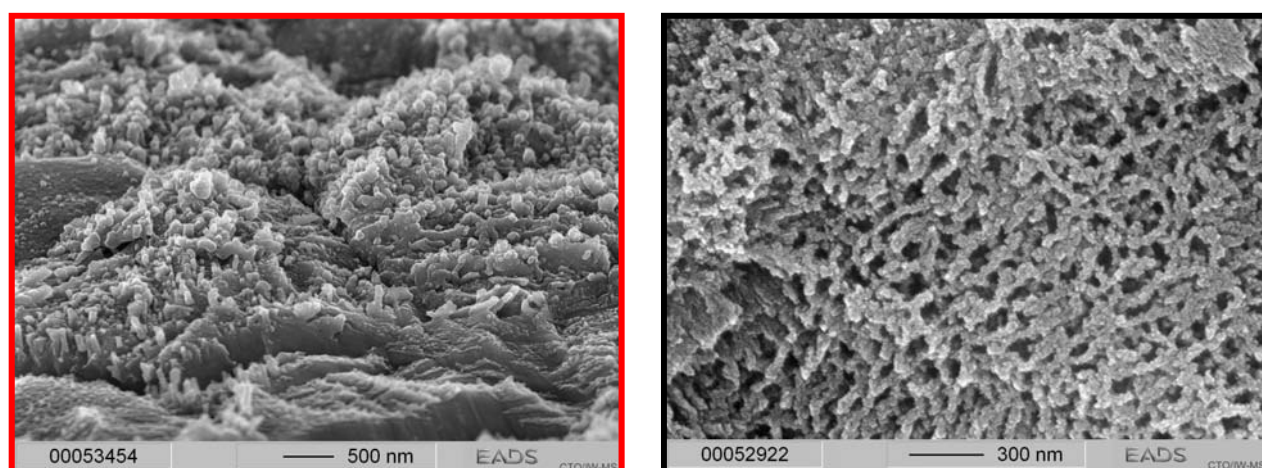


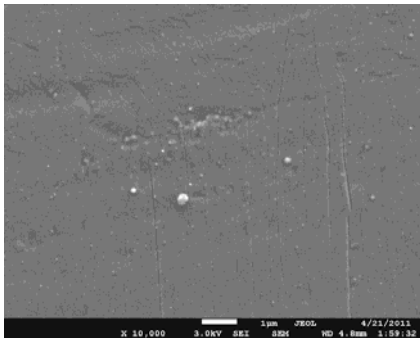
Figure 50: Beneficial surface structures on Titanium for achieving highest adhesion: Micro structure / columnar nano structure (left); micro structure / basket wave nano structure (right) © EADS, Fraunhofer IWS

For stainless steel and pre-painted steel, the optimal surface conditions for bonding are summarised as follows:

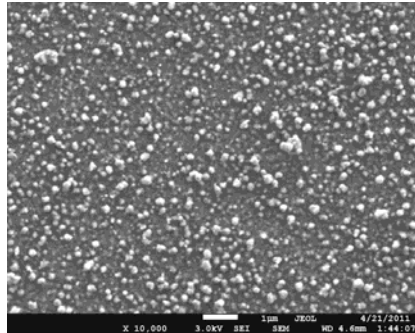
Stainless steel:

For stainless steel, the situation is similar to what was observed for titanium. A nano/micro-rough silica layer should be deposited onto the smooth stainless steel substrate in order to enhance bonding strength. But, in comparison to titanium, additional factors need to be considered, like formation of loose powder/particles on silica layer (nozzle distance, gas mixture) and low adherence of silica onto stainless substrate.

Example of surface structure for 'bad' adhesion: smooth silica layer



Example of surface structure for 'bad' adhesion: formation of loose powder/particles on stainless steel substrate.



Example of surface structure for 'good' adhesion: nano-structured silica film without powder/particles.

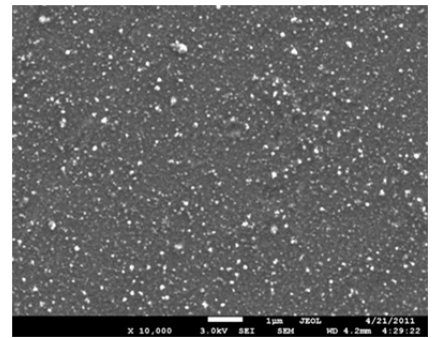


Figure 51: Examples of different surface structures resulting in 'good' and 'bad' adhesion © OCAS, Fraunhofer IWS

Pre-painted steel

For pre-painted steel, low-temperature plasma treatments enhance adhesion by deposition of a very thin layer consisting of amine and silanol functionalities. Here, the adhesion mechanism is considered to be mostly chemical surface functionalization. Plasma activation (by N_2/CO_2) and plasma coating (by N_2/CO_2 + APEO precursor) result in significant chemical surface changes. Surface energy measurements showed the increase of the surface polarity. The changes in the chemical composition of the surface were also evidenced in XPS measurements. The consequences of these changes in surface properties are found in higher adhesion strength after the lamination process.

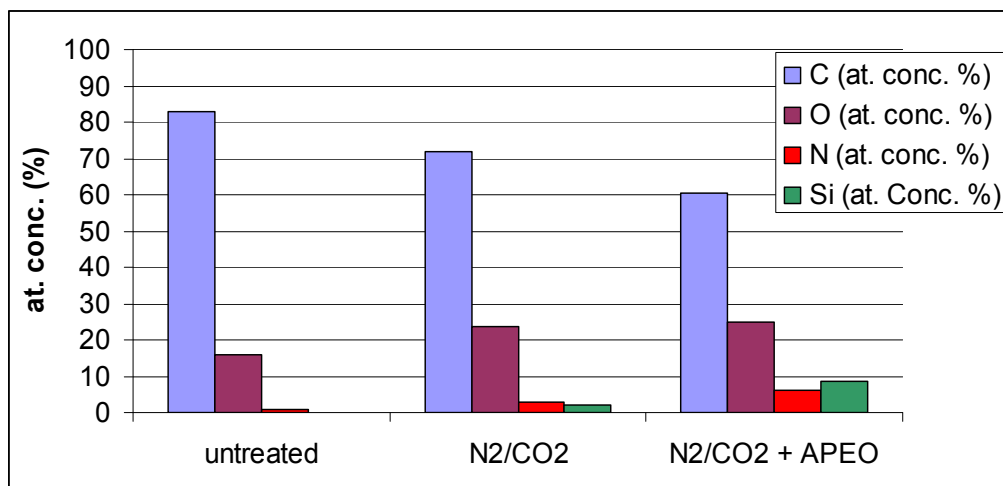


Figure 52: Surface composition of pre-painted steel after aerosol assisted DBD plasma with and without APEO precursor. © OCAS, Vito

2.5.2 Application Demonstrator for Interface Technologies

2.5.2.1 Objectives

The applications for both aeronautics and automotive are aiming for a step-change in production technology. Essential for these two applications is that any production technology for 3D nano-structuring must be applicable on big (immobile) shaped parts.

The applications for steel industry are aiming for high efficient, mass production of pre-manufactured parts which can be used, e.g. for materials saving light-weight construction (honeycomb structures with high stiffness). Essential for these applications are high adhesive joint strength and long-term durability due to nano-surface structuring/functionalisation of flat or embossed sheets/bands from steel.

From materials point of view the three applications are looking for a substantial increase of adhesion due to 3D nano-surface structuring/functionalisation.

Scope of WP 10 is the transfer of the results, developed on small flat laboratory samples in WP 9, to 3D shaped components or flat coils with high processing speed in industrially relevant perimeter.

The demonstrator systems:

- Three application demonstrator (each for aeronautics, automotive, and steel applications) were built based on the technologies being developed in WP9 for polymer/metal materials surface structuring. Objectives were:
- Aircraft application:
- Increased bond strength, toughness, and lifetime (e.g. corrosion resistance); target performance:
- Adhesion on CFRP: > 80% cohesive failure in adhesive
- Adhesion on Ti: > 70 % cohesive failure in adhesive
- Substitute dangerous handcraft work by automated equipment, avoid environmental impact by aggressive chemicals
- Target processing cost < cost of Chromic Acid Anodisation
- Automotive application: Increased performance of organic coating systems on big coachwork parts
- Reduction of the failure rates regarding the usual automotive test standards to well below 1 % also with not adhesion optimized substrate materials.
- Target performance for paint-bonding: <10 % failure in steam-jet test after temperature cycling (special specification of automotive industry)
- Cost reduction by possible application of not adhesion optimized plastics.
- Substitution of aggressive primer chemicals; avoid any environmental impact by substituting wet chemical approach by gas phase plasma chemistry.
- Steel application:
- Increase of adhesion strength for sandwich panels for construction (stainless steel or pre-painted galvanised steel skin + lightweight core)
- High strength and durability of adhesive joints are required in combination with an ultra-low failure rate; reduced 'accidental' surface contamination (process stability)
- Substitution of primer and cleaning chemicals by eco-friendly atmospheric plasma process
- Demonstration of atmospheric plasma process as high-speed etching or functionalization treatment for flat steel surfaces.

2.5.2.2 Application demonstrators for aeronautics industry

Application oriented testing on Titanium

- Wedge tests (DIN 65448): To compare the adhesion of specimen coated with the coater head device and the robot-capable technology head device wedge test samples were prepared and tested. Main conclusions from these tests are:
- The adhesion and durability of the specimen prepared by coater head and (prototype scale) technology head are in the same range. The resulting crack length is significantly lower in comparison to those of the commercially available etch-cleaner. Interface coatings prepared with HMDSO as precursor show lower crack growth during ageing compared to those prepared with TEOS as precursor. The HMDSO based interface coating can be used with and without bonding primer
- Roller peel test (DIN EN 1464): The test was selected aiming to verify the positive results of the wedge test by using an alternative test with modified loads. This test is used as a standardised test for qualification of adhesive bonds. Main conclusions from these tests are:
- Without ageing all pre-treatments lead to a peel resistance of 9-11 kN/m and cohesive failure. After aging however alkaline etch and TEOS based interface show strong decrease of peel strength due to partly adhesive failure.

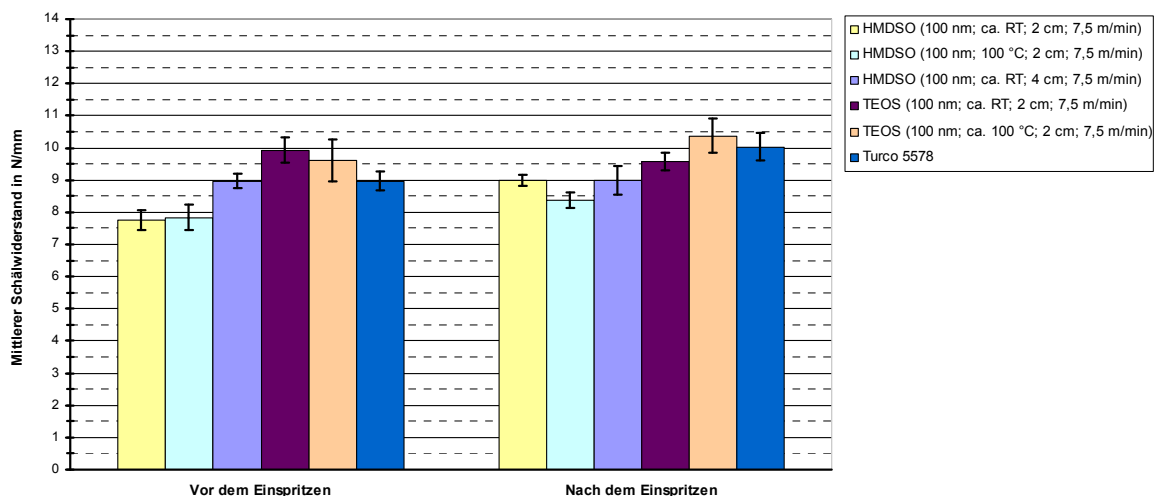


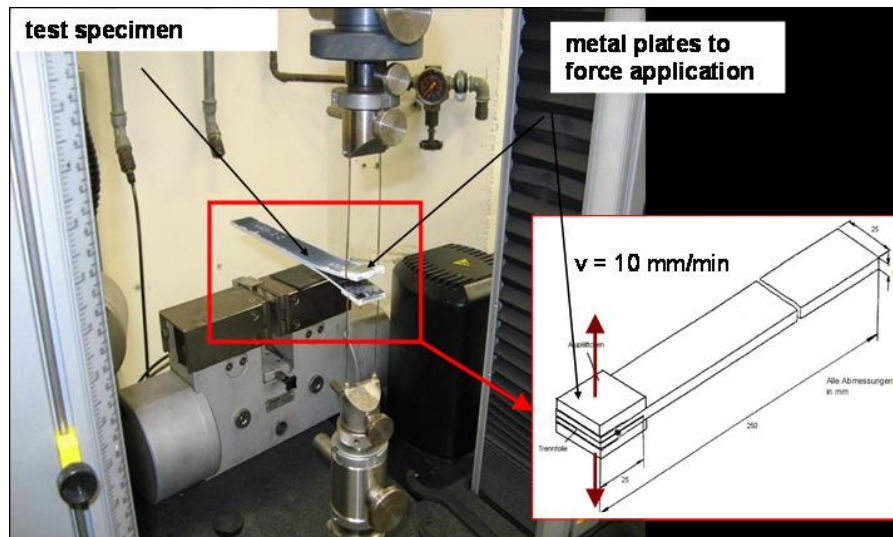
Figure 53: Results of Peel test (DIN EN 1464)

- Cross Cut Test (ISO 2409)
- Besides adhesive bonding the use of plasma based interfaces on paint adhesion was investigated. Independent from type of paint (water/solvent based) and precursor (HMDSO/TEOS) the surface chemical treatments exhibit an excellent paint adhesion on Titanium (in initial state as well as after ageing (336 hrs water storage)

Application oriented testing on CFRP

- G1c Test (AITM 1-0053)

The most representative test for the evaluation of pre-treatments for bonding of CFRP is the G1c energy of bonded joints (mode I). Mode I define a crack that extends as a result of peel forces test (Airbus standard AITM 1-0053). Scope of the test is the determination of fracture toughness perpendicular to the crack plane.



G1c test set-up for CFRP bonds © EADS

The results show a distinct influence of the distance of the technology head to the substrate. Up to 40 mm working distance a good adhesion with cohesive failure mode is demonstrated. At 70 mm distance partly adhesive failure leads to a strong scattering of results.

Application oriented testing on hybrid joints Ti to CFRP

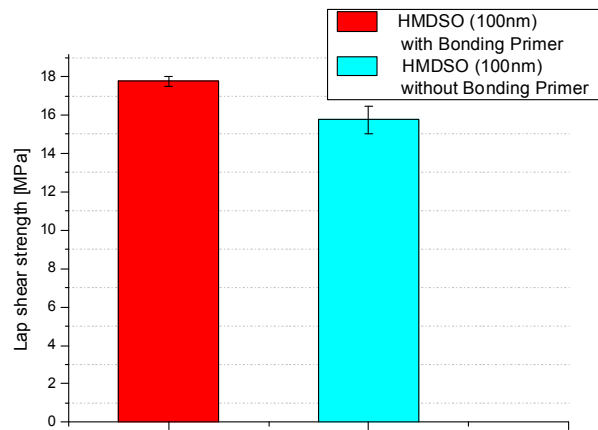
To demonstrate, that different types of materials like metals (Titanium) and plastics (carbon fibre reinforced plastic – CFRP) can be treated with the same atmospheric plasma equipment, plates of titanium and CFRP were plasma modified and adhesively bonded, to prepare lap shear test specimen (Lap Shear Test: ISO 1465) . The adjustment to the different materials is done by adjustment of process parameters and feeding of suitable plasma and – where needed – precursor gases.

To show the applicability of the developed technology head for this goal Titanium and CFRP plates were plasma treated with the optimised parameters evaluated during the process development period. The treated samples were adhesively bonded to prepare lap-shear specimen.

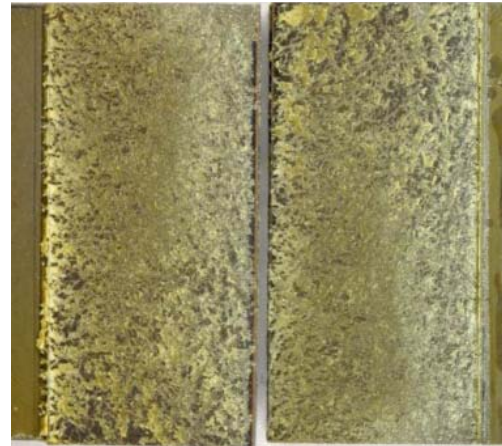
Main results of testing:

- Ti/CFRP hybrid samples exhibit a lap shear strength of 18 – 19 MPa
- This lap shear strength is in the same range as for specimen Ti/Ti
- Fracture mode is cohesive in the glue (as for the Ti/Ti specimen)

In summary the results prove, that hybrid structures (Ti/CFRP) can be produced showing the same performance as monolithic structures (Ti/Ti or CFRP/CFRP).



Ti/Ti



Failure mode Ti/CFRP: cohesive

Fig. 66 Lap Shear test (EN 2243): Results © EADS

Material demonstrator

Final goal of the N2P project for aeronautics was to prepare a hybrid material demonstrator by adhesive bonding with Titanium and CFRP as substrate material. The design of the demonstrator is representative for a component based on a Titanium structure with CFRP cladding. The use of Titanium directly bonded to CFRP is due to the better galvanic compatibility of these two materials compared to Al/CFRP joints (high risk of galvanic corrosion).

Design of demonstrator

The demonstrator is composed of two u-shaped profiles, 40 mm in height bonded together with an overlap. The Titanium profile is placed on the inner side simulating a supporting structure and CFRP is placed on the outer side simulating a cladding.

The components are plasma treated using the equipment demonstrator and the parameter window evaluated within the N2P project – plasma coating on the outer side for Titanium and plasma activation on the inner side for CFRP.

The bond strength and integrity of such a bonded component was demonstrated by single lap shear test.

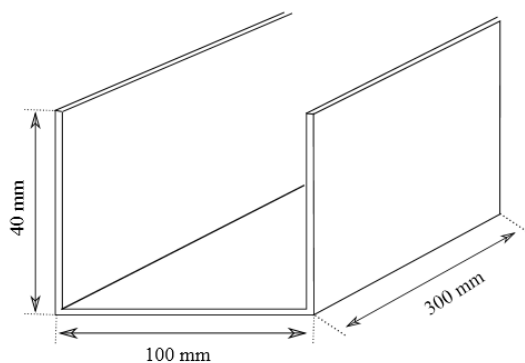


Figure 54: Sketch of aeronautic demonstrator

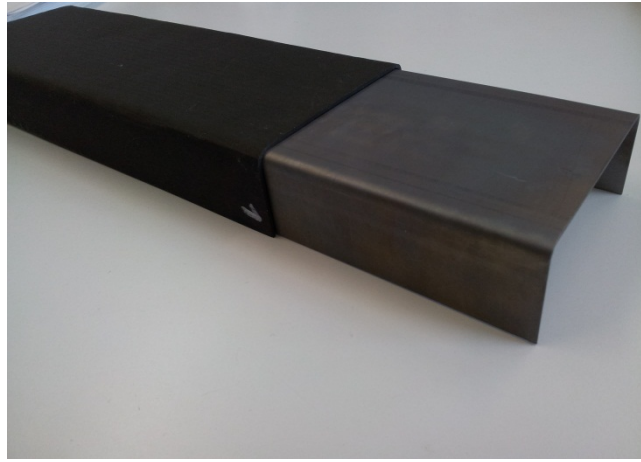


Fig. 66: Application demonstrator aeronautics © EADS

Atmospheric plasma equipment and process parameters developed during the N2P project were successfully utilized for demonstration. The postulated beneficial influence of nano-structuring could be demonstrated within the project period.

2.5.2.3 Conclusions

Within the N2P project it was demonstrated, that atmospheric plasma treatment, based on linearly extended and stabilized DC arc plasma with a length of 150 mm is suitable for Titanium as well as CFRP substrates to achieve long term stable adhesive bonding and painting.

The technical functionality of the prepared surfaces matches the target performance. The process developed is in a state of a concept process.

In comparison to competing approaches for pre-treatment of hybrid structures (e.g. wet chemical and laser processes), the plasma process has distinctive advantages:

Flexibility: technology is not material specific – different material classes can be treated by the same technology/equipment → economic benefit

Throughput: technology is not limited in size (e.g. bathes) and can be implemented in assembly lines → increase of productivity

Durability: there is no heat impact of substrate (as it is for laser)

Sustainability: no waste (e.g. used electrolytes, waste water) is produced → sustainable and ecologic process

Application demonstrators for steel industry

Two types of demonstrators for steel industry have been selected:

- lightweight panel composed of two pre-paint galvanized steel or two primed zinc steel skins, and PP honeycomb core or LDPE full core material;
- lightweight stainless steel composed of one flat and one embossed sheet.

The objectives were the following:

- Optimize surface modification process for demonstrator materials, assuring process stability and improved adhesion.
- Demonstrate applicability of plasma process at large scale, assuring good treatment uniformity

- Test demonstrator according to specification (application related tests) and evaluate results



Figure 55: Light-weight panels composed of plastic core (honeycomb and full core) and painted galvanised steel or primed zinc steel skins (left and middle); Light-weight panel composed of flat and embossed stainless steel sheets (right) © OCAS, Fraunhofer IWS

Demonstrators for pre-painted galvanised steel and zinc sheets

Aerosol assisted DBD plasma technology was used to chemically modify the surface of pre-painted steel and primed zinc sheets. The achieved process speeds (up to 10 m/min) are compatible with the speed of a sandwich manufacturing line. Both lab tests and application oriented tests showed improved adhesion and durability results, making the DBD plasma process a potential candidate for in-line pre-treatment of painted and primed surfaces. It has been shown that the uniformity of the treatment is very good and reproducible. The DBD plasma meets the main objectives, namely improvement of adhesion and durability, and higher product quality (reduced failure rate).

To simulate industrial production, steel samples (30 x 100 cm²) were transferred after plasma treatment at VITO to an industrial sandwich production line. At the line, the metal skins were joined to the lightweight cores by means of a thermoplastic PE or PE/PP based film (depending on the core material). After assembly, the panels were cut into pieces and adhesion was assessed by floating roller tests (ISO 1464).

Treatment @ VITO

Lamination @ industrial line

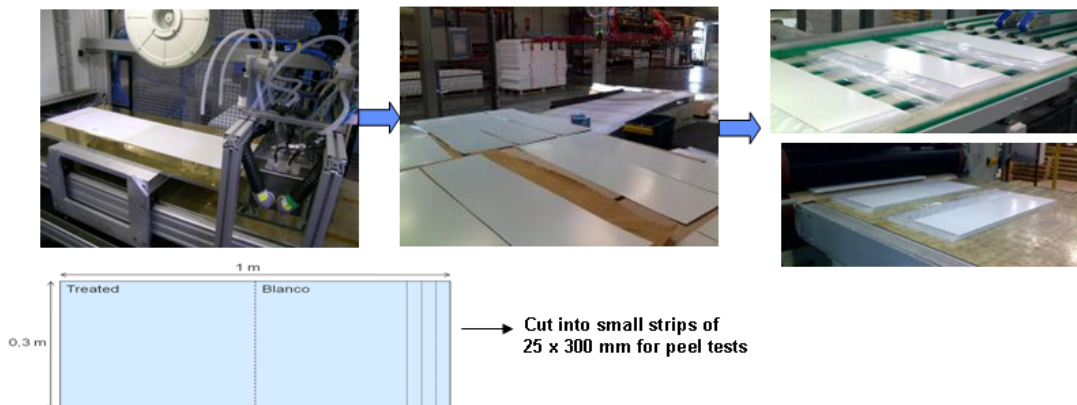


Figure 56: Production scheme of semi-industrial sandwich panels after plasma treatment ©VITO, OCAS

The stability of the plasma source was very high, resulting in reproducible chemical modifications of the polymer surfaces over the full width of the panels. For pre-painted steel as well as for primed galvanised (zinc) steel, a significant increase in adhesion strength was observed when using the APEO pre-cursor, along with a strongly reduced deviation in peel values. Both properties are a clear indication of enhanced product quality.

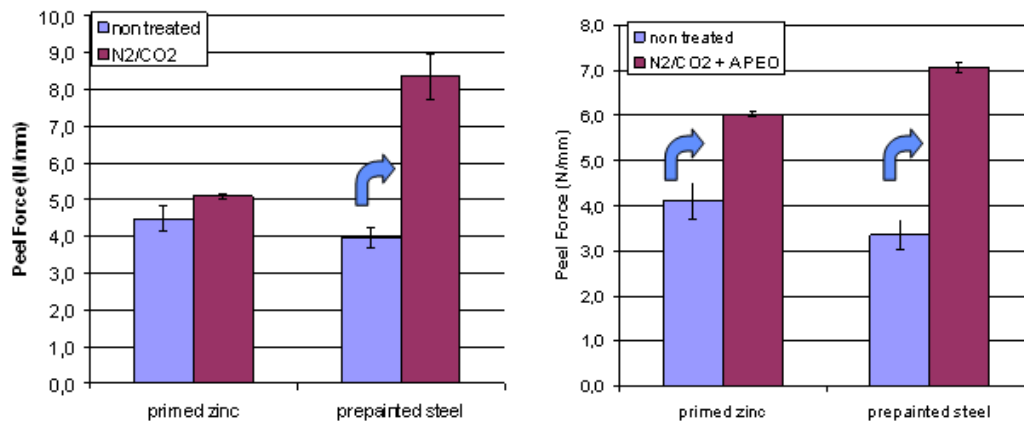


Figure 57: Peel values for plasma treated pre-painted steel and primed zinc panels.

Durability of the plasma treated sandwich panels was also strongly increased compared to untreated panels.

Stainless steel demonstrators

Adhesion tests on flat and embossed stainless steel sheets – treated at the IWS lab test bench – reconfirmed that substrate pre-heating, temperature control and gas feeding were the most critical parameters in order to achieve adhesion promoting silica layers.

The final demonstrators were manufactured by joining one flat and one embossed stainless steel sheet. The steel was treated by using the demonstrator plasma head at IWS and glued by an epoxy upon arrival at OCAS. Plasma settings were selected based on a detailed parametric study of process variables on the PA-CVD lab test bench. In contrast to untreated stainless steel, the adhesion strength could be increased and was very reproducible for the plasma treated samples (high product quality).

2.6 WP11: Cross-cutting equipment development

2.6.1 Objectives

Aim for WP11 was the development of cross-cutting equipment to demonstrate feasibility of industrial production of 3D nano-structured surfaces, comprising:

- new plasma sources for high throughput atmospheric pressure processing
- tailored power supplies for atmospheric pressure plasma source operation
- equipment and dedicated software for process monitoring and quality assurance

The application specific development of equipment for continuous high throughput plasma-chemical etching of 3D nano-structures and of processes for high throughput deposition of 3D nano-structured materials was subject of the vertical workpackages concerned, see WP1 to WP10

2.6.2 Plasma sources

2.6.2.1 Extended DC-Arc plasma source

Targeting to the equipment demonstrators for both plasma chemical etching of silicon for c-Si-PV (WP1/2) and surface chemical treatment for adhesion control the pre-existing extended DC Arc plasma source was up-graded:

A re-design of the gas distribution system inside of the plasma source based on results of an extensive characterisation and fluid dynamic simulations lead to an improved homogeneity of the remote plasma.

For 3D nano-surface structuring and functionalization for improved adhesion (WP9) lab-scale equipment based on an extended DC-Arc plasma source and a “technology head” for the treatment of shaped parts was developed. With the linear substrate movement system velocities of up to 50 m/min are possible. Also slightly bended substrates can be treated with this setup. Fluid dynamic simulations of the lab-scale test bench equipment were performed. One conclusion of these simulations is the use of a total plasma flow of minimum 120 slm to ensure the plasma reaching the substrate.

An additional precursor injection unit for thin film deposition was installed, allowing the injection of gases into the remote plasma. A hole type nozzle system with a reduced gas extraction area was designed allowing high speed PE-CVD coating. The film thickness homogeneity was increased by tilting the plasma source.

Optical emission spectroscopy (OES) and Fourier transform infrared emission spectroscopy (FTIR) have been used to identifying active species in the afterglow of the DC-Arc plasma. The results suggest that oxygen atoms are present at distances up to 12 cm from the plasma source. OH, CN and C₂ radicals are also clearly present at all distances measured. The FTIR spectra are dominated by vibrationally excited CO₂ emissions and furthermore CO as a dissociation product can be seen at most distances.

2.6.2.2 Microwave plasma source

An 11“ cylinder resonator type microwave plasma source (CYRANNUS, 10 kW microwave power; investment outside N2P) was set into operation and evaluated as a basis for plasma chemical etching at atmospheric pressure. As the optimal type of plasma gas supply a circular slit nozzle on the top of the plasma source was evaluated enabling a highly energetic, homogenous plasma extraction.

To evaluate the plasma homogeneity, the gas temperature of the plasma gas extracted from the plasma source was determined. A high concentration of argon in the plasma gas causes a homogenization of the plasma extraction. Up to a total gas flow of 90 slm nitrogen injection

increases the gas temperature. With further increase of the total gas flow, the gas temperature of the extracted plasma gas decreases as the delivered microwave energy is no longer sufficient.

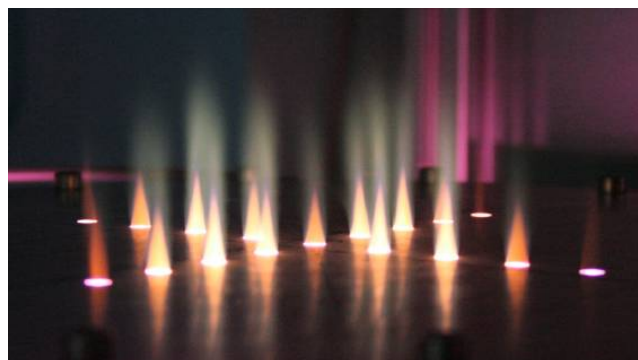
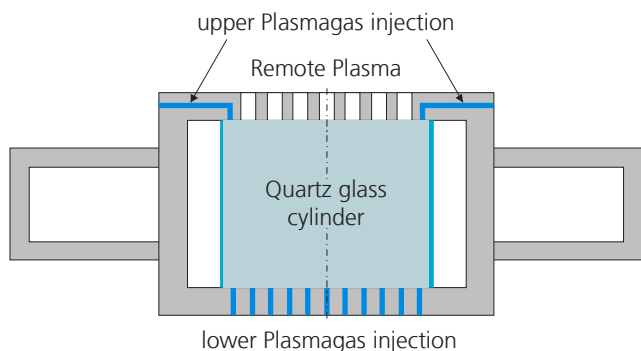


Figure 58: Microwave plasma source: flow scheme (left); test set-up for measuring plasma activity distribution (right) © Fraunhofer IWS

2.6.2.3 GD-DBD based plasma sources

A diffuse (glow) dielectric barrier discharge provides a large area, non thermal plasma at atmospheric pressure and has demonstrated significant potential for deposition and surface treatment combining low substrate temperatures with low power consumption. However, when operating in gases other than helium, the discharge readily transits to a highly filamentary condition, which although used commercially for surface activation of polymers, is less suited to the in-situ deposition of inorganic materials. The key objective of this work was to provide a visually diffuse discharge capable of providing uniform activation, operating in nitrogen to provide a cost effective and scalable process.

The developed power supply enables a diffuse, cost effective nitrogen discharge suited to coating and etching processes. The approach is scalable to large areas and highly compatible with online installation. A novel, low cost atmospheric pressures etch process has been developed with a head constructed and under evaluation in WP3/4. This complements and builds on the enhanced TCO growth facilitated by the provision of upgraded thermal CVD equipment, providing a strong technology platform for the demonstrator phase.

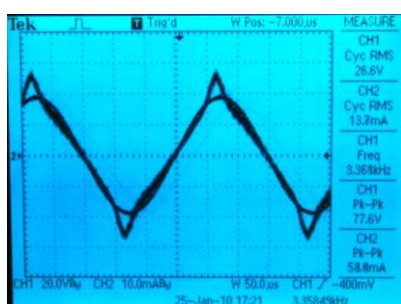


Figure 59: Oscilloscope trace showing the plasma current and primary voltage waveforms for a visually diffuse discharge using a 60 mH choke to prevent high frequency spikes on the current trace (left); nitrogen discharge operating over a 3 mm gap (right) © USAL-cvd

The design of a modular coating head was initiated to enable variable path lengths for exploring different chemistries and allowing further optimization of zinc and aluminium based films. Such evaluation could steer future designs, maximizing process efficiency and film properties, enabling a cost effective technical solution.

This platform technology was incorporated into head designs, applied in-situ for the deposition of anti-microbial coatings (WP6) and remotely for an activated etch process for the surface modification of thin film TCO for TF-PV applications (WP4).

2.6.2.4 Ultra-short pulse DBD

The feasibility of a newly developed nanosecond short pulse generator for DBD based CVD applications was successfully demonstrated. Short pulses resulted in higher plasma activity and hence, deposition rates, in comparison with conventional sinus wave excitation of the discharge.

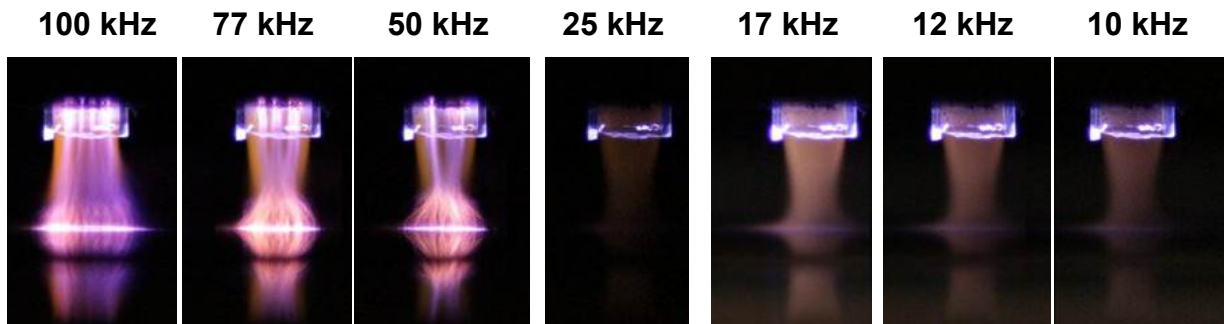


Figure 60: Characteristics of the Pulse-DBD with Ar-N₂ plasma gas mixture: discharge voltage of 4.7 kV with frequencies from 100 kHz to 10 kHz (increased exposition time for 17-10 kHz) © Fraunhofer IWS, Regatron, Baur

The DBD torch setup modifications to prevent short cuts and streamers at higher power were insufficient. Therefore, a new linear DBD source concept was designed and realized. Also, the test of alternative gases for chemical surface modification and etching (e.g. NH₃ or HCl) was successful. The feasibility for coating was confirmed.

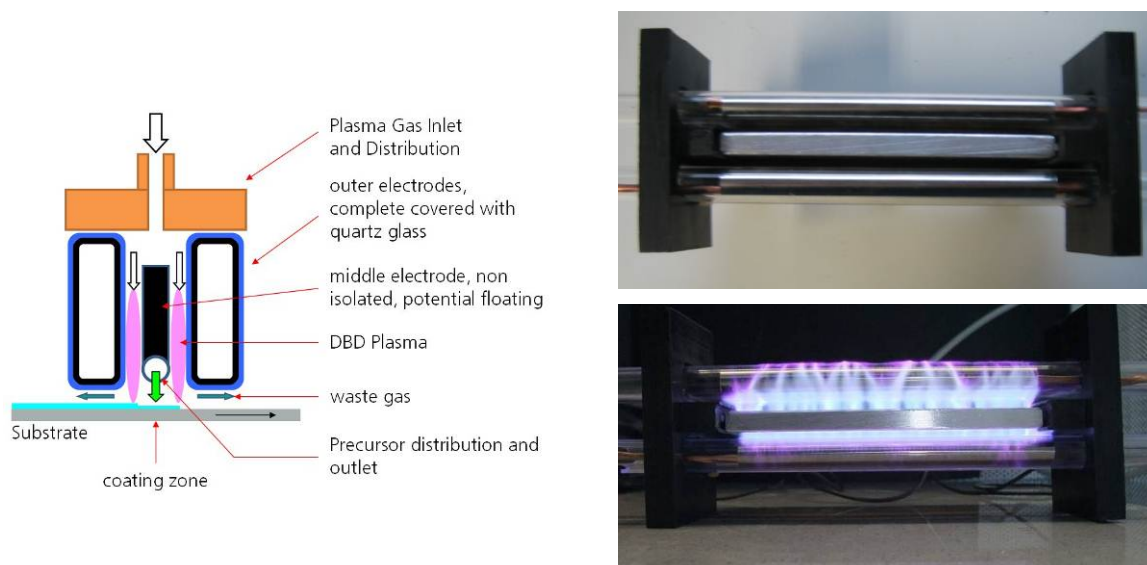


Figure 61: Principle (left) and first set-up (top right) of linear DBD source, discharge in the linear DBD equipment, 20 slm Ar, 5 kV, 100 kHz, 68 °C, position of the middle electrode 5 mm, duty cycle 30% (bottom right) ©Fraunhofer IWS

2.6.3 Power supplies

2.6.3.1 Power supply for extended DC Arc plasma sources

The extended DC Arc plasma systems as used in WP 1/2 and WP 9/10 are driven by up-graded REGATRON TopCon power supplies. These have proven stable and reliable operation during the project work. By using the capability of TopCon to be connected either in parallel, in series or even in matrix mode, changing requirements on currents and/or voltages or power can easily be adapted.



Responsible Partner: REGA

Name: TopCon, 2 modules

Power: 2x32 kW

Frequency: DC

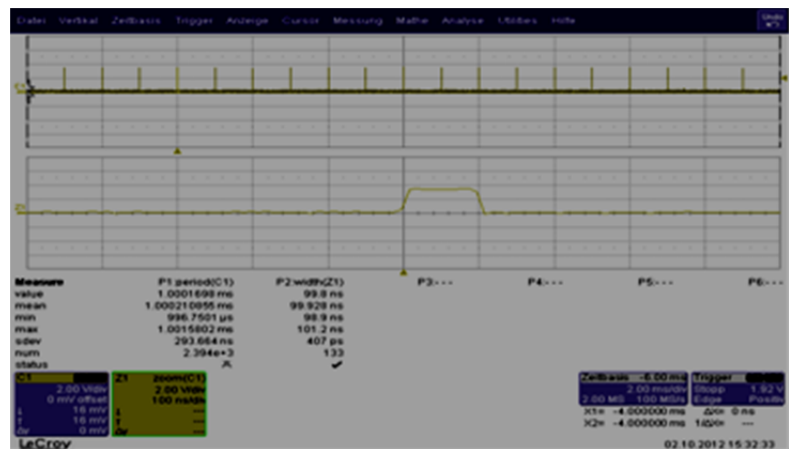
Cooling: Air cooling / water cooling on demand

Figure 62: Power supply for Extended DC Arc plasma source, picture and main technical parameters ©Regatron

2.6.3.2 Power supply for Ultra Short Pulses (DBD)

The development of the USPP (Ultra Short Plasma Pulser) is aiming for:

- DBD type sources with enhanced plasma activity and improved homogeneity (see above)
- N2P spin-of applications, e.g. high rate magnetron sputtering and cable fault detection in Power Cables



Responsible Partner: REGA, BAUR

Name: NPQ10.100.3kW-BAUR

Maximum Pulse voltage: 10 kV

Maximum Pulse current: 30 A

Maximum Power: 3 kW

Pulse Repetition rate: 1 – 100 kHz

Cooling: liquid cooling circuit for HV switch

Figure 63: Ultra Narrow Pulse Generator (left), Scope screen of a Narrow Pulse train and zoomed portion (right)

©Regatron, Baur

N2P spin-of application: cable fault detection in Medium Voltage Power Cables

The USPP had to be modified to allow pulse forming in a Power Cable. Simulation and literature reference indicated that power cables with a typical impedance of $40\ \Omega$ require higher currents for forming a proper HV pulse with steep flanks. Therefore the USPP was modified:

Maximum Pulse Voltage: 10 kV
Maximum Pulse Current: 200 A
Pulse Repetition Rate: 0.1 - 100 Hz and a "single shot" mode
Air cooled HV switch

Cable faults can be detected via time domain reflectometry (TDR): As an example, a reflexion of a simulated cable fault ($100\ \Omega$ resistor) between two cable sections of 300 m each is shown in Figure 64.

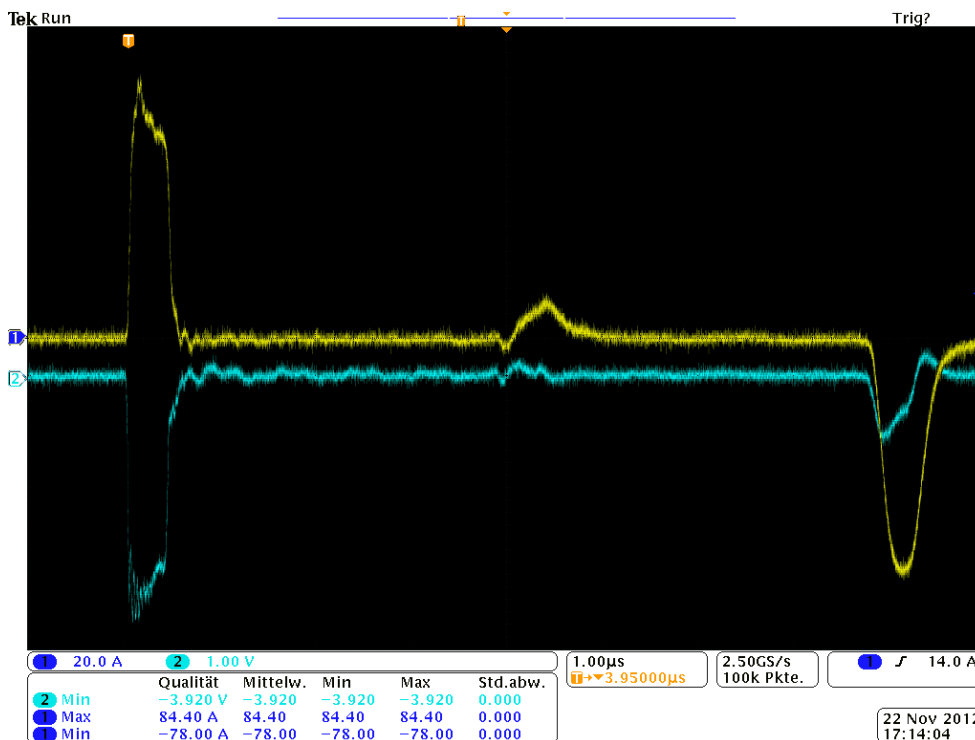


Figure 64: Reflection of a simulated cable fault ($100\ \Omega$ resistor) between two cable sections of 300 m each; Pulse 4 kV, pulse width 500 ns, Pulse Runtime for 600 m cable forth and back about 8 µs; The upper trace is the current, the lower the voltage (displayed inverse): Left is the original starting pulse, in the middle the reflection of the cable fault, right the reflection from the open cable end. ©BAUR

Using TDR for cable fault detection in power cables is by no means a new approach; however, using strong high voltage pulses for this technique holds the promise of higher detection ranges and a better sensitivity for intermitted cable faults.

2.6.3.3 Power supply for filamented DBD with enhanced frequency

Standard corona power supplies were adapted for use up to 100 kHz in DBD plasma reactors by AFS (Figure 65 left). A setup with different inductors and capacitors that can easily be switch in and out the first circuit of the transformer is applied to match the power supply with the DBD plasma reactor. In this way the resonance frequency of the system can be adapted and plasma discharges can be generated at any chosen frequency with minimum power losses. When working at resonance frequency, current output (blue) from the power supply and voltage output (yellow) out of the transformer results in sinusoidal signals (Figure 65 right). To work at frequencies up to 100 kHz,

a new IGBT system was developed with higher driver power for stable operation of the power supply.

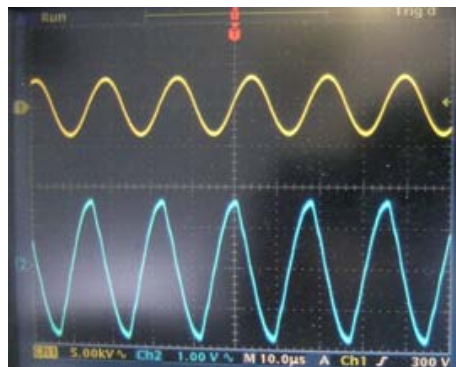


Figure 65: Power supply with power load matching regulators (left) and current (blue) and voltage (yellow) signal at resonance (right). ©AFS

2.6.4 Process monitoring and control

2.6.4.1 Optical surface monitoring

Using an OceanOptics HL-2000-FHSA (tungsten halogen source) and the OceanOptics 2000+ various optical arrangements were investigated to enable accurate measurement of the reflection spectra. To determine the film thicknesses to $\pm 1\text{nm}$ and refractive indices to ± 0.001 the reflection needed to be accurately measured to better than $\pm 0.5\%$. To achieve this on an in-line system requires the following points were addressed:

1. The reflected intensity needs to be strong enough to avoid troublesome noise on the detected signal;
2. The distance from the detection head to the reflecting surface should not be too sensitive to changes in distance;
3. The tolerance to tilt or wobble of the reflecting surface should not be too critical;
4. A reliable reference surface needs to be used to accurately determine the reflectivity.

The optical arrangement, using two 10 mm lens and 600 μm fibre was been found to give a good signal to noise ratio, and some insensitive to distance and tilt.

A fused silica plate has been used has a reference surface for calibrating the reflection spectra intensity. The advantage of using the silica plate is that the index is accurately known and hence the expected reflection spectra can be determined.

This arrangement was then packaged to make it more rugged and suitable for installing on a production line. The schematic outline of the new arrangement is shown in Figure 66.

Schematic of On-line Reflectometer

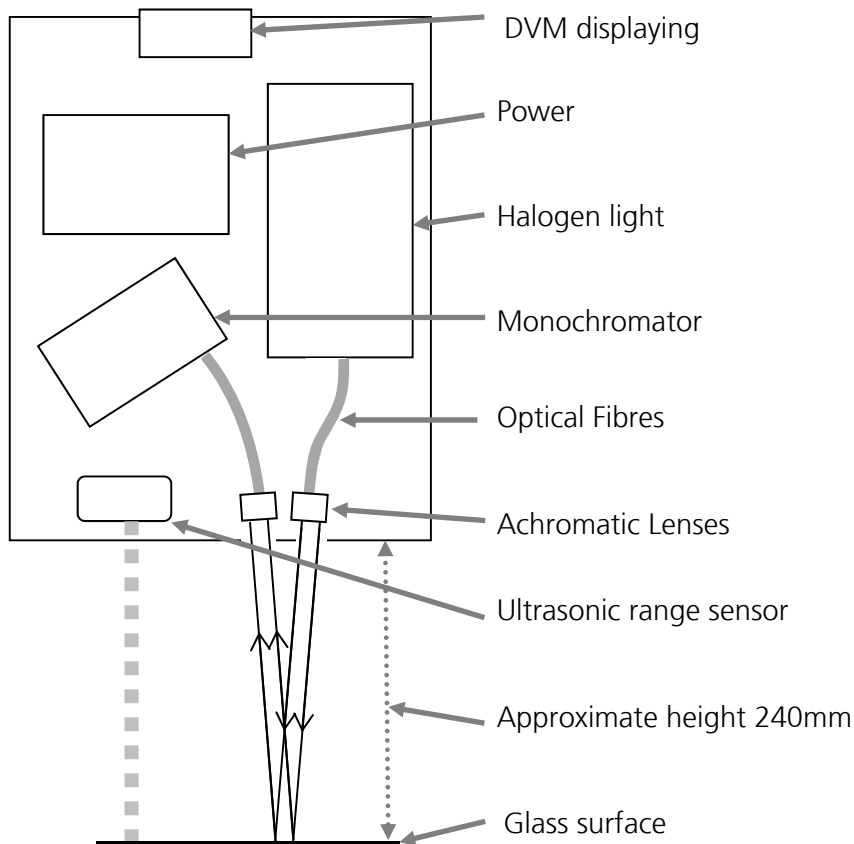


Figure 66: Schematic of the on-line reflectometer showing the main components ©CTEC

This arrangement was then integrated into the in-line demonstrator system at CTEC. A multi-capability surface monitoring platform was designed and installed on the in-line coater to allow the simultaneous measurement of reflection and haze.



Figure 67: Online analysis equipment, in-situ on the demonstrator system © CTEC

2.6.4.2 Gas phase monitoring by laser and FTIR spectroscopy

A range of techniques must be used to monitor the processes involved in the production of 3D nanostructured surfaces. The multispecies and multipoint NIR diode laser monitoring instrument has been developed and its performance improved to enable data collection to go towards the identification of a correlation with surface measurements.

Initial results in WP3 demonstrate the strong capabilities for continuously monitoring key species of AP-CVD processes, e.g. HCl and H₂O. The measurements can also be used to validate CFD models of the reactor system.

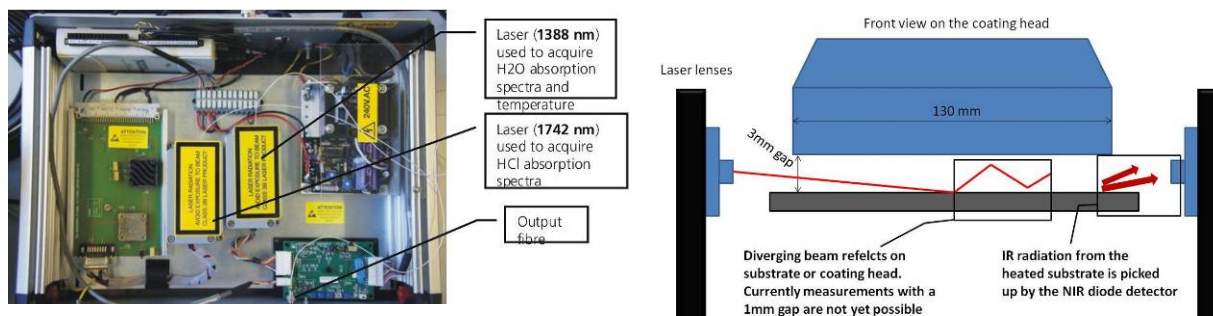


Figure 68: Photograph shows the internal view of the combined HCl, H₂O and temperature monitoring instrument (left); multispecies and multipoint NIR diode laser absorption spectrometer installed at the coating reactor (right)
©TDL

FTIR spectroscopy, both in situ and in line has been shown to be extremely useful for monitoring purposes. Despite being less sensitive than the laser methods FTIR absorption and emission spectroscopy has a wide wavelength coverage and can thus detect a range of species. Time-resolved FTIR has been shown to be less successful due to the increased electrical and vibrational noise present. These issues can be surmounted.

The methodology for correlating process parameters and chemical species with film properties appears to be promising and merits further investigation especially in the application of chemometric principles such as PCA.

2.7 Dissemination activities and exploitation of results

(refer to the separate file which summarises measures for dissemination and exploitation of results)